CENTRO DE INVESTIGACIONES EN AGRIGENÓMICA

INSTITUTO HISPANOLUSO DE INVESTIGACIONES AGRARIAS

DEPARTAMENTO DE MICROBIOLOGÍA Y GENÉTICA

AREA: GENÉTICA

Nuevas estrategias para la regeneración de tejidos y la defensa de las plantas frente a *Ralstonia solanacearum*, *Pseudomonas syringae* y *Botrytis cinerea*

TESIS DOCTORAL

-Alejandro Alonso Díaz-

Directores:

Núria Sánchez Coll

Marc Valls Matheu

Tutor:

Ernesto Pérez Benito

Nuevas estrategias para la regeneración de tejidos y la defensa de las plantas frente a *Ralstonia solanacearum*, *Pseudomonas syringae* y *Botrytis cinerea*

Tesis presentada por D. Alejandro Alonso Díaz para optar al grado de Doctor en Agrobiotecnología

Fdo.: Alejandro Alonso Díaz

VºBº

Los directores de la tesis

Tutor de la tesis

Dra. Núria Sánchez Coll

Dr. Marc Valls Matheu

Dr. Ernesto Pérez Benito

Barcelona, 11 de Julio de 2019

Dra. Núria Sánchez Coll, Investigadora Ramón y Cajal del Centro de Investigaciones en Agrigenómica (CSIC-IRTA-UAB-UB), **Dr. Marc Valls Matheu**, Profesor Titular de Genética de la Universidad de Barcelona y **Dr. Ernesto Pérez Benito** Profesor Titular de Genética de la Universidad de Salamanca.

CERTIFICAN:

Que la presente Memoria titulada "**Nuevas estrategias para la regeneración de tejidos y la defensa de las plantas frente a *Ralstonia solanacearum*, *Pseudomonas syringae* y *Botrytis cinerea***" ha sido realizada en el Departamento de Microbiología y Genética y el Centro de Investigaciones en Agrigenómica (CSIC-IRTA-UAB-UB de Barcelona, bajo nuestra dirección y tutoría, por **D. Alejandro Alonso Díaz**, y que cumple las condiciones exigidas para optar al grado de Doctor en Agrobiotecnología por la Universidad de Salamanca.

Para que así conste, firmamos el presente certificado en Barcelona/Salamanca, a 11 de Julio de 2019.

Fdo: Dra. Núria Sánchez Coll

Fdo: Dr. Marc Valls Matheu

Fdo: Dr. Ernesto Pérez Benito

Dr. Carlos Nicolás Rodríguez, Coordinador del Programa de Doctorado en Agrobiotecnología (RD 99/2011) de la Universidad de Salamanca

CERTIFICA:

Que la memoria titulada "**Nuevas estrategias para la regeneración de tejidos y la defensa de las plantas frente a *Ralstonia solanacearum*, *Pseudomonas syringae* y *Botrytis cinerea***" presentada por **D. Alejandro Alonso Díaz** para optar al grado de Doctor en Agrobiotecnología por la Universidad de Salamanca, ha sido realizada bajo la dirección de la Dra. Núria Sánchez Coll, el Dr. Marc Valls Matheu y tutorada por el Dr. Ernesto Pérez Benito, en el Centro de Investigaciones en Agrigenómica (CSIC-IRTA-UAB-UB) en Barcelona.

Y para autorizar su presentación y evaluación por el tribunal correspondiente, firmo este certificado en Salamanca, a 11 de Julio de 2019.

Fdo: Dr. Carlos Nicolas Rodríguez

Dr. Luis Román Fernández Lago Director del Departamento de Microbiología y Genética de la Universidad de Salamanca

CERTIFICA:

Que la memoria titulada "**Nuevas estrategias para la regeneración de tejidos y la defensa de las plantas frente a *Ralstonia solanacearum*, *Pseudomonas syringae* y *Botrytis cinerea***" presentada por **D. Alejandro Alonso Díaz** para optar al grado de Doctor en Agrobiotecnología por la Universidad de Salamanca, ha sido realizada bajo la dirección de la Dra. Núria Sánchez Coll, el Dr. Marc Valls Matheu y tutorada por el Dr. Ernesto Pérez Benito, en el Centro de Investigaciones en Agrigenómica (CSIC-IRTA-UAB-UB) en Barcelona.

Y para autorizar su presentación y evaluación por el tribunal correspondiente, firmo este certificado en Salamanca, a 11 de Julio de 2019.

Fdo: Dr. Luis Román Fernández Lago

Dr. Jose Luis Riechmann Fernández Director del Centro de Investigaciones de Agrigenómica (CSIC-IRTA-UAB-UB) en Barcelona

CERTIFICA:

Que la memoria titulada "**Nuevas estrategias para la regeneración de tejidos y la defensa de las plantas frente a *Ralstonia solanacearum*, *Pseudomonas syringae* y *Botrytis cinerea***" presentada por **D. Alejandro Alonso Díaz** para optar al grado de Doctor en Agrobiotecnología por la Universidad de Salamanca, ha sido realizada bajo la dirección de la Dra. Núria Sánchez Coll, el Dr. Marc Valls Matheu y tutorada por el Dr. Ernesto Pérez Benito, en el Centro de Investigaciones en Agrigenómica (CSIC-IRTA-UAB-UB) en Barcelona.

Y para autorizar su presentación y evaluación por el tribunal correspondiente, firmo este certificado en Salamanca, a 11 de Julio de 2019.

Fdo: Dr. Luis Román Fernández Lago

AGRADECIMIENTOS

Agradecimientos.

Me gustaría agradecer especialmente a Núria Sánchez y Marc Valls por darme la oportunidad de poder formar parte de su maravilloso grupo de investigación, por su cercanía y forma de motivarme para seguir adelante.

También hay un agradecimiento especial para Ernesto Pérez, por introducirme en el apasionante mundo de la ciencia y la investigación. También por su infinita paciencia.

Quisiera también dedicar parte de estos agradecimientos a Montse Capellades, que sin su extraordinaria ayuda esta Tesis no hubiera sido la misma.

Que decir a todos mis compañeros de camino, agradeceros de todo corazón el haberme ayudado de una manera u otra a enriquecerme con vuestra presencia y compañía. Me gustaría agradecer especialmente a mis colegas de laboratorio; Saul, Marc, Marina, Eugenia, Jose, Pau, Anurag, Roger, Ujjal, Montse, Liang y un largo etcétera. Sabéis que más que compañeros de laboratorio sois muy buenos amigos. En mi memoria quedarán muy buenos recuerdos.

Debo de hacer una mención especial a mi madre, ya que ella ha sido la que me ha impulsado a hacer lo que realmente quiero sin ningún tipo de barrera, a motivarme a luchar por conseguir un objetivo y a tender la mano para tocar un sueño. A Carlitos por darnos esos grandes momentos de risa y buen rollo y a mi hermano César por estar siempre a mi lado. Muchas gracias a todos por vuestra infinita paciencia.

ÍNDICE

Contenido

AGRADECIMIENTOS ... 13

ÍNDICE ... 17

RESUMEN SIGNIFICATIVO ... 1

INTRODUCCIÓN GENERAL ... 5

Nanomateriales y sus aplicaciones en defensa de la planta ... 7

Biomateriales y biofilms: celulosa bacteriana ... 7

Biosíntesis y estructura ... 7

Aplicaciones y usos: como matriz y soporte de elementos ... 9

Nanotecnología ... 11

Nanopartículas de plata ... 11

Métodos de síntesis de AgNPs ... 11

Híbrido de celulosa bacteriana y nanopartículas de plata ... 12

Propiedades antipatogénicas ... 13

Interacción *R. solanacearum-A. thaliana*: sistema modelo ... 14

***R. solanacearum*: taxonomía, clasificación, y distribución geográfica** ... 14

Ciclo de vida, infección, colonización y síntomas ... 15

Virulencia y mecanismos de infección ... 17

Producción de exopolisacáridos (EPS) ... 17

Sistema de secreción tipo III ... 18

OBJETIVOS ... 21

Chapter 1 ... 25

Enhancing localized pesticide action through the plant foliage by silver-cellulose hybrid patches. ... 25

Summary ... 25

Introduction ... 27

Results and discussion ... 29

Materials and Methods ... 39

Supplementary information ... 49

Bibliography ... 53

Chapter 2 ... 59

Type III secretion-dependent and -independent phenotypes caused by Ralstonia solanacearum in Arabidopsis roots ... 59

Summary ... 59

Introduction ... 61

Results 63

In vitro infection with *R. solanacearum* causes a triple phenotype on Arabidopsis roots 63

***R. solanacearum hrp* mutants are altered in their capacity to cause the triple root phenotype** 65

***R. solanacearum* strains unable to cause the triple root phenotype are non-virulent on Arabidopsis** 68

***R. solanacearum*-triggered root hair formation is mediated by plant auxins** 70

Absence of the triple root phenotype in Arabidopsis might reveal new sources of resistance to strain GMI1000 72

Discussion 74

Plant host root phenotypes appear as early symptoms of colonization by *R. solanacearum* 74

Auxin signaling alterations caused by *R. solanacearum* infection likely trigger root structure rearrangements, resulting in root hair formation 75

Absence of the triple root phenotype to screen for *R. solanacearum* virulence factors or resistance in Arabidopsis 76

Materials and Methods 78

Bibliography 87

CONCLUSIONES 91

BIBLIOGRAFIA 95

RESUMEN

Resumen de la Tesis

Debido al constante cambio climático que existe y al aumento de la población, es necesario el desarrollo de nuevas estrategias moleculares para poder hacer frente a los patógenos que producen grandes pérdidas en las cosechas. Por lo tanto, en esta Tesis hemos tratado de desarrollar dentro de las estrategias mecánicas, un biomaterial con propiedades antipatogénicas. Y por otra parte, dentro del ámbito molecular, la caracterización de la interacción fenotípica entre *R. solanacearum* y *A. thaliana*.

Así los capítulos 1 de esta Tesis engloban la caracterización del biomaterial y evaluación de sus propiedades antipatogénicas. Y los capítulos 2 se ha centrado en el análisis en detalle de la interacción fenotípica producida en el patosistema *A. thaliana-R. solanacearum* en infecciones de raíz *in vitro*, y sus posibles usos para la búsqueda de bases genéticas para la defensa de la planta frente a este patógeno.

En el segundo objetivo analizamos los posibles efectos antipatogénicos de un material híbrido formado por BC unida covalentemente a nanopartículas de plata (BC-AgNPs). Las nanopartículas de plata se sabe que poseen un alto poder antimicrobiano y su uso ha sido altamente estudiado, motivo por el cual decidimos usar este tipo de nanopartículas. Este material híbrido tenía un claro efecto inhibidor del crecimiento *in vitro* de los patógenos bacterianos *Escherichia coli* y *Pseudomonas syringae* así como del hongo necrótrofo *Botrytis cinerea*. Este mismo efecto inhibidor del crecimiento pudo observarse igualmente en ensayos de infección en planta utilizando *P. syringae* y *B. cinerea*. Ya que los mecanismo de acción de las nanopartículas de plata y los iones de plata son la rotura de la pared celular y la permeabilidad de la membrana y también actuar sobre las moléculas de ADN hasta causar la muerte del patógeno. Estos resultados se publicaron en la revista *ACS Biomaterials Science & Engineering*, de alto índice de impacto (Alonso et al., 2019). Este material además, puede constituir una alternativa sostenible para tratamientos antipatogénicos a nivel local, ya que las nanopartículas de plata no se desprenden de la BC.

Habiendo dado respuesta de manera eficaz, mediante el uso del híbrido de BC-AgNPs a la infección que existe entre los patógenos antes mencionados y las diversas plantas de interés agrícola usadas, quisimos seguir aportando conocimiento a esta problemática que tantas pérdidas produce a nivel mundial. Por lo que decidimos seguir trabajando con uno de los patógenos más virulentos que hay, con el que se trabaja en nuestro

laboratorio, y así poder ayudarnos de las herramienas moleculares que ya disponemos, con el objetivo de poder estudiar su interacción con la planta modelo *A. thaliana*.

Para comprender mejor los mecanismos de defensa de la planta a nivel molecular se utilizó el patosistema *Ralstonia solanacearum-A. thaliana*. *R. solanacearum* es una bacteria patógena vascular que infecta las plantas a través de las raíces. Es considerado el responsable de la marchitez bacteriana y tiene un rango de hospedadores que abarca más de 200 especies de más de 50 familias diferentes. Uno de los objetivos de esta tesis es la búsqueda de nuevas formas de resistencia para combatir a *R. solanacearum*, mediante la identificación de nuevos genes implicados en defensa. Para ello, nos centramos inicialmente en establecer un sistema *in vitro* de infección para estudiar de una manera high-throughput los fenotipos causados por *R. solanacearum* en raíces de *A. thaliana*. Esto nos llevó a la identificación de 3 claros fenotipos de raíz: inhibición del crecimiento radicular, formación de pelos radiculares y muerte celular en la punta de la raíz, que fueron publicados (Lu, Lema, Planas et al., 2018). Este método es una herramienta fácil de usar y con un alto rendimiento que permite estudiar de manera eficiente la interacción de *R. solanacearum* en *A. thaliana*, en comparación con los tradicionales métodos de patogenicidad de inoculación por empapamiento en el suelo que requieren de mayor tiempo y espacio de crecimiento en condiciones controladas.

INTRODUCCIÓN GENERAL

Nanomateriales y sus aplicaciones en defensa de la planta

Biomateriales y biofilms: celulosa bacteriana

La celulosa es la molécula polisacárida insoluble en agua más abundante de la tierra (Jonas & Farah, 1998). Puede ser sintetizada por muy diversos organismos; plantas, algas verdes, oomicetos, hongos y múltiples bacterias (Römling, 2002; Stone, 2005; Kimura & Itoh, 2007; Sarkar et al., 2009; Morgan et al., 2012). La celulosa bacteriana se diferencia de la celulosa de origen vegetal por su elevado grado de pureza, ya que se encuentra libre de ligninas, hemicelulosas y pectinas (Bielecki et al., 2002). Este biopolímero extracelular insoluble puede ser producido por varios tipos de bacterias de diferentes géneros como *Acetobacter*, *Agrobacterium*, *Sarcina* y *Rhizobium* (Jonas & Farah, 1998).En los últimos tiempos la celulosa de origen bacteriano (BC) ha ido ganando importancia debido a sus extraordinarias propiedades como alto grado de cristalización, elasticidad, alta capacidad de absorción de agua, alta resistencia a la presión y durabilidad (Zeng et al., 2014; Klemm et al., 2011). Una vez purificada, la celulosa bacteriana no produce toxicidad, no es alérgica, es biocompatible y biodegradable (Portela et al., 2019).

Biosíntesis y estructura

Las bacterias del género *Acetobacter* producen celulosa a partir de fuentes de carbono como son la glucosa, glicerol, manitol o sacarosa (Oikawa et al., 1995; Biyik & Coban, 2017). *Glucanocetobacter xylinum* (anteriormente *Acetobacter xylinum*) (Ross et al., 1991) se ha convertido en un organismo modelo para la producción y estudio de la celulosa bacteriana debido a su alta capacidad productora, alta pureza y estructura similar a la celulosa de origen vegetal (Klemm et al., 2011; Nishi et al., 1990). Dependiendo de las condiciones de cultivo, la macroestructura de la celulosa bacteriana presenta características diferentes (M. Iguchi et al., 2000; Watanabe et al., 1998). Por lo que en condiciones estáticas *G. xylinum* genera una película en la interfase aire/líquido (Figura 1).

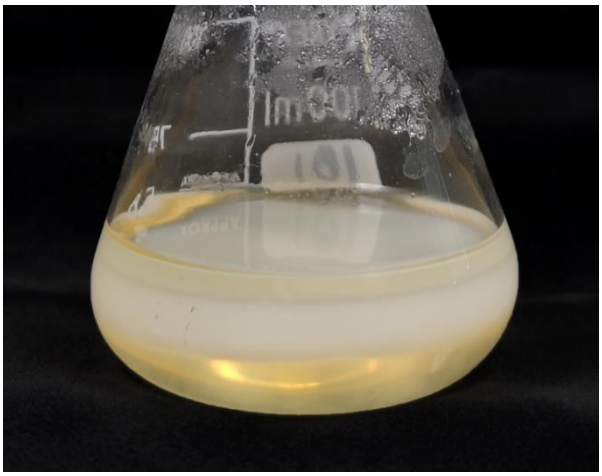

Figura 1: Película de celulosa bacteriana (añadir foto nuestra).

G. xylinum produce dos tipos diferentes de celulosa (tipo I y tipo II) (Chawla et al., 2008). Durante el proceso de síntesis, las protofibrillas (1,5 nm de ancho) de la cadena de glucosa se secretan a través de la pared celular de las bacterias en el medio de cultivo, y se agregan y entrelazan con otras fibras por puentes de hidrógeno y fuerzas de Van der Waals (Figura 2) producidas por otras células formando haces de nanofibrillas de celulosa como se explica en la figura 3 (Ross et al., 1991). Estas cintas construyen la estructura de red con matriz altamente porosa (Dahman, 2009) y forman una capa gelatinosa (Brown, 1996). Al final del proceso de síntesis se produce una estructura reticulada con una elevada resistencia mecánica (Jonas & Farah, 1998).

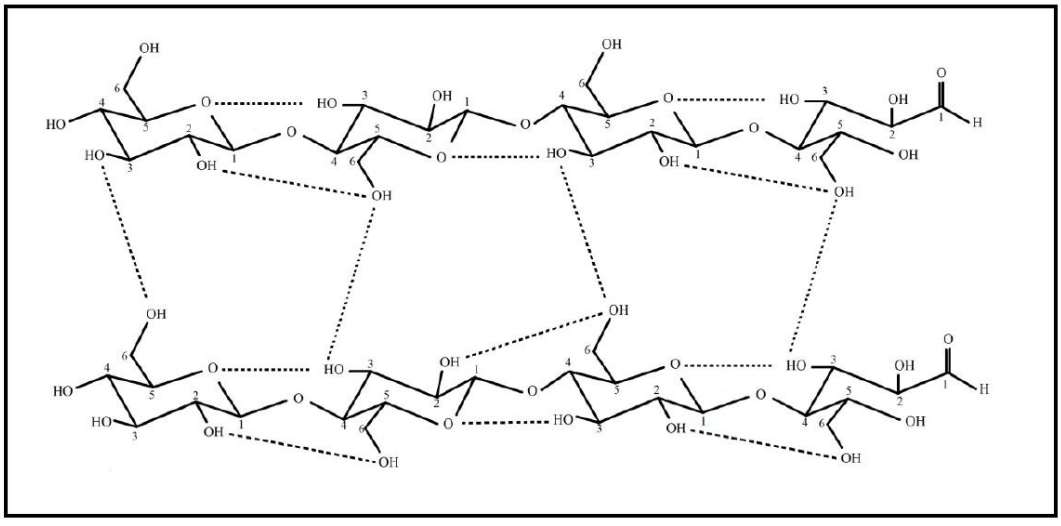

Figura 2: Proceso esquemático de nanoestructura de la celulosa (Festucci-Buselli et al., 2007)

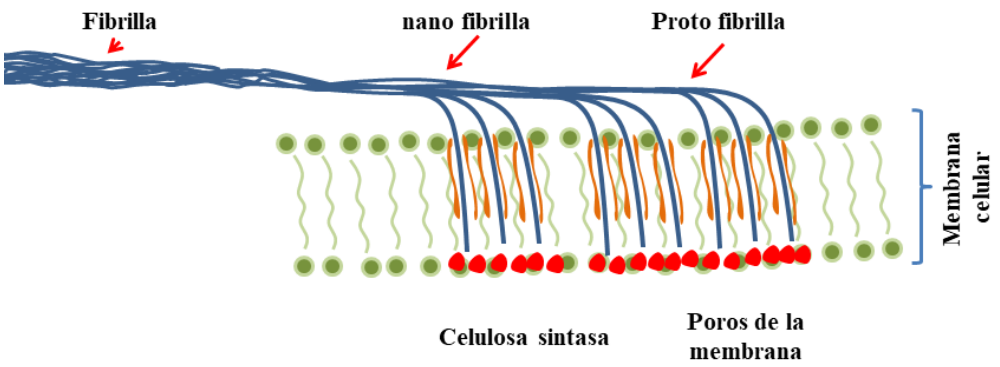

Figura 3: Producción de fibrillas a partir de proto fibrilla y nano fibrilla de celulosa bacteriana.

Aplicaciones y usos: como matriz y soporte de elementos

Gracias a la pureza de la celulosa bacteriana (Bielecki et al., 2002), y a que puede ser esterilizada sin que se vea afectada su estructura y propiedades, esta puede ser utilizada para diversas aplicaciones biomédicas (Czaja et al., 2005), ya que no produce toxicidad o alergia al contacto con otro tejidos (Dourado et al., 2017; Portela et al., 2019). En la figura 5 se muestran algunos ejemplos de usos de la celulosa bacteriana en el campo de la biomedicina.

Figura 5: Aplicaciones de la BC en biomedicina (Ullah et al., 2016).

Además de las aplicaciones que pueda tener en biomedicina, la celulosa bacteriana también tiene otros usos en campos tan diversos como la alimentación, electrónica, producción de papel, cosmética, administración de medicamentos o matriz para albergar nanomateriales que podemos resumir en algunos ejemplos en la siguiente tabla.

Categoría	**Aplicación**	**Referencia**
Alimentación	Espesante y estabilizante	Thompson & Hamilton, 2001
	Nata de coco	M. Iguchi et al., 2000
	Agente gelificante	Okiyama et al., 1993
	Absorbente de grasa	Purwadaria et al., 2010
Electrónica	Celdas de combustible	Sun et al., 2009
	Transductores acústicos	Ciechanska et al., 2002
Papel	Papel de alta calidad	Surma-ślusarska & Presler, 2008
	Papel más resistente	Gao et al., 2011
Cosmética	Máscara facial	Amnuaikit et al., 2011; Almeida et al., 2014; Legendre, 2009
Administración de medicamentos	Liberación de antibióticos	Stoica-Guzun et al., 2007
	Efecto antimicrobiano	Rouabhia et al., 2014; Butchosa et al., 2013; Pinto et al., 2013
Matriz de unión a nanomateriales	Propiedades antibacterianas y antifúngicas	Alonso-Díaz et al., 2019; Roig-Sanchez et al., 2019

Tabla: aplicaciones de la celulosa bacteriana.

Nanotecnología

La nanotecnología es la creación de materiales, dispositivos y sistemas y de escala nanoscópica (1 a 100 nm) (Russell et al., 2004), que debido a su tamaño microscópico, adquieren nuevas propiedades fisicoquímicas. Por ejemplo, el oro es un material estable e inerte, pero sus nanopartículas pueden convertirse en reactivas (Savage et al., 2007). Otro ejemplo de cambio de comportamiento y propiedades son los nanotubos de carbono, que presentan una mayor resistencia y dureza que el carbono a nivel macroscópico (Saeed & Ibrahim, 2013). Los nanomateriales tienen un uso muy relevante en el campo de la biomedicina, ya que su tamaño facilita una rápida movilización por el organismo. Otra propiedad que les confiere una gran ventaja es la relación área/volumen en comparación con un material macroscópico. Debido a sus características, los nanomateriales permiten que muy diversas moléculas (antibióticos, proteínas, biosensores…) sean combinadas con ellos por medio de enlaces covalentes, interacciones electrostáticas u otros tipos de uniones, dejando accesible una mayor cantidad de moléculas activas (Caruthers et al., 2007).

Nanopartículas de plata

La plata ha tenido a lo largo de la historia una gran importancia, también, gracias a sus propiedades antimicrobianas, ya que se ha utilizado en ámbitos tan diversos como la potabilización del agua (Heggers et al., 2012; Castellano et al., 2007), la cicatrización de heridas (HJ., 2000), el tratamiento de infecciones bacterianas (Chopra, 2007; Melaiye & Youngs, 2005), el tratamiento de quemaduras (Moyer et al., 1965). En la actualidad, gracias a sus propiedades antibacterianas, antifúngicas y antivirales (Jo et al., 2009; Oka et al., 1994; Hajipour et al., 2012), las nanopartícuas de plata son el nanomaterial más utilizado para productos de consumo (Vance et al., 2015) y se está estudiando su uso para combatir las cepas de bacterias resistentes a los antibióticos más potentes (Dhanalakshmi et al., 2013).

Métodos de síntesis de AgNPs

Los métodos de síntesis de nanopartículas se pueden clasificar en métodos químicos, físicos y biológicos. Los métodos químicos son los más utilizados (Iravani et al., 2013), ya que permiten preparar las nanopartículas en grandes cantidades y con un tamaño de partícula más homogéneo. Dentro de los métodos químicos existen diferentes procesos como la reducción química, método de poliol, proceso radiolítico o la reducción

fotoquímica mediante radiacción de microondas entre otros (Gudikandula & Charya Maringanti, 2016; Iravani et al., 2013). Para la síntesis química de nanopartículas de plata en disolución se requiere de tres componentes que son; el precursor metálico ($AgNO_3$), un agente reductor y un disolvente o agente estabilizante. La nucleación y el crecimiento son las etapas necesarias para obtener nanopartículas de plata mediante este proceso (Figura 7). El proceso de nucleación requiere una alta energía para activar la reducción de la plata, al contrario del proceso de crecimiento, donde la energía necesaria es menor (Monge, 2009).

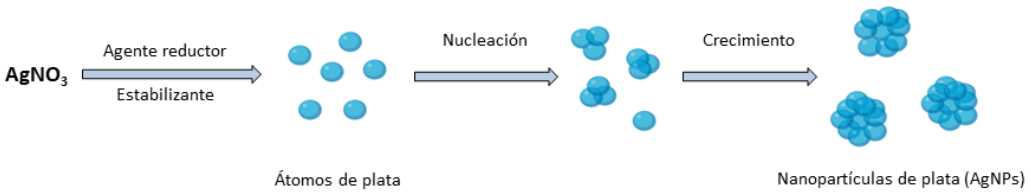

Figura 7: Formación de nanopartículas a partir de la reducción química del precursor $AgNO_3$. Modificada de Monge et al., 2009.

Híbrido de celulosa bacteriana y nanopartículas de plata

En este trabajo, el método utilizado para la síntesis de nanopartículas y posterior unión covalente a la celulosa bacteriana ha sido la reducción térmica mediante radiacción de microondas (Figura 8). Los compuestos utilizados fueron; $AgNO_3$ como precursor metálico, el etilenglicol como agente reductor y la polivinilpirrolidona (PVP) como agente estabilizante, ya que se ha comprobado que es de los agentes protectores más eficaces para estabilizar nanopartículas de plata (Iravani et al., 2013).

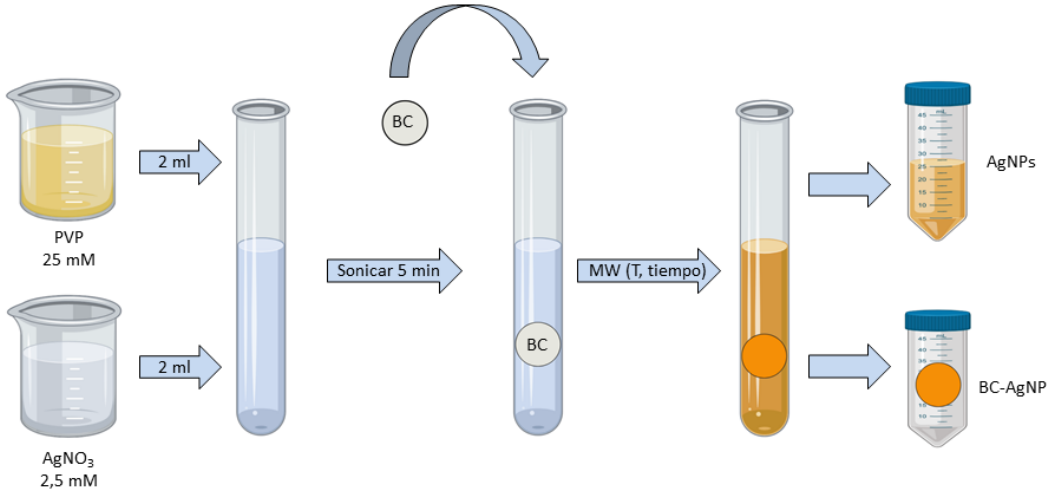

Figura 8: Esquema de la síntesis de híbridos de celulosa bacteriana y nanopartículas de plata (BC-AgNPs) usado en este trabajo. Se mezcla una relación 1:10 en volumen entre el precursor ($AgNO_3$) y el agente reductor y estabilizante (PVP). Se somete la mezcla a sonicación durante 5 minutos para una perfecta homogeneización. Posteriormente se introduce una pieza de BC y se trata con microondas durante 10 min a 120ºC y 300W de potencia. Como producto final se obtiene una suspensión de nanopartículas de plata (AgNPs) e híbridos (BC-AgNPs).

Existen otros métodos para la producción de híbridos que se han descrito con anterioridad como es la impregnación de la BC en $AgNO_3$ y posterior reducción de los iones de plata (Ag^+) en nanopartículas elementales (Ag^0) dentro de la BC usando como agente reductor $NaBH_4$ (Mohite & Patil, 2016; Maneerung et al., 2008) o la combinación con otros materiales (Wu et al., 2018; Yang, et al., 2017; De Moura et al., 2012; Li et al., 2017; Kishanji et al., 2017; Rieger et al., 2016). El inconveniente de este método de impregnación es que no se garantiza la unión entre las nanopartículas de plata y la BC, por lo que una gran cantidad de ellas se desprenden y pueden producir toxicidad en otros seres vivos (Ratte, 1998; Johnston et al., 2010).

Propiedades antipatogénicas

Se cree que el efecto inhibitorio de las nanopartículas de plata frente a patógenos (Figura 9) es debido a los iones de plata (Ag^+), que se liberan en presencia de humedad e interactúan con las paredes del microorganismo que presentan carga negativa. Los iones Ag^+ desplazan a los iones Ca 2^+ y Zn 2^+, mientras que las partículas de plata inhiben las enzimas celulares, permeabilizan la membrana y finalmente conducen a la

lisis celular, rotura de las moléculas de ADN y la muerte (Ratte, 1998; Sambhy et al., 2006; Choi et al., 2008; Kędziora et al., 2018)

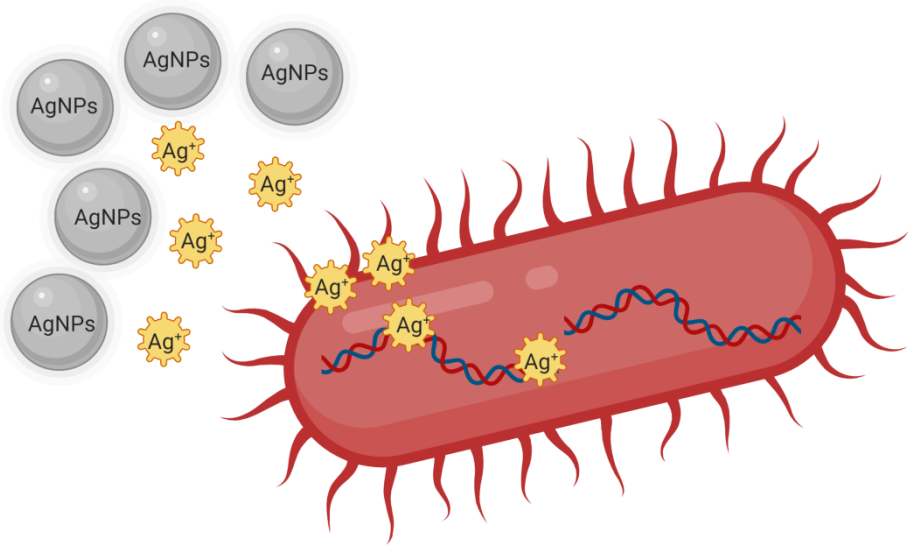

Figura 9: Modo de acción de las nanopartículas de plata e iones de plata.

Interacción *R. solanacearum*-*A. thaliana*: sistema modelo

R. solanacearum: taxonomía, clasificación, y distribución geográfica

Ralstonia solanacearum (antiguamente llamada *Bacillus solanacearum* y *Pseudomonas solanacearum)* es una β-proteobacteria (Hayward, 1964). Es un patógeno de cuarentena en la Unión Europea (DOCE 2000 y modificaciones), pero es especialmente endémica en las regiones tropicales y subtropicales del mundo, ya que su temperatura de crecimiento óptima es de alrededor de 30ºC. *R. solanacearum* ha sido clasificada tradicionalmente en 5 razas y 6 biovares teniendo en cuenta, respectivamente, el rango de hospedador y las propiedades bioquímicas (Buddenhagen, 1962; He et al., 1983), (Hayward, 1964). Recientemente se ha establecido una clasificación donde se agrupan las cepas en cuatro grupos monofiléticos (filotipos). De este modo, las cepas que provienen de países de Asia, África y América, corresponden a los filotipos I, II y III.

Por otra parte, en filotipo IV englobaría a las cepas que han sido aisladas en países como Australia, Japón e Indonesia.

R. solanacearum es el agente responsable de la marchitez bacteriana, una enfermedad de las más destructivas sobre la agricultura a nivel mundial. El rango de hospedadores de *R. solanacearum* es extremadamente amplio, ya que abarca a más de 200 especies de más de 50 familias diferentes, entre las que se encuentran cultivos de gran importancia agronómica como la patata, tomate, pimiento, tabaco, berenjena o banana (Elphinstone 2005; Hayward, 1994b).

Ciclo de vida, infección, colonización y síntomas

R. solanacearum es un patógeno que habita en el suelo (Figura 10) y en las vías fluviales durante largos periodos de tiempo (Álvarez et al., 2008). La bacteria ingresa en la planta por medio de heridas o aberturas naturales que hay en la raíz. Hay una adhesión más precisa a zonas de elongación de la raíz que suelen ser puntos importantes de exudados que producen un efecto de atracción sobre *R. solanacearum*, promoviendo la adherencia (Yao & Allen, 2006), y raíces laterales emergentes o ya desarrolladas (Vasse et al., 1994). La motilidad mediada por el flagelo tipo "*twitching*" y las fimbrias de tipo IV juegan un papel importante en estas etapas precoces de la infección (Kang et al., 2002); (Liu et al., 2001). Una vez que la bacteria se encuentra en el interior de la raíz, avanza a través del córtex por el apoplasto o espacio intercelular, donde puede obtener nutrientes de la lámina media por acción de las enzimas pectinolíticas (Schell, 2000). Pasados unos días del inicio de la infección, las bacterias ya se encuentran en los vasos del xilema y el cilindro vascular donde proseguirán la infección (Digonnet et al., 2012). En el xilema, la bacteria se multiplica enormemente, alcanzando densidades de 10^{10} UFC (Unidades Formadoras de Colonia) / ml (Vasse et al., 1995). Esta multiplicación y la producción de exopolisacáridos (EPS) acaban bloqueando la vasculatura de la planta y llevando a su colapso por bloqueo del flujo de agua (Denny & Baek, 1990); (Mcgarvey et al., 1999).

Una vez que la planta muere, la bacteria puede sobrevivir varios años en los restos de tejido vegetal marchito enterrado en el suelo o liberarse al medio y propagarse por el agua de riego o vías fluviales y así completar el ciclo de vida (Hong et al., 2008).

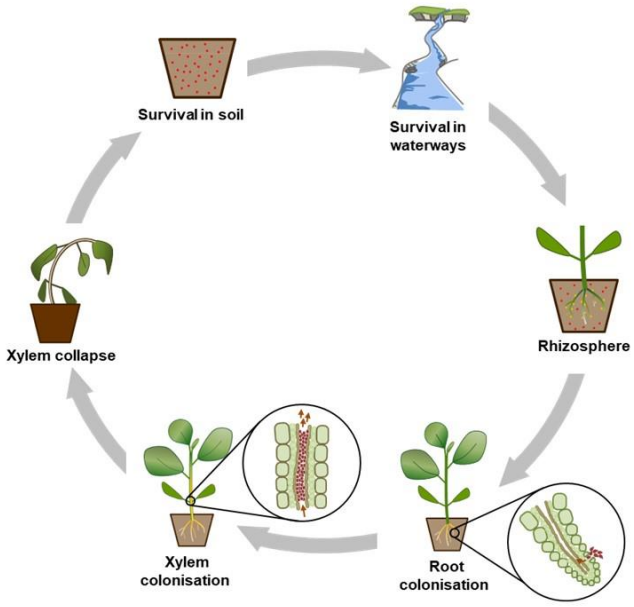

Figura 10: Ciclo de vida de *R. solanacearum.*

La marchitez bacteriana (Figura 11) fue descrita por primera vez en 1914 en África y en 1995 en España en cultivos de patata (Caruso et al., 2017). Posteriormente se han detectado nuevos focos de infección en diferentes provincias como Andalucía, Castilla y León, Castilla La Mancha, Extremadura, Comunidad de Madrid y País Vasco en patata y tomate (Caruso et al., 2017). En todas estas zonas se llevó a cabo las medidas de erradicación oportunas que establece la legislación (BOE 1999, 2007). Más importante es su amenaza en Canarias, debido a su clima subtropical (BOE Nº153. 2002). Sin embargo, la bacteria parece haberse establecido en algunos hábitats naturales (como el río Tormes, Salamanca) (BOCyL nº12. 2001).

Figura 11: Planta de *A. thaliana* sana (izquierda) y planta mostrando síntomas de marchitez bacteriana por la infección de *R. solanacearum* (derecha).

Virulencia y mecanismos de infección

Producción de exopolisacáridos (EPS)

Uno de los más importantes factores de virulencia de *R. solanacearum* es la producción de exopolisacárido (EPS), un polímero secretado compuesto principalmente por tres unidades principales: N-acetilgalactosamina, 2-N-acetil-2-desoxi-galacturónica y 2-N-acetil-4-N- (3-hidrozxibutanoilo) -2. 4,6, tri-desoxi-D-glucosa (Orgambides et al., 1991; Mcgarvey et al., 1999). Se ha considerado que el EPS es el causante directo de la marchitez, ya que directamente bloquea el transporte de agua a través de los vasos conductores del xilema (Figura 12) (Denny & Baek, 1990), o la rotura de los vasos por el exceso de presión hidrostática en su interior (Schouten, 1989); (Van Alfen, 1989). La producción de EPS está controlada por el operón *eps* que contiene más de 12 genes transcritos por un mismo promotor (Huang & Schell, 1995). El EPS podría ayudar a la defensa de la propia bacteria frente a los mecanismos de reconocimiento por parte de la planta huésped (Araud-razou et al., 1998); (Mcgarvey et al., 1998).

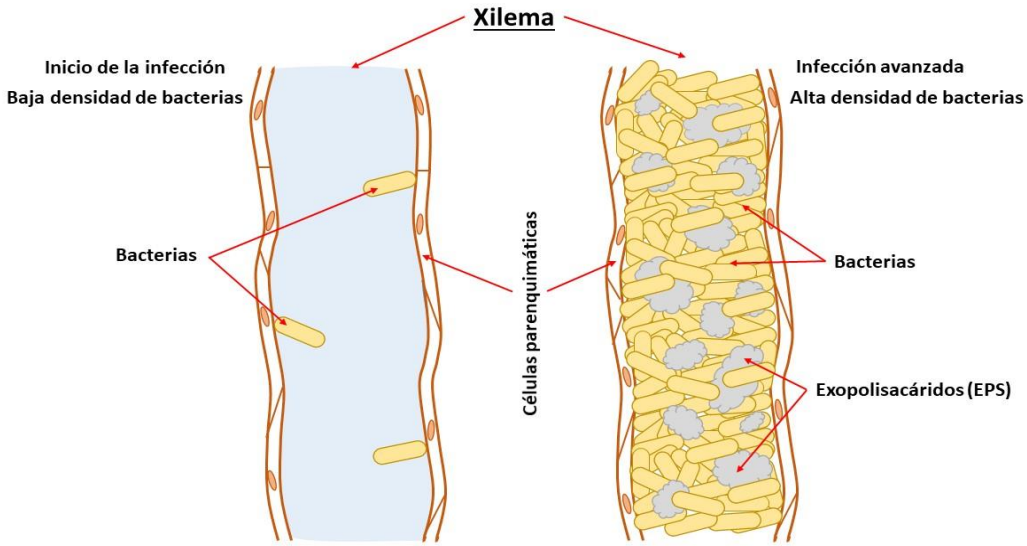

Figura 12: Colapso del xilema de la planta por *R. solanacearum* durante la infección. Al inicio de la infección la densidad de bacterias es muy baja y no impide el transporte de agua a lo largo del xilema. En estadíos más avanzados de la enfermedad, *R. solanacearum* coloniza el xilema hasta que la alta densidad de bacterias y exopolisacárido impiden la circulación del agua y provocan marchitez y muerte de la planta.

Sistema de secreción tipo III

El T3SS está considerado el principal determinante de la virulencia en la mayoría de las bacterianas patógenas gram-negativas. Este sistema de secreción actúa inyectando un conjunto de proteínas efectoras para tratar de modificar o alterar los sistemas de defensa de la planta (Cornelis and Van Gijsegem, 2000). El T3SS está codificado por los genes *hrp* situados en un *cluster* génico de 23-kb, (Genin y Boucher, 2002). Se estima que *R. solanacearum* puede producir más de 70 efectores de tipo III (Peeters et al. 2013). Además de su función en virulencia, muchos de los efectores actúan como proteínas de avirulencia, desencadenando una respuesta de defensa de la planta cuando son específicamente reconocidas por los receptores de la planta (Keen, 1990). En plantas resistentes, se desarrolla una interacción incompatible, que se caracteriza por la respuesta hipersensible (HR), lo que se conoce como interacción “gen a gen” (Alfano y Collmer, 2004). Existen proteínas efectoras de *R. solanacearum* que inducen una respuesta de HR como es el caso de AvrA en plantas de tabaco (Carney y Denny, 1990; Robertson et al., 2004).

Entre los genes *hrp* o alrededor del *cluster*, se encuentran los reguladores del sistema. La transcripción de los genes hrp y sus efectores relacionados es activada por HrpB, el regulador aguas abajo de una cascada reguladora bien descrita inducida por el contacto con la pared celular de la planta (Brito et al., 2002), como se describe en la figura 13. La cascada incluye el receptor de membrana PrhA, el transductor de señal PrhI y los reguladores transcripcionales PrhJ y HrpG (Brito et al., 2002). HrpG está más abajo de PrhJ y controla directamente la expresión de HrpB (y, por tanto, la expresión de los genes T3SS), pero también activa una serie de determinantes de virulencia independientes de HrpB, como los genes para la síntesis de etileno (Valls et al., 2006).

Se ha demostrado que mutantes de *hrp* aunque mantienen la capacidad de invadir la raíz de tomate y llevar a cabo la colonización del sistema vascular, provocan una disminución considerable de la concentración de bacteria en la planta (Etchebar et al. 1998; Vasse et al. 2000).

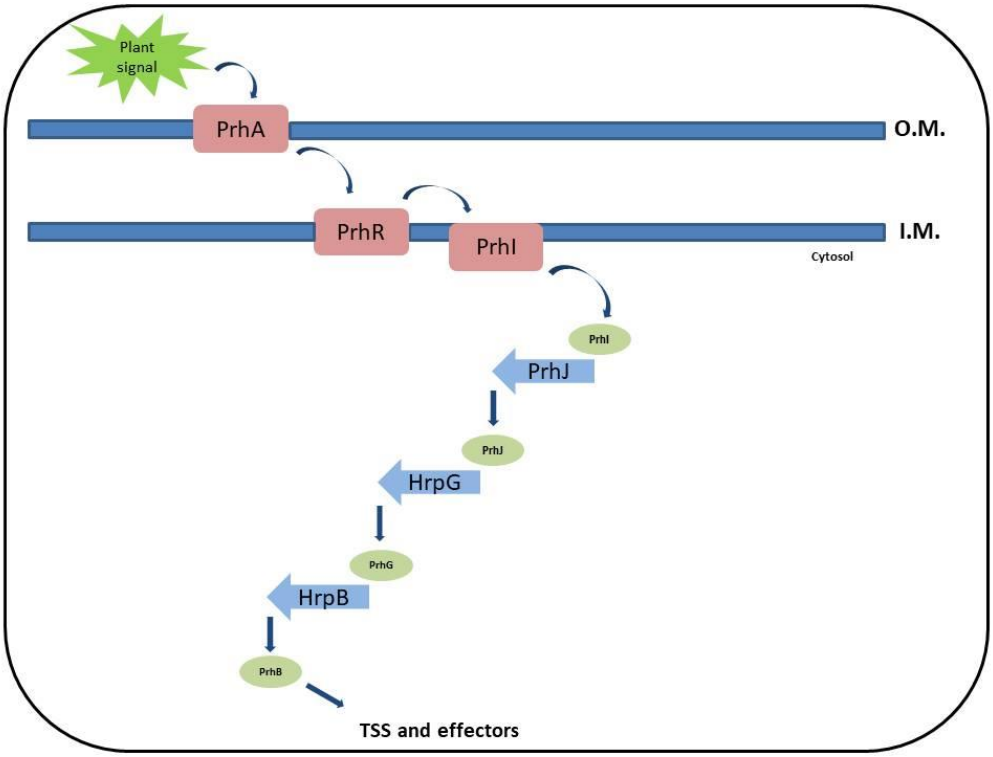

Figura 13: Cascada de señalización del T3SS.

OBJETIVOS

En este trabajo, se han abordado dos cuestiones importantes:

- Por una parte, el estudio de la Celulosa Bacteriana (BC) y a su vez comprobar su posible uso como matriz de soporte para el anclaje de nanomateriales, con el objetivo de potenciar sus aplicaciones. Para ello se planteó el siguiente objetivo:

1- **Evaluar las propiedades antimicrobianas del híbrido formado de BC y nanopartículas de plata (BC-AgNPs) y su aplicabilidad.**

- Por otra parte, se ha realizado el análisis detallado de la interacción *A. thaliana-R. solanacearum* en infecciones de raíz *in vitro*. Para dar respuesta a esta cuestión, se diseñaron un objetivo:

2- **Identificar los fenotipos producidos a tiempos tempranos en la raíz durante la infección *in vitro* del patógeno vascular *R. solanacearum* en *A. thaliana.***

Chapter 1

Enhancing localized pesticide action through the plant foliage by silver-cellulose hybrid patches.

Summary

Efficacy and efficiency of pesticide application in the field through the foliage still faces many challenges. There exists a mismatch between the hydrophobic character of the leaf and the active molecule, low dispersion of the pesticides on the leaves' surface, runoff loss and rolling down of the active molecules to the field, decreasing their efficacy and increasing their accumulation to the soil. We produced bacterial cellulose-silver nanoparticles hybrid patches by *in situ* thermal reduction under microwave irradiation in a scalable manner and obtaining AgNPs strongly anchored to the BC. Those hybrids increase the interaction of the pesticide (AgNPs) with the foliage and avoids runoff loss and rolling down of the nanoparticles. The positive anti-bacterial and anti-fungal properties were assessed *in vitro* against the bacteria *Escherichia coli* and two agro-economically relevant pathogens: the bacterium *Pseudomonas syringa*e and the fungus *Botrytis cinerea*. We showed *in vivo* inhibition of the infection in *Nicotiana Benthamiana* and tomato leaves, as proven by the suppression of the expression of defense molecular markers and reactive oxygen species production. The hydrogel-like character of the bacterial cellulose matrix increases the adherence to the foliage of the patches.

The results presented in this Chapter have been published in the *ACS Biomaterials Science & Engineering* research journal (Anexo).

Enhancing localized pesticide action through the plant foliage by silver-cellulose hybrid patches.

Alejandro Alonso-Díaz[1], Jordi Floriach-Clark[2], Judit Fuentes[2], Montserrat Capellades[1], Núria S. Coll[1*], Anna Laromaine[2*]

[1] *Centre for Research in Agricultural Genomics (CRAG), CSIC-IRTA-UAB-UB, Campus UAB, Bellaterra, Barcelona, 08193, Spain.*

[2] *Institute of Material Science of Barcelona (ICMAB), CSIC, Carrer dels Til.lers, Campus UAB, Bellaterra, Barcelona, 08193, Spain.*

[*]*Corresponding authors: alaromaine@icmab.es, nuria.sanchez-coll@cragenomica.es*

KEYWORDS bacterial cellulose, silver nanoparticles, preventing infection, Nicotiana benthamiana, pseudomonas.

Introduction

Food security and the need to increase sustainably crop yields for a rapidly growing world population are among the greatest social and economic challenges of our century. The most extended agricultural practice to enhance crop yield is to increase host plant density, which in turn tends to increase the severity of plant diseases (Sundström et al., 2014). Most plant diseases occurring in agriculture are caused by fungal pathogens (Agrios, 2005). Diseases caused by pathogenic bacteria are less prevalent; but their effects are also devastating (V. Rajesh Kannan, 2015).

To fight against pathogens, pesticides are effectively used in agriculture, securing a stable crop yield (FAO, 2014). However, the efficacy and efficiency of the pesticides application in the field still faces many challenges. Pesticides sprayed through the leaves experience a mismatch of their hydrophobic character between the foliar tissue and the active molecule, which promotes low dispersion of the pesticides on the leaves' surface, a runoff loss and rolling down of the pesticides to the field, decreasing their efficacy and increasing their accumulation in the soil.

Several active ingredients with anti-pathogenic and anti-bacterial properties, such as several metal ions, have been explored in crops (Lemire et al., 2013). Currently, novel smart-based nanomaterials for pesticides have been developed since they can improve the low solubility issues of the active ingredients in water and its dispersions. The small size, big surface area and target modified properties of nanomaterials holds promise as

nano-based pesticides (X. Zhao et al., 2017). Silver compounds have been commonly used as active ingredients in commercial pesticides (Agency, 1992), despite their toxic properties including DNA damage, inhibition of key enzyme activities or disruption of the bacterial membrane (Lemire et al., 2013; Oka et al., 1994; Nasrollahi et al., 2009). Silver compounds prepared as nanoparticles showed an increased efficacy and specificity as anti-bacterial and antimicrobial agents (Lemire et al., 2013; Hajipour et al., 2012). Price of those smart pesticides are not comparable to common bulk products currently used; however they suit high value applications such as vineyards, fruit trees or rare/valuable tree specimens.

We present a hybrid anti-bacterial and anti-fungal patch, which exploits the potential of smart-based nanomaterials; silver nanoparticles (AgNPs) as anti-bacterial active component. AgNPs are anchored to the bacterial cellulose matrix by *in situ* thermal reduction under microwave irradiation which prevents the release of the NPs to the environment and their runoff loss during application; improving the efficiency and environmental sustainability of this patch.

Cellulose is the most abundant biopolymer (Jonas & Farah, 1998) and is the main constituent of the cell wall of plants (Heredia et al., 1995). However, cellulose can also be produced by different microorganisms, including bacterial species such as *Komagataeibacter xylinus (Kx). Kx* produces cellulose film as a sub-product of its metabolism, which has a hydrogel texture holding up to 90 times its weight on water (Zeng et al., 2014; Hestrin & Schramm, 1954). Bacterial cellulose (BC) is obtained as an ultra-fine and highly pure tridimensional network exhibiting high water holding capacity, gel-like formulation (Zeng et al., 2014) and biocompatibility, thus displaying high potential in regeneration and wound healing applications, Figure S1 (Boateng & Catanzano, 2015). The bacterial cellulose matrix has similar chemical composition to the plant cellulose present in leaves but shows higher purity, crystallinity and water absorbance (Zeng et al., 2014; Klemm et al., 2011). We took advantage of the hydrogel-like nature of the bacterial cellulose matrix to *in situ* synthesize and embedded AgNPs in order to confer anti-pathogenic properties to the patches. Different authors exploited the combination of cellulose with silver nanoparticles, from impregnation (Mohite & Patil, 2016; Maneerung et al., 2008; to *in situ* synthesis in cellulose, oxidized cellulose or combination with other materials (Wu et al., 2018; Yang et al., 2017; De Moura et al., 2012; Li et al., 2017; Kishanji et al., 2017; Riegeret al., 2016) and evaluated them as

anti-bacterial materials. However, the release of the NPs was commonly observed on those materials or not evaluated, even though its environmental hurdles. To avoid any runoff loss to the environment, we exploited the synthesis by *in situ* thermal reduction under microwave irradiation (Gonzalez-Moragas et al., 2015; Zeng et al., 2014; Xu, Wang et al., 2016), in order to strongly anchor the AgNPs to the bacterial cellulose matrix.

Results and discussion

Briefly, BC films were immersed in an $AgNO_3$ and PVP solution to ensure a homogeneous distribution of the precursor inside the cellulose network. After 10 min of microwave radiation, we observed the change of color of the BC films from translucent white to dark brown indicating the incorporation of the AgNPs into the cellulose scaffold (Figure 1a). SEM of BC-AgNPs hybrid films confirmed the homogeneous distribution of AgNPs within the film (Figure 1b) and by TEM we measured the diameter width of spherical shape metallic silver nanoparticles to 13±4 nm (Figure 1c). We analyzed the leaching process of BC-AgNPs hybrid films, immersing them in water for 14 days in gentle stirring (<60 rpm). We did not detect any change in the size, shape or color of the films. We semi-quantitatively measured BC-AgNPs leaching by analyzing the color change of the hybrid film by ImageJ software (grey scale) and we could not appreciate any change of color indicative of detachment of the particles from the hybrid films (Figure 1e). The content of silver on those films upon immersion was quantitatively measured by Coupled Plasma – Mass Spectroscopy (ICP-MS) and we did not observe any change. ICP-MS data confirmed that the release to the solution was of approximately 57 ppb in 14 days. Together, these data confirms the strong attachment of AgNPs to the BC matrix similar to what has been previously reported with iron oxide nanoparticles (Zeng et al., 2014). In addition, the release and degradation of the nanoparticles from the BC matrix is slow. The combination of the anti-pathogenic properties of the BC-AgNPs films and the slow release contributes to obtain a material that could be safer for the environment and more sustainable than most common pesticides used nowadays.

In order to obtain commercial products, it is important to have good reproducibility and scalability of the materials produced. We confirmed the reproducibility of 30 films

produced in 5 different batches and synthesized by different users using different techniques such as thermogravimetric analysis, TEM, SEM and color analysis.

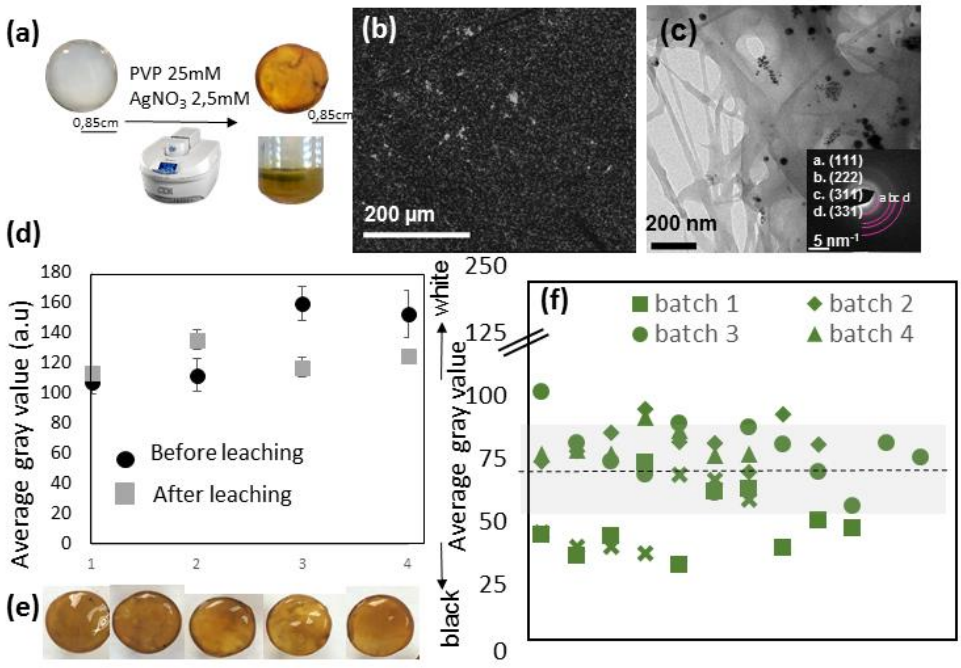

Figure 1. (a) Production of the AgNP-BC hybrid film by reduction of $AgNO_3$ assisted by microwave radiation; (b) SEM BSE image of AgNP-BC surface indicating high homogeneity; (c) TEM image and SEAD of AgNP-BC composite; (d) Qualitative measurement of the amount of Ag-NPs of the hybrids upon leaching. (e) Images of BC-AgNPs hybrids produced in the same batch. (f) Qualitative measurement of the reproducibility and amount of Ag-NPs in the BC-AgNPs hybrids from five batches. Average gray value is 69 (dashed line); ±1σ range is shaded; σ=19; n=30.

We analyzed the *in vitro* growth inhibitory effects of BC-AgNPs against a range of bacteria and fungi. We choose *Escherichia coli* as a reference species because of its known sensitivity against a wide range of antibiotics and *Pseudomonas syringae pv tomato* DC3000, causing the bacterial speck disease in tomato and a model plant pathogen. Growth inhibition of *E. coli* could be observed as a halo around a particular treatment (Figure 2a) and was quantified by measuring its diameter (1,2mm). In contrast, wet BC (BC-wet) film without AgNPs did not show any obvious inhibitory effect on bacterial growth. SEM observed higher bacterial densities in the positive control and BC-wet in comparison to the BC-AgNP treatment as shown in Figure 2b. As expected, gentamicin and $AgNO_3$ caused a transparent halo on the culture media. Figure 2c also shows that the BC-AgNPs film resulted in a transparent halo in *P. syringae*

DC3000, demonstrating that this composite is also toxic for phytopathogenic bacteria. Even though BC-AgNPs films showed a low leaching and slow release of silver, we observed those films have anti-bacterial properties.

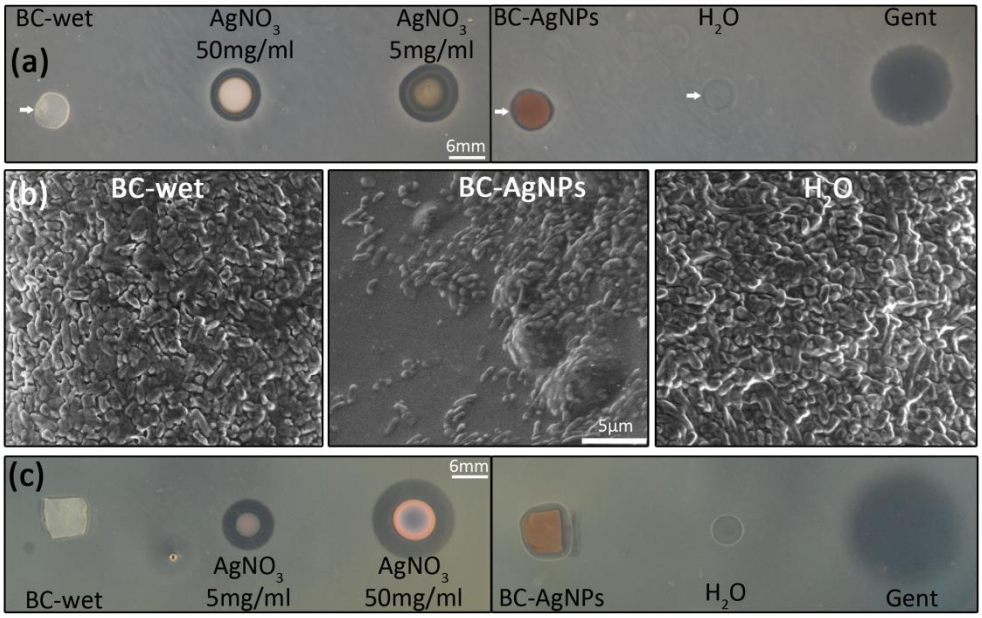

Figure 2: Toxicity assay of BC-AgNPs in bacteria (*E. coli* and *P. syringae*). (a) Toxicity assay using *E. coli*. strain OP50. Bacteria was growth in LB plate at 37ºC, and different treatments were applied: BC-wet (piece of 6 mm diameter), 5 µl $AgNO_3$ (50 mg/ml), 5 µl $AgNO_3$ (5 mg/ml), BC-AgNPs (piece of 6 mm diameter), 5 µl sterile miliQ water and 5 µl Gentamicin (10 mg/ml). (b) SEM images of BC-wet, BC-AgNPs and sterile miliQ water-treated bacteria were taken from areas pointed by white arrows. (c) Toxicity assay using *P. syringae* (DC3000). Bacteria were growth in KB plate at 28ºC, and different treatments were applied: BC-wet (piece of 6 mm diameter), 5 µl $AgNO_3$ (50 mg/ml), 5 µl $AgNO_3$ (5 mg/ml), BC-AgNPs (piece of 6 mm diameter), 5 µl sterile miliQ water and 5 µl Gentamicin (10 mg/ml). All photos were taken at 24 hours after treatment. Scale bar: 5 µm and 6 mm.

Potentially toxic effects of hybrid BC with silver nanoparticles are commonly tested only in bacteria and not assessed using fungal phytopathogens (Maneerung et al., 2008; J. Wu et al., 2014; Yang et al., 2012; Barud et al., 2011; Maria et al., 2010; Z. Li et al., 2015; J. Yang et al., 2013). Previous reports showed that bacterial cellulose-copper oxide nanocomposites had anti-microbial activity against bacteria and yeast (Araújo et al., 2017). Therefore, to determine whether hybrid films were only toxic for bacteria or their effect could be extended to unrelated phytopathogens, we tested the patches against the plant pathogenic fungus *Botrytis cinerea* (B05.10 strain), the causal agent of

gray mold disease and one of the most important fruit postharvest pathogens (Oirdi & Bouarab, 2007). The fungal mycelium was allowed to develop for 9 days (Figure 3a) and after that, spores were extracted and quantified separately from a fixed area surrounding each treatment (Figure 3b). As expected, the strongest effect was caused by the AgNPs alone due to their ability to diffuse in the medium, which inhibited fungal colonization and spore production, as it has been reported in previous publications (Villamizar-Gallardo et al., 2016; Kim et al., 2012). The BC-AgNPs also inhibited spore production ($4.75 \cdot 10^5$ spores/ml) compared to the control treatment ($3.6 \cdot 10^6$ spores/ml), and resulted in reduced fungal colonization, similar to what has been previously reported (Adepu & Khandelwal, 2018). BC-wet alone did not significantly inhibit spore formation, although fungal colonization was slightly reduced. The growth inhibition and toxicity of BC-AgNPs on the fungal mycelium can be clearly observed in the images shown in Figure 3c. The 5 mm^2 area adjacent to each different treatment (BC-AgNPs, BC-wet and untreated) was visualized using SEM. Untreated and BC-wet-treated mycelia showed no growth defects. In contrast, mycelia treated with BC-AgNPs had obvious signs of damage and cell death, with an apparent loss of turgor, deformation of the chitin cell walls and no spore production, indicating the toxicity reaction caused by the patch.

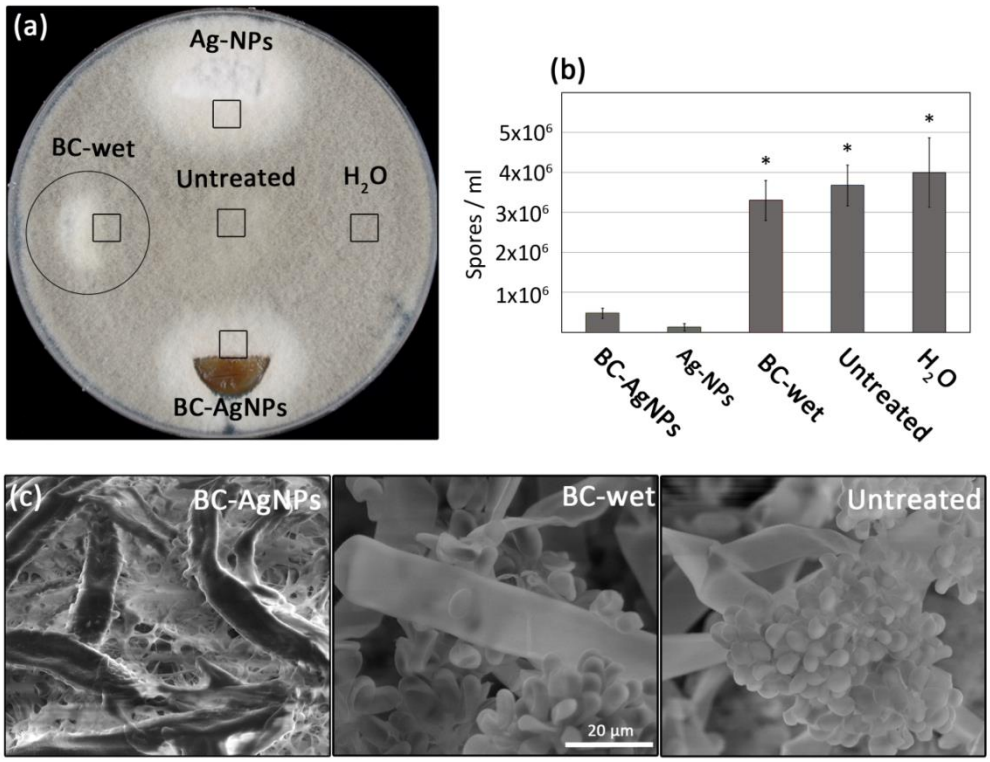

Figure 3: Toxicity assay of BC-AgNPs in *B. cinerea*. (a) Toxicity assay in PDA medium. 7,5 µl *B. cinerea* concentration 10^5 sp/ml inoculum were add in the center of the PDA plate: Top image corresponds to 15 µl AgNPs (0.53mg/ml), right image corresponds to BC-wet, left image corresponds to 15 µl sterile miliQ water and below image corresponds to BC-AgNPs. (b) Spore count using a toxicity assay plate. A piece of PDA plate of 2.7 cm diameter (marked with a circle) was excised for each treatment; BC-AgNPs, BC, AgNPs, untreated and sterile miliQ water. (c) SEM images were taken 9 days post infection (dpi) of a portion of the mycelia close to each treatment (marked with a square); BC-AgNPs, BC and untreated.

Then we evaluated the *in* vivo effects of BC-AgNPs; by infecting leaves of the model plant *Nicothiana benthamiana* with the bacterial pathogen *P. syringae* DC3000 on well-delimited 1-cm diameter areas. Then, the infected areas were left uncovered or covered for 6 days with BC film alone, or with BC-AgNPs film. *P. syringae* DC3000 caused a necrotic reaction on *N. benthamiana* in the uncovered control (Figure 4b and 4c). This reaction was mostly inhibited in the leaf area covered with BC-AgNPs, indicating that the film had a strong anti-bacterial effect on leaves. Interestingly, the BC film alone caused a slight inhibition of necrosis caused by bacterial infection. This effect might be the result of additive factors including an altered environment for the bacteria (lower oxygen availability and reduced light intensity) and the material properties (porosity,

thickness and roughness) added to the possibility that *Kx*-secreted molecules may have remained embedded in the BC matrix, providing supplementary anti-bacterial properties.

The reduction of necrosis correlated with a decrease of bacterial growth in the areas covered with BC-AgNPs and BC alone (Figure 4d). As expected, this inhibition of bacterial growth was more dramatic in BC-AgNPs than in BC-covered samples, in which only a minor, although significant, decrease of bacterial growth was observed. The anti-bacterial effect of BC-AgNPs was not restricted to N. *benthamiana* plants. We performed a *P. syringae* infection experiment using tomato, a crop of high agricultural value, observing similar effects (Figure S3). Curiously, in tomato we did not observe a significant decrease of bacterial growth in BC-treated samples.

Importantly, BC and BC-AgNP films strongly adhered when placed wet on the surface of leaves. These films stayed attached for long periods (more than 7 days) on the leaf surface under normal growth conditions (Figure 4a). In contrast, an analogous patch made of wet plant cellulose (filter paper) only stayed 1 day adhered to the leaves. As previously described, BC has high water absorbance and its composites retain this property. Therefore, we believe that the hydrogel consistency of the BC-AgNP film allows it to dry slowly; while it dries, it embeds the leaf trichomes (hair-like cells on the leaf adaxial surface) within the BC matrix, favoring the adhesion of the patches to the leaves. This strong adherence of BC may significantly contribute to the anti-pathogenic effects of the BC-AgNPs hybrid film, as it provides a stable, strongly anchored matrix in which the AgNPs can exert their toxic effect on the bacteria in close contact to the leaf, without detaching with time.

Anti-fungal activity of the BC-AgNPs and BC-wet alone in plants were tested on *N. benthamiana* leaves inoculated with a droplet of *B. cinerea* spore solution. Twenty-four hours after, the infection sites were covered with BC-AgNPs, BC-wet alone or left uncovered. After 6 days of treatment, effects were evaluated by taking pictures of the infected leaves (Figure 4e) and lesion size was measured (Figure 4f). The typical symptom caused by *B. cinerea* on *N. benthamiana* leaves is tissue necrosis, as it could be clearly observed in the uncovered control. Strikingly, the BC-AgNPs film totally inhibited the development of any visual fungal infection symptoms. In contrast, both

BC-wet and uncovered treatment did not block disease progression. This indicates that the BC-AgNPs hybrid film has also a strong anti-fungal effect on plants.

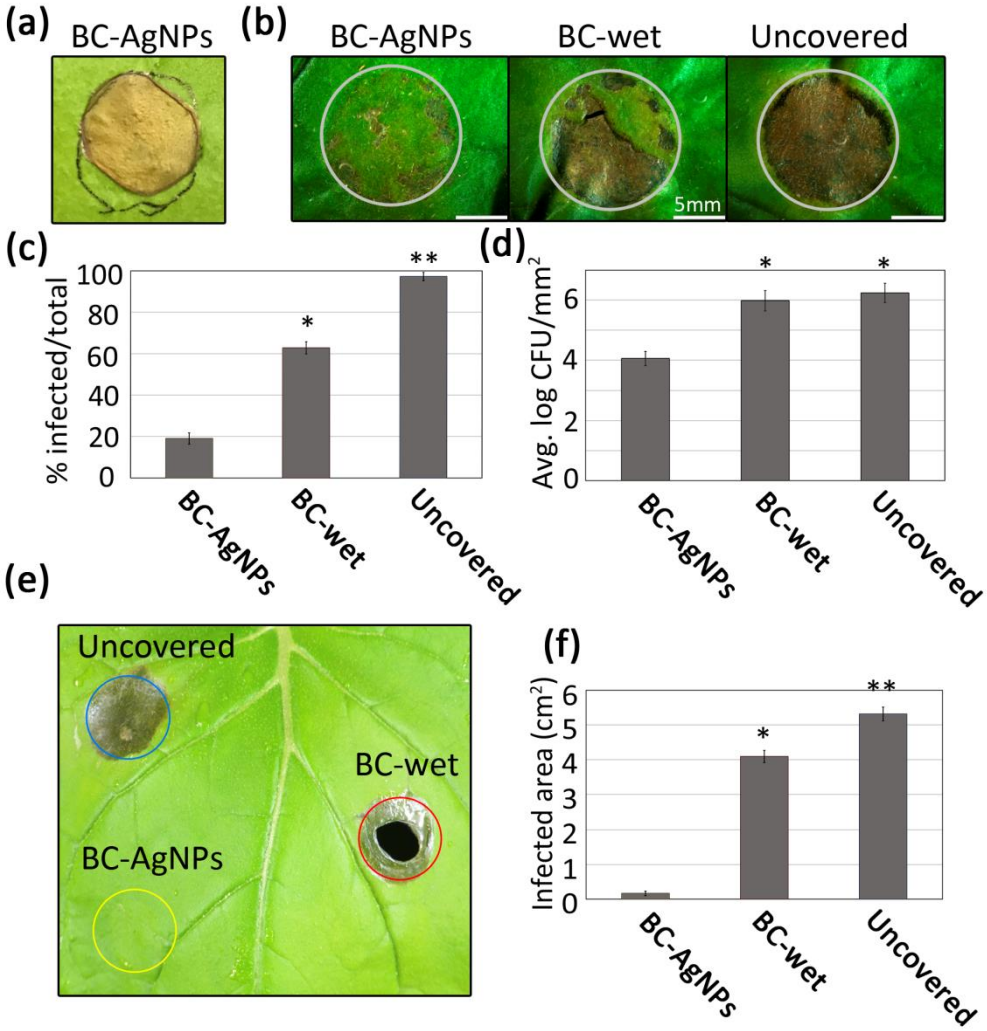

Figure 4: Anti-bacterial and anti-fungal activity of BC-AgNPs in *N. benthamiana* against *P. syringae* and *B. cinerea* (a) BC-AgNPs adhered to a *N. benthamiana* leaf (b) Three week-old *N. benthamiana* plants were infiltrated with *P. syringae* (DC3000) at an $O.D._{600}$ of 0.0008. After infiltration infected areas were covered with different treatments: BC-AgNPs, BC or left uncovered. Photos were taken 6dpi. (c) The area of necrotic tissue was measured with the ImageJ software at 6dpi d) Bacterial growth within a 1 cm-diameter infected area was measured as the average of colony forming units (CFUs) (logarithmic scale) per square millimeter of infected tissue. (e) Three week-old *N. benthamiana* leaves were infected with a 5 µl drop of 10^5 *B. cinerea* spores/ml and kept under 100 % humidity. After 24 h infected areas were covered with BC-AgNPs, BC-wet or left uncovered. After 6dpi the treatments were removed and digital

pictures were taken. f) The area corresponding to the necrotic tissue was measured with ImageJ software at 6dpi.

The anti-pathogenic effect of BC-AgNPs could occur as a result of pathogen growth inhibition or by an enhancement of the plant defenses. To test a potential immune boosting effect of BC-AgNPs on bacterial infection, we quantified the expression of *PATHOGENESIS-RELATED 1a* (*PR1a*), a plant defense marker gene (Ward et al., 1991) *PR1a* was expressed in BC-AgNPs -treated infected tissue, although to very low levels, 18 times lower than the uncovered control (Figure 5a). The BC-AgNPs patch strongly inhibited pathogenic bacteria perception and the subsequent immune response of the plant. BC-wet film alone also caused partial inhibition of *PR1a* expression to approximately 1.6 times lower than untreated leaf levels. This result correlates with the decreased extent of pathogen-triggered necrosis observed upon infection in BC-AgNPs-covered leaf areas when compared to the untreated control (Figure 5a and 5e).

In parallel, we analyzed gene expression profiles of *HOMEOBOX 1* (*HB1*) and *HARPIN-INDUCED GENE* (*HIN1*) after fungal infection with *B. cinerea*. *HBI* is a gene which is expressed in pathogen-induced cell death and its expression is dependent on jasmonic acid signaling, which is activated upon necrotrophic fungal infection (Yoon et al., 2009). On the other hand, *HIN1* is a marker of pathogen-triggered cell death (Pontier & Tronchet, 1998). Figure 5b shows that these genes are upregulated in inoculated tissue that was either uncovered or covered with tape, indicating pathogen perception and response by the plant. In contrast, BC-AgNPs-covered tissue shows minor upregulation of the two marker genes, suggesting that BC-AgNPs may directly inhibit *B. cinerea* infection, previous to the activation of the plant immune system. This indicates that fungal growth arrest may occur at very early stages of infection.

Recognition of a pathogen by a plant results in a rapid burst of reactive oxygen species (ROS), which can be measured as an output of plant defense responses (Torres, 2010). Previous reports showed also an increase of ROS upon exposure of AgNPs to some plants (Pratley & Haig, 2018). Production of hydrogen peroxide (H_2O_2), one of the main ROS produced by the plant upon pathogen infection, was visualized in leaf areas infected with *P. syringae* DC3000 using 3, 3 –diaminobenzidine (DAB) staining. Figure 5c-d clearly shows that infection results in accumulation of H_2O_2 in uncovered tissue, when compared to uninfected or mock-inoculated leaf tissue ($MgCl_2$). In contrast, *P. syringae*-inoculated tissue covered with BC-AgNPs displays a drastic reduction on

H_2O_2 accumulation. This observation corroborates the previous findings indicating that defense responses are not induced in inoculated tissue covered with BC-AgNPs. Together, these data corroborate that the anti-bacterial effect of BC-AgNPs does not result from enhanced plant defense responses. BC-wet film alone did not prevent ROS accumulation in the inoculated tissue, which is not surprising, considering that the extent of bacterial growth inhibition caused by this film is minor when compared to BC-AgNPs. Previous reports indicated an increase of ROS caused by nanoparticle exposure, potentially harmful for living cells and tissues. The fact that the leaf treatment with the BC-AgNPs hybrid does not result in ROS production might constitute another indication that AgNPs are not released from the BC matrix, avoiding any effects derived from AgNPs treatment alone and preventing their release to the environment".

ROS produced as a result of *B. cinerea* infection were absent in the BC-AgNPs-covered sample; in contrast to inoculated samples covered with BC-wet which showed ROS production levels comparable to those of the uncovered control (Figure 5e and 5f).These data corroborate our previous observation indicating that BC-AgNPs completely blocks fungal invasion at very early stages. Thanks to this rapid elimination of the pathogen, the plant does not even perceive it and thus, unnecessary defense reactions are prevented.

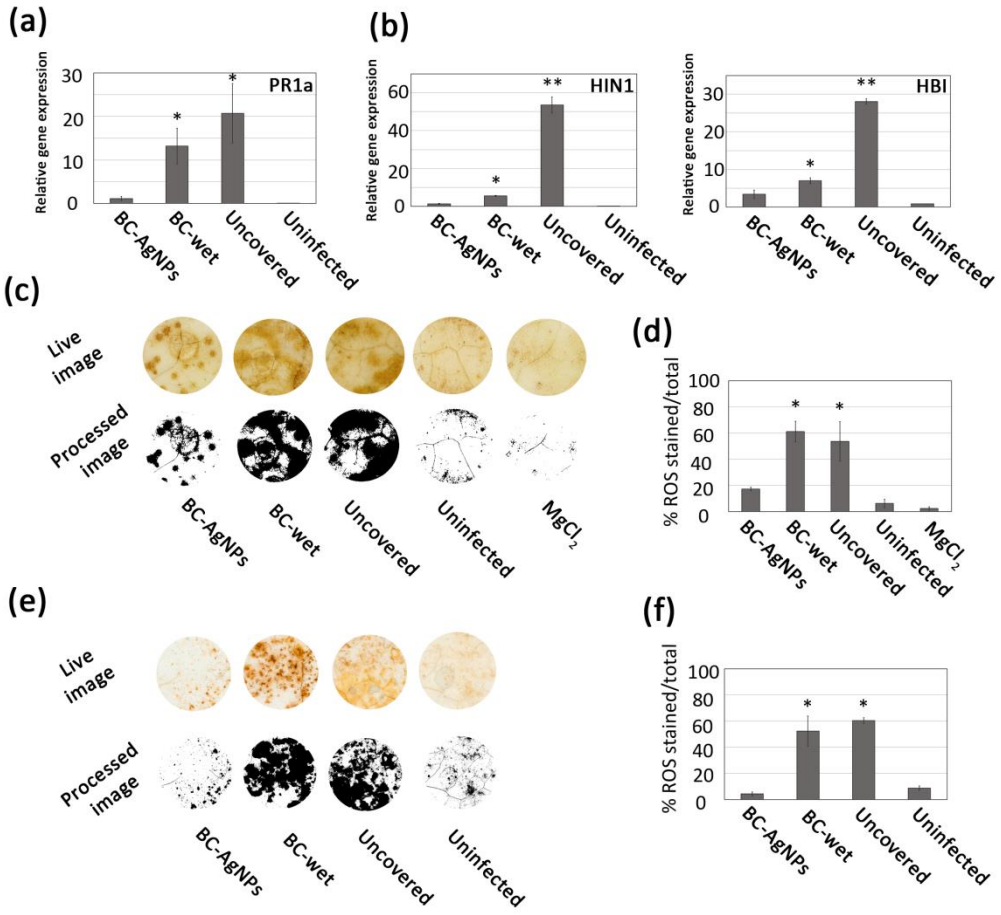

Figure 5: Defense molecular markers and reactive oxygen species (ROS) (a-b) Quantitative PCR (qPCR) analysis of defense marker genes. Three week-old N. benthamiana plants were infiltrated with (a)P. syringae DC3000 at an O.D.600 of 0.001, (b)Three week-old plants were sprayed with either 105 spores/ml of B. cinerea and keep for 24 hours under 100% humidity.Then, the infected zones were covered with the different treatment (BC-AgNPs, BC-wet and uncovered) during 12 hours and then RNA was extracted. qPCR was performed with specific primers for N. benthamiana (a) PR1a, (b) HIN1, HBI and Tubulin (control) genes as described in Material and Methods. (c) to (f) ROS production analysis. (c) Three week-old *N. benthamiana* leaves were infected with *P. syringae* DC3000 (*avrRpm1*) at an $O.D._{600}$ of 0.01 and then covered with: BC-AgNPs and BC or left uncovered. As a negative control uninfected tissue was used. After 12 hpi the infected zones with different treatments were stained using the H_2O_2 stain 3,3′-diaminobenzidine (DAB). Stained leaves were imaged using a digital camera. (d) Quantification of the images shown in (c) as the percentage of DAB stain present using the Image J software. (e) Three week-old *N. benthamiana* leaves were infected with *B. cinerea* at 10^5 spores/ml concentration and keep for 24 hours under 100% humidity. Then, the infected zones were covered with BC-AgNPs, BC-wet and uncovered and after 12 hpi. The infected

zones and uninfected control were stained using DAB and images were taken using a digital camera. Previously staining leaves were processed with ImageJ. (f) Quantification of the images shown in (e) as the percentage of DAB stain present using the ImageJ software.

In summary, we have developed environmentally friendly nanocomposite patches based on bacterial cellulose and silver nanoparticles in a reproducible and scalable manner; with positive results against the bacteria *Escherichia coli* and *Pseudomonas syringae* and the fungus *Botritis cinerea.* Thanks to their hydrogel-like consistency, we obtained a strong adherence to *N. benthamiana* leaves inoculated *B. cinerea* spore solution. We confirmed the pathogen inhibitory properties of the material by quantitative gene expression profiling of various plant defense marker genes, and by reactive oxygen species quantification in the inoculated tissue, showing no defense response activation probably due to an early neutralization of the pathogen on site by the nanocomposite. The slow release of silver nanoparticles from the bacterial cellulose makes this material potentially safer for the environment than most current pesticides. Thus, this bacterial cellulose silver nanoparticle composite shows promise as a new generation pesticide, potentially overcoming bottlenecks to increase efficacy and efficiency of current foliar pesticides.

Materials and Methods

Production of BC films

Bacterial strain of *Komagataeibacter xylinus*, (*Kx*) (ATCC 11142) was obtained from CECT (Spanish Type Culture Collection, Spain). Glucose, peptone, yeast extract and agar were purchased from Conda lab, NaOH, $Na_2HPO_4 \cdot 12H_2O$ and citric acid monohydrate were bought from Sigma-Aldrich and used as received. Liquid HS culture media(Zeng, Laromaine Sagué, et al., 2014) for *Kx* consisted of 20 g/L glucose, 5 g/L peptone, 5 g/L yeast extract, 1.15 g/L citric acid monohydrate and 6.8 g/L $Na_2HPO_4 \cdot 12H_2O$ in distilled (DI) water. Solid media for *Kx* was obtained adding 15 g/L agar to liquid media. *Kx* was grown on solid agar at 30ºC and for the pre-inoculum 4 single colonies were picked out, and each one was transferred into a test tube with 5 mL of liquid culture media and let grown for 3 days at 30 ºC under static conditions. Then, 20 ml of the *Kx* suspension cultures were transferred to an Erlenmeyer flask containing 280 mL of HS liquid media and gently mixed, obtaining the inoculum. Then, 2 mL of this inoculum solution were transferred to each well of a 24-well culture plate (Thermo

Fisher Scientific, USA) and kept at 30ºC. Thin films of BC grew on the surface of the liquid media in each well and they were harvested after 3, 6 or 8 days of culture. BC films harvested from the air/liquid interface were immersed in DI water:ethanol (1:1) for 10 minutes. Then, they were transferred to DI water and boiled for 40 minutes, then boiled two more times with 0.1 M NaOH at 90°C for 20 minutes, and finally, neutralized with DI water twice until neutral pH was reached.

After 3 and 6 days of culturing *Kx*, we obtained BC films with an averaged thickness of 1.5±0.2 mm (n=60) measured by a digital micrometer and a density of 8.2±0.6 g/m^2 (n=4). Their thickness and density of BC films was not substantially modified with time. However, the thickness of BC films grown up to 8 days computed for 1.8±0.4 mm (n=3) (Figure S1e). BC films used were grown for 6 days if not stated otherwise. BC films were used as never-dried and we will refer to them to as BC-wet; otherwise they were dried at room temperature (BC-RT) until complete dryness and its use will be stated explicitly in the text. Figure S1.

Synthesis of BC-hybrids

Silver nitrate BioChemica ($AgNO_3$) precursor, acetone technical grade and ethylene glycol (EG) pure were purchased from AppliChem Panreac. and polyvinyl pyrrolidone (PVP) with average molecular weight 10 kDa was purchased from Sigma-Aldrich and all used as received.

BC-AgNPs hybrids were synthesized by *in situ* reduction of $AgNO_3$ by microwave-assisted method using a CEM Discover focused microwave oven. 2 mL of 2.5 mM $AgNO_3$ (aq) and 2 mL of 25 mM PVP (aq) (capping agent) were transferred to a 10-mL, borosilicate glass microwave (MW) tube and sonicated for 5 minutes. Then a BC film was added to the tube and was fully impregnated with the precursors' solution. The solution was heated in the MW oven for 10 minutes at 120ºC, radiation frequency of 2.45 GHz and maximum power of 300 W. BC films changed color from translucent white to dark brown indicating the incorporation of the AgNPs in the cellulose network, and the solution turned dark brown. The BC-AgNPs hybrid films were harvested from the solution, profusely rinsed with acetone and water and stored in DI water. AgNPs in suspension were separated adding 20 mL of acetone with 10 µL of PVP and centrifuged at 6000 rpm for 10 min, twice. The AgNPs were re-dispersed in 2 mL DI water and 10 µl PVP.

We previously reported the *in situ* microwave assisted thermal decomposition process to synthesize iron oxide nanoparticles onto the cellulose fibers. Those nanoparticles were also strongly anchored and we did not observed leaching for more than 2 months.(Zeng, Laromaine, Feng, et al., 2014) We postulated that microwave radiation selectively heated the hydroxyl groups in the cellulose backbone promoting those spots as the anchoring points to synthesize the nanoparticles. We hypothesized that a similar mechanism could take place in the case of BC-AgNPs hybrid, providing a strong link of the nanoparticles to the cellulose matrix.

Characterization of BC and BC composites films

Bacterial cellulose thickness

BC-wet thickness (never-dried films) was measured with QuantuMike Micrometer (Mitutoyo America Corporation, sensitivity of 0.001 mm). The BC film was placed between two glass slides and then measured with the micrometer. Since BC is spongy, the measure ended when the film started to oppose to compression. Thickness of the glass slides was subtracted.

Ultraviolet-Visible spectroscopy (UV-Vis)

UV-Vis absorbance spectrum of BC-wet films, BC-AgNPs hybrids films and AgNPs suspensions were obtained with a UV-Vis-NIR spectrophotometer Varian Cary 5000 in the wavelength range from 300 to 800 nm. AgNPs suspensions were sonicated for 5 minutes and measured in 1-cm wide quartz cuvettes. Films were sandwiched vertically between a holed metal plate and a glass slide cover. DI water was used as a blank for suspensions and a BC-wet film for BC-AgNPs hybrid films.

Transmission Electron Microscopy (TEM)

BC-AgNPs hybrid films were dried and obliquely cut with a scalpel in a 1x2 mm rectangle size, deposited on the copper grid and placed in the TEM sample holder with a TEM grid onto them. TEM images were obtained with the JEOL 1210 electron microscope operating at 120 kV. AgNPs mean size and standard deviation was measured using Image J software, computing 420 nanoparticles. The resulting size histogram was fitted to a Gaussian function.

TEM images indicated that the AgNPs were a bit larger in suspension (39±12 nm, n=193) than in the hybrid films (13±4 nm, n=206) (Figure S2). Peaks at 411 nm and 419

nm in the UV-Vis spectrum confirmed the presence of the AgNPs in the films and in solution, respectively. The red-shift agrees with the increase of size of the NPs suspended in the solution compared to the BC-AgNPs hybrid films (Figure S1g). FTIR-ATR analysis of the samples confirmed the presence of characteristic peaks corresponding to cellulose, AgNPs and the surfactant PVP (Figure S1h).

Scanning Electron Microscopy (SEM)

BC and BC-AgNPs hybrids were cut in a 0.5x0.5 cm^2 piece and placed on a SEM aluminum stub covered with a carbon tape adhesive. Samples were imaged with the QUANTA FEI 200 FEG scanning electron microscope under low-vacuum conditions, an acceleration voltage of 10 kV, an electron beam spot of 3.5, a water steam pressure of 60 Pa, and a working distance of 8-10 mm.

For the analysis of the mycelium of *B. cinerea* and *E. coli* the samples from the toxicity experiments were used. Samples were not treated. They were imaged under the environmental SEM mode (ESEM) conditions, an acceleration voltage of 10-15 kV, an electron beam spot of 3.5-4, a water steam pressure of 13-31Pa, and a working distance of 8-10.1 mm.

Thermogravimetric Analysis (TGA)

BC-AgNPs hybrids were cut and weighed before the analysis. TGA of the BC-AgNPs hybrid films was performed with the TGA-DSC/DTA analyzer (model STA 449 F1 Jupiter from NETZSCH) supplier at a heating rate of 10 °C/min from room temperature to 800 °C in air. For calculations, the mass at 120ºC was used as a reference to ensure that water was not affecting the weight value.

Previously, we reported the scalability and reproducibility of the *in situ* microwave thermal decomposition reaction for the synthesis of iron oxide nanoparticles.(Gonzalez-Moragas et al., 2015) We confirmed the production of BC-AgNPs hybrid films in a reproducible manner and up to 6 BC-AgNPs hybrid films in a single batch. We analyzed the reproducibility of 30 films produced in 5 different batches and synthesized by different users. We compared by color analysis the content of AgNPs within the films (Figure 1f). In all cases, the BC-AgNPs hybrid films were homogeneous and the content of AgNPs were similar within a narrow dispersion of color (Figure 1e).

Thermogravimetric analysis allowed us to compute the load of AgNPs being a 2.5% of the total weight (35 µg AgNPs) and this was also confirmed by ICP-MS 34±1 µg.

Inductively Coupled Plasma – Mass Spectroscopy (ICP-MS)

BC-AgNPs hybrid stability was assessed by detecting Ag leached from films under agitation conditions with ICP-MS analytical technique. The value obtained includes AgNPs or Ag+ released from degradation of the nanoparticles. The samples were prepared by adding one hybrid to 8 ml of DI water in a vial and stirring it at low rate (<60 rpm) for 14 days. The vial was tightly covered with aluminum foil to avoid photoreduction of possible released silver species. The solution was then filtered with a 0.42 µm syringe filter to remove fibers and stored in a new covered vial. The ICP_MS equipment used was the AGILENT model 7500ce.

Fourier Transformed InfraRed spectroscopy (FTIR)

FTIR analysis was performed to determine the chemical structure of BC. The Samples analyzed were BC-RT and BC-AgNPs. They were folded five times to increase the total signal intensity, and placed over the Universal Diamond ATR top-plate (Perkin-Elmer) and compressed with a force of 120 pN (90%). Readings were performed with a FTIR Perkin-Elmer Spectrum One spectrophotometer. The FTIR spectra were examined in a mid IR range (4000-450cm^{-1}) with a working range of 450 to 4000 cm^{-1} and a U-ATR resolution of 4 cm^{-1}. A number of 4 scans per sample was taken.

Dynamic Light Scattering (DLS)

Samples of the suspensions of AgNPs obtained were dispersed in water and sonicated for 10 minutes to achieve highly diluted samples. The measurement of the NPs hydrodynamic size distribution was performed in water at 25ºC with a Zetasizer Nano ZS (Malvern Instruments).

Image Analysis

The ImageJ software (v.1.50i; National Institutes of Health, Bethesda, MD, USA) was used for image analysis. The processed images were converted to a greyscale, 8-bit image, and then analyzed as white color (255) and black color (0).

Biological Material and Growth Conditions

Plants

All pathogenicity tests were performed on *Nicotiana benthamiana* plants. *N. benthamiana* seeds were sown on 5" plastic pots filled with sphagnum peat substrate (Gramoflor, profi-substrat, Spain) and allowed to germinate for a week under constant conditions 50-60% humidity and a long day photoperiod (16h light / 8h dark) with 23-26ºC during the light period and 21-22ºC during the dark period. A week later plantlets were transferred individually to 5" pots filled with sphagnum peat substrate and grown under the above mentioned conditions for 3 more weeks.

Bacterial infection were performed also in tomato (*Solanum lycopersicum*) var. Marmande plants. *Tomato* seeds were grown on 7x7 cm pots with sphagnum peat substrate (Gramoflor, profi-substrat, Spain) under costant conditions 50-60% humidity and long day photoperiod (16h light / 8h dark) with 22-23ºC during 3 weeks.

Pathogens

Escherichia coli strain (OP50, uracil auxotroph) was purchased from Caenorhabditis Genetics Center (CGC) from the University of Minnesota (EEUU) and grown at 37ºC in Luria-Bertrani (LB) broth at 200 rpm or on petri dishes filled with LB agar. *Pseudomonas syringae pathovar (pv) tomato* strains DC3000 were grown in King´s B (KB) with bactoagar (Becton Dickinson, EEUU) at 28ºC. *Botrytis cinerea* strain (B05.10) was grown in Potato Dextrose Agar (PDA) (Becton Dickinson, EEUU) at 23ºC in dark conditions.

Toxicity experiments

To test their growth inhibitory effect on bacteria, we placed a circle of 6 mm diameter BC-AgNPs on top of a plate containing *E. coli* grown to confluence. As positive controls, we used 5 µl of $AgNO_3$ at 5 and 50 mg/ml and 5 µl of gentamicin at 10 mg/ml. As negative controls, we used the same size of a BC-wet film and 5µl of sterile Milli-Q water. In the case of *P. syringae* we used a square of 0.5x0.5 cm of BC-AgNPs and BC.

Bacteria

E. coli was streaked on a LB agar plate and grown overnight. A single colony was transferred to 2 ml of LB broth and grown overnight in agitation. The bacterial

suspension was diluted to O.D.$_{600}$ 0.5 and 1.5 ml was plated on a LB agar plate (120 x 120 mm) using sterile crystal balls. The plated bacterial suspension was allowed to dry for 30 minutes. The following treatments were applied to the plate: 5 µl of filter-sterilized gentamicin (AppliChem, EEUU) (10 mg/ml), 5 µl of sterile miliQ water, 5 µl of filter-sterilized $AgNO_3$ (50 and 5 mg/ml), a circle of 6 mm diameter BC film and a circle of 6 mm diameter BC-AgNPs film. The plate was incubated overnight at 37ºC and after that time, the growth inhibitory effect of the different treatments was visually evaluated after digital photographs were taken.

P. syringae (DC3000) was streaked on a KB selective agar plate containing rifampicin (AppliChem, EEUU) (50 µg/ml) and kanamycin (AppliChem, EEUU) (50 µg/ml) and grown overnight at 28ºC. Bacteria were scraped from the plate with a sterile spreader, plated onto a fresh KB agar selective plate and grown overnight at 28ºC. Bacteria were then resuspended with 10 ml of 10 mM $MgCl_2$, transferred to a flask containing 150 ml of 10 mM $MgCl_2$ and incubated in agitation (150 rpm) at room temperature for 5 minutes. Then, a bacterial suspension at an OD_{600} of 0.5 was prepared, and 1.5 ml was plated onto a KB agar selective plate (120 x 120 mm) using sterile crystal balls and allowed to dry for 30 minutes. After that, the same treatments described above to assess toxicity, except the BC and BC-AgNPs that were a 0.5cm^2 square, were applied onto the plate, following an overnight incubation at 28ºC. The growth inhibitory effect of the different treatments was evaluated visually after digital photographs were taken.

Fungi

A 7.5 µl drop of $1 \cdot 10^5$ spores/ml of *B. cinerea* (B05.10) was placed on the center of a PDA plate. After that, the treatments; 15 µl AgNPs (0.53mg/ml), 15 µl sterile MiliQ water, BC-AgNPs and BC-wet were immediately applied onto the plate, following an incubation step at 23ºC for 9 days to allow the development of the fungal mycelium. The growth inhibitory effect of the different treatments was analyzed by excising agar plugs of 2.7 cm diameter around each treatment. These plugs were placed into 50 ml tubes containing 5 ml of sterile ultra-pure water. The tubes were vortexed 2 min to release the spores from the mycelium and filtered using Miracloth™ paper (Calbiochem, EEUU). The spores were diluted ten times and finally, the spores of different treated areas were counted using a Neubauer chamber (Marienfeld, Germany) under an optical microscope (Leica DM LB, Germany).

Anti-bacterial activity in *N. benthamiana* leaves

To prepare *P. syringae* for leaf inoculation, bacteria were processed as described above for toxicity assays, but in the final dilution step, $O.D._{600}$ was adjusted to 0.0008. Three-week-old *N. benthamiana* leaves were infiltrated with a syringe on three different points of the reverse side of a fully expanded leaf. The infiltrated area was of a smaller diameter than the BC films (1.7 cm). Infiltrated areas were covered with BC-AgNPs, BC-wet alone or left uncovered. Seven days later, leaves were photographed and 1 cm leaf disks corresponding to the inoculated areas were extracted using a cork borer to perform the different analyses described.

Anti-bacterial activity in *tomato* leaves

P. syringae bacteria were processed as described above for toxicity assays, but in the final dilution step, $O.D._{600}$ was adjusted to 0.0008. Three-week-old *tomato* leaves were infiltrated with a syringe on three different points of the reverse side of leaf. The infiltrated area was of a smaller diameter than the BC films (1.7 cm). Infiltrated areas were covered with BC-AgNPs, BC-wet alone or left uncovered. Five days later, leaves were photographed and 0,6 cm leaf disks corresponding to the inoculated areas were extracted using a cork borer to perform the different analyses described.

Bacterial growth curves

Three leaf disk replicates from each type of inoculated sample (covered with BC-AgNPs, BC-wet alone or uncovered) were placed in 1.5 ml tubes containing 500 µL of 10 mM $MgCl_2$ and were ground using an electric tissue homogenizer (Potter, B. Braun-Biotech SA, Spain). Serial 10-fold dilutions were plated on selective KB agar plates and incubated at 28ºC for 48 hours. The number of colonies were counted and the $\log(CFU/mm^2)$ leaf tissue was calculated according to(Y. Zhao et al., 2003).

Anti-fungal activity in *N. benthamiana* against *B. cinerea*

Three week-old fully-expanded *N. benthamiana* leaves were inoculated with a 10 µl drop of a *B. cinerea* spore suspension containing $1 \cdot 10^5$ spores/ml. Plants were then

grown for 24 h under 100% relative humidity at a constant temperature of 23ºC and a long-day photoperiod (16h light / 8h dark). Then, inoculated areas were covered with BC-AgNPs film, BC-wet film alone or left uncovered after 24 hours of inoculation. Subsequently, the films were removed after 4 days of infection. Then, pictures were taken and 1 cm leaf disks corresponding to the inoculated areas were extracted using a cork borer to perform the different analyses described.

Quantitative reverse transcriptase-polymerase chain reaction (RT-qPCR)

RNA was extracted from *N. benthamiana* leaves using Maxwell 16 LEV Plant RNA Kit (Promega, Australia) according to the manufacturer´s recommendations. RNAs were treated with DNase-free RNase (Promega, Australia). cDNA was synthesized from 2 µg RNA using High Capacity cDNA Reverse Transcription Kit (Applied Biosystems, USA). Melting curves were determined using the software LightCycler V1.5 (Roche, Switzerland). This software was used to detect the amplification level and was programmed with an initial step of 10 min at 95ºC followed by 45 cycles using 95ºC during 10 sec, 60ºC during 30 sec and 72ºC during 30 sec. All samples were run in 3 technical replicates for each 3 biological replicates, and the average values were used for quantification. The relative quantification of target genes were calculated using the Light Cycler V1.5 software (Roche, Switzerland) and the values of target genes were normalized to an endogenous control gene (*N. tabacum* tubulin beta-2 chain; LOC107775153).

Reactive oxygen species (ROS) staining with 3,3'-Diaminobenzidine (DAB)

N. benthamiana leaf disks were stained with 3,3'-Diaminobenzidine (DAB) to detect H_2O_2, following the protocol described in this publication.(Torres, Dangl, & Jones, 2002) Three week-old fully-expanded *N. benthamiana* leaves were used for the staining. 40 mg of DAB were added in a 50-ml tube with 40 ml of distilled water and 16 µl of HCl 37% (Sigma, EEUU) to lower the pH. Then, the tube was covered with aluminum foil and incubated 1 h at 37ºC on the shaker until the solution turned yellow-red in color. After that, 4-5 leaves per treatment were placed in a capped syringe with both ends closed. Vacuum was applied to the solution by pulling the plunger 4 times. Leaves were then transferred to a closed dark plastic box on top of paper towels saturated with DI water and kept for 7-8h at RT. After that, leaves were transferred to a 15 ml tube

containing the de-staining solution (Ethanol: Lactic acid: Glycerol, 3:1:1) and shaken at room temperature overnight. Leaves were then photographed using a digital camera.

Quantification and Statistical Analysis

All statistical analyzes were carried out using an ANOVA ($p < 0.05$, $\alpha = 0.05$).

Supplementary information

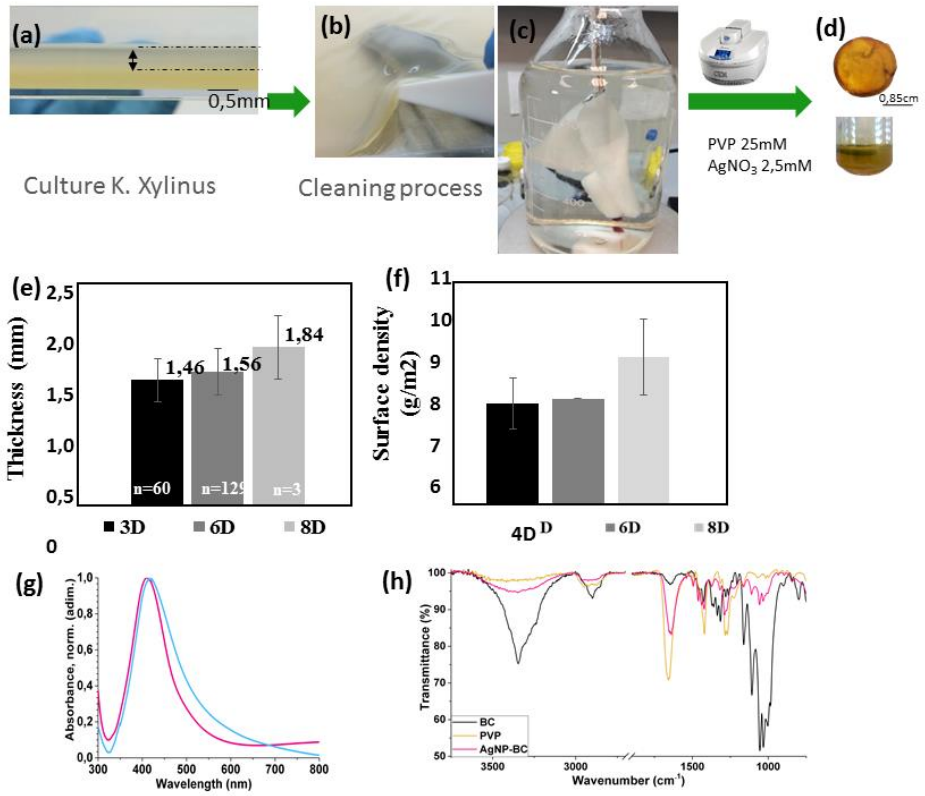

Figure S1: Process to produce Bacterial Cellulose films. (a) BC films were grown in the bacterial media after different days at 30ºC. (b) BC films harvested from the air/liquid interface were immersed in DI water:ethanol (1:1) for 10 minutes. In this picture we can visualize the texture of hydrogel of the BC films. (c) Process of cleaning of the BC films. Then, they were transferred to DI water and boiled for 40 minutes, two more times with 0.1 M NaOH at 90°C for 20 minutes, and finally, neutralized with DI water twice until neutral pH is reached. (d) Then AgNPs were synthesized on the films by thermal decomposition reaction assisted by microwave. (e) Measurement of the thickness of the bacterial cellulose film after 3, 6 and 8 days of culture; measured by a micrometer. (f) Evaluation of the changes by surface density (g/cm^2). (g) UV-Vis spectrum of the composite (blue) and the suspension (pink); (h) FTIR-ATR spectrum of the BC film (black), AgNP-BC hybrid (pink) and PVP,10k (yellow).

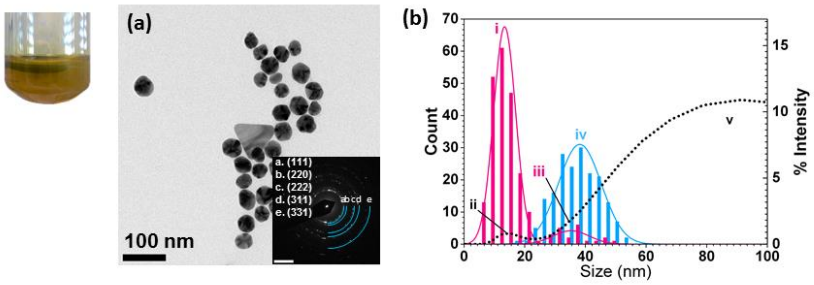

Figure S2: (a) TEM measurement of the size and shape of the AgNPs produced while generating BC-AgNPs hybrids. (b) NP size distribution in the composite (blue) and the suspension (pink) and, in the right axis, DLS measure of AgNPs' hydrodynamic diameter in suspension (black spotted line).

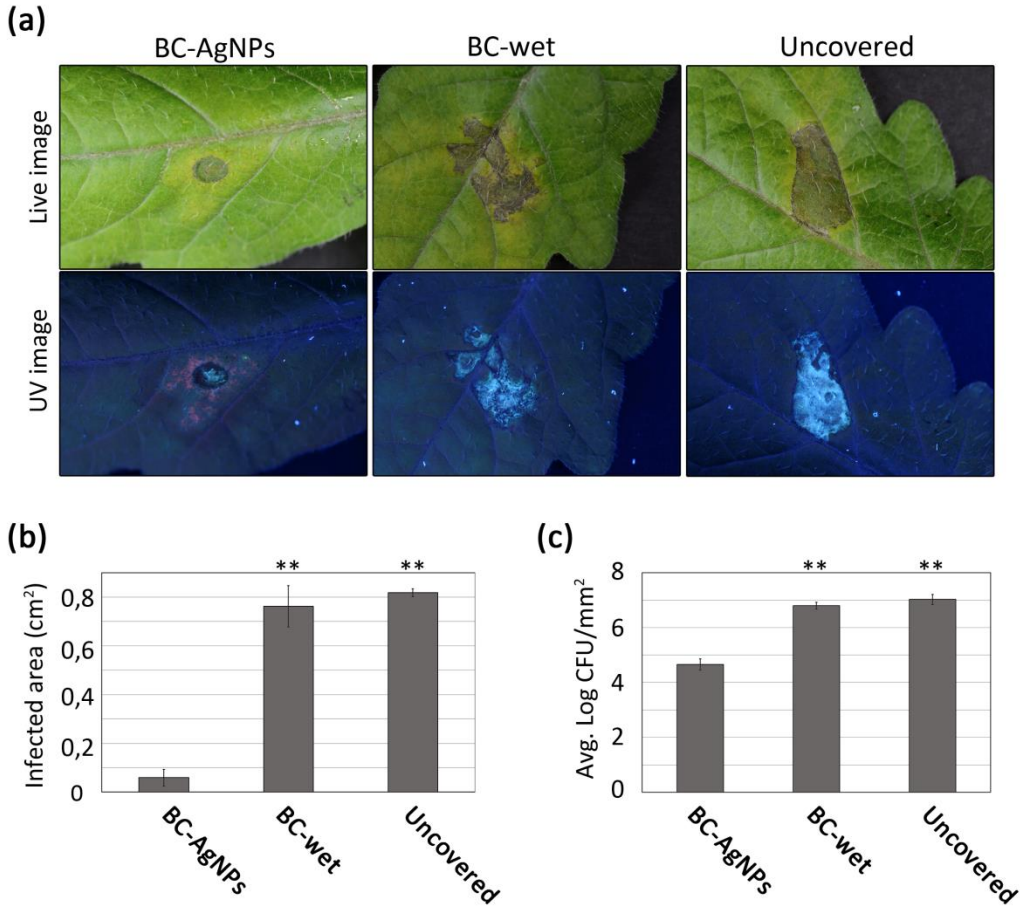

Figure S3: Anti-bacterial activity of BC-AgNPs in tomato (*Solanum lycopersicum* variety Marmande) (a) Three-week-old *tomato* plants were infiltrated with *P. syringae* (DC3000) at an $O.D._{600}$ of 0.0008. After infiltration, the infected areas were covered with different treatments: BC-AgNPs, BC-wet or left uncovered. Photos were taken 5dpi. Cell death was visualized with UV light. (b) The necrotic tissue areas were measured using ImageJ software at 5dpi (c) Bacterial growth within a 0,6 cm-diameter infected area was measured as the average of colony forming units (CFUs) (logarithmic scale) per square centimeter of infected tissue.

Conflicts of interest

There are no conflicts of interest to declare.

Acknowledgements

We acknowledge financial support from the Spanish Ministry of Economy and Competitiveness (MINECO) with grants 2016-78002-R (AGL) and RyC 2014-16158 (NSC), MAT2015-64442-R, FIP and through the "Severo Ochoa Programme for Centres of Excellence in R&D" (SEV-2015-0533 and SEV-2015-0496). This work was also supported by the CERCA Programme / Generalitat de Catalunya, the Generalitat de Catalunya for the 2017SGR765 project. The authors would like to thank all members of the "bacterial plant diseases and cell death" lab for helpful comments.

Bibliography

Adepu, S., & Khandelwal, M. (2018). Broad-spectrum antimicrobial activity of bacterial cellulose silver nanocomposites with sustained release. *Journal of Materials Science*, *53*(3), 1596–1609. https://doi.org/10.1007/s10853-017-1638-9

Agency, U. S. E. P. (1992). Silver in Business. Retrieved from http://www.empower-yourself-with-color-psychology.com/silver-in-business.html

Agrios, G. N. (2005). *Plant Pathology. Quinta edición. Academic Press. Nueva York.*

Araújo, I. M. S., Silva, R. R., Pacheco, G., Lustri, W. R., Tercjak, A., Gutierrez, J., … Barud, H. S. (2017). Hydrothermal synthesis of bacterial cellulose–copper oxide nanocomposites and evaluation of their antimicrobial activity. *Carbohydrate Polymers*, *179*(2018), 341–349. https://doi.org/10.1016/j.carbpol.2017.09.081

Barud, H. S., Regiani, T., Marques, R. F. C., Lustri, W. R., Messaddeq, Y., & Ribeiro, S. J. L. (2011). Antimicrobial bacterial cellulose-silver nanoparticles composite membranes. *Journal of Nanomaterials*, *2011*. https://doi.org/10.1155/2011/721631

Boateng, J., & Catanzano, O. (2015). Advanced Therapeutic Dressings for Effective Wound Healing - A Review. *Journal of Pharmaceutical Sciences*, *104*(11), 3653–3680. https://doi.org/10.1002/jps.24610

De Moura, M. R., Mattoso, L. H. C., & Zucolotto, V. (2012). Development of cellulose-based bactericidal nanocomposites containing silver nanoparticles and their use as active food packaging. *Journal of Food Engineering*, *109*(3), 520–524. https://doi.org/10.1016/j.jfoodeng.2011.10.030

FAO. (2014). *Food and Agriculture Organization, the international code of conduct on pesticide management*.

Gonzalez-Moragas, L., Yu, S. M., Murillo-Cremaes, N., Laromaine, A., & Roig, A. (2015). Scale-up synthesis of iron oxide nanoparticles by microwave-assisted thermal decomposition. *Chemical Engineering Journal*, *281*, 87–95. https://doi.org/10.1016/j.cej.2015.06.066

Hajipour, M. J., Fromm, K. M., Akbar Ashkarran, A., Jimenez de Aberasturi, D., Larramendi, I. R. de, Rojo, T., … Mahmoudi, M. (2012). Antibacterial properties of nanoparticles. *Trends in Biotechnology*, *30*(10), 499–511. https://doi.org/10.1016/j.tibtech.2012.06.004

Heredia, A., Jiménez, A., Guillén, R., & Guillénn, R. (1995). Composition of plant cell walls. *Zeitschrift Für Lebensmittel-Untersuchung Und -Forschung*, *200*(1), 24–31. https://doi.org/10.1007/BF01192903

Hestrin, S., & Schramm, M. (1954). Synthesis of cellulose by Acetobacter xylinum. 2. Preparation of freeze-dried cells capable of polymerizing glucose to cellulose*. *Biochemical Journal*, *58*(2), 345–352. https://doi.org/10.1042/bj0580345

Jonas, R., & Farah, L. F. (1998). Production and application of microbial cellulose. *Polymer Degradation and Stability*, *59*(1–3), 101–106. https://doi.org/10.1016/S0141-3910(97)00197-3

Kim, S. W., Jung, J. H., Lamsal, K., Kim, Y. S., Min, J. S., & Lee, Y. S. (2012). Antifungal effects of silver nanoparticles (AgNPs) against various plant pathogenic fungi. *Mycobiology*, *40*(1), 53–58. https://doi.org/10.5941/MYCO.2012.40.1.053

Kishanji, M., Mamatha, G., Obi Reddy, K., Varada Rajulu, A., & Madhukar, K. (2017). In situ generation of silver nanoparticles in cellulose matrix using Azadirachta indica leaf extract as a reducing agent. *International Journal of Polymer Analysis and Characterization*, *22*(8), 734–740. https://doi.org/10.1080/1023666X.2017.1369612

Klemm, D., Kramer, F., Moritz, S., Lindström, T., Ankerfors, M., Gray, D., & Dorris, A. (2011). Nanocelluloses: A new family of nature-based materials. *Angewandte Chemie - International Edition*, *50*(24), 5438–5466. https://doi.org/10.1002/anie.201001273

Lemire, J. a, Harrison, J. J., & Turner, R. J. (2013). Antimicrobial activity of metals: mechanisms, molecular targets and applications. *Nature Reviews. Microbiology*, *11*(6), 371–384. https://doi.org/10.1038/nrmicro3028

Li, Y. T., Lin, S. Bin, Chen, L. C., & Chen, H. H. (2017). Antimicrobial activity and controlled release of nanosilvers in bacterial cellulose composites films incorporated with montmorillonites. *Cellulose*, *24*(11), 4871–4883. https://doi.org/10.1007/s10570-017-1487-3

Li, Z., Wang, L., Chen, S., Feng, C., Chen, S., Yin, N., … Xu, Y. (2015). Facilely green synthesis of silver nanoparticles into bacterial cellulose. *Cellulose*, *22*(1), 373–383. https://doi.org/10.1007/s10570-014-0487-9

Maneerung, T., Tokura, S., & Rujiravanit, R. (2008). Impregnation of silver nanoparticles into bacterial cellulose for antimicrobial wound dressing. *Carbohydrate Polymers*, *72*(1), 43–51. https://doi.org/10.1016/j.carbpol.2007.07.025

Maria, L. C. S., Santos, A. L. C., Oliveira, P. C., Valle, A. S. S., Barud, H. S., Messaddeq, Y., & Ribeiro, S. J. L. (2010). Preparation and antibacterial activity of silver nanoparticles impregnated in bacterial cellulose. *Polímeros*, *20*(1), 72–77. https://doi.org/10.1590/S0104-14282010005000001

Mohite, B. V., & Patil, S. V. (2016). In situ development of nanosilver-impregnated bacterial cellulose for sustainable released antimicrobial wound dressing. *Journal of Applied Biomaterials & Functional Materials*. https://doi.org/10.5301/jabfm.5000257

Nasrollahi, Y.-K., Kim, B. H., & Jung, G. (2009). Antifungal Activity of Silver Nanoparticles on some fungi. *Plant Disease*, *93*(10), 1037–1043. https://doi.org/10.1094/PDIS-93-10-1037

Oirdi, M. El, & Bouarab, K. (2007). Plant signalling components EDS1 and SGT1 enhance

disease caused by the necrotrophic pathogen Botrytis cinerea, *175*(1), 131–139. https://doi.org/10.1111/j.1469-8137.2007.02086.x

Oka, H., Tomioka, T., Tomita, K., Nishino, a, & Ueda, S. (1994). Inactivation of enveloped viruses by a silver-thiosulfate complex. *Metal-Based Drugs*, *1*(5–6), 511. https://doi.org/10.1155/MBD.1994.511

Pontier, D., & Tronchet, M. (1998). Activation of hsr 203, a plant gene expressed during incompatible plant-pathogen interactions, is correlated with programmed cell death. *Mol Plant Microbe Interact*, *11*(6), 544–554. https://doi.org/10.1094/MPMI.1998.11.6.544

Pratley, J. E., & Haig, T. (2018). *Metal-Based nanomaterials and oxidative stress in plants: current aspects and overview.* (Vol. 26). https://doi.org/10.1007/978-3-319-76708-6

Rieger, K. A., Cho, H. J., Yeung, H. F., Fan, W., & Schiffman, J. D. (2016). Antimicrobial Activity of Silver Ions Released from Zeolites Immobilized on Cellulose Nanofiber Mats. *ACS Applied Materials and Interfaces*, *8*(5), 3032–3040. https://doi.org/10.1021/acsami.5b10130

Sundström, J. F., Albihn, A., Boqvist, S., Ljungvall, K., Marstorp, H., Martiin, C., … Magnusson, U. (2014). Future threats to agricultural food production posed by environmental degradation, climate change, and animal and plant diseases - a risk analysis in three economic and climate settings. *Food Security*, *6*(2), 201–215. https://doi.org/10.1007/s12571-014-0331-y

Torres, M. A. (2010). ROS in biotic interactions. *Physiologia Plantarum*, *138*(4), 414–429. https://doi.org/10.1111/j.1399-3054.2009.01326.x

Torres, M. A., Dangl, J. L., & Jones, J. D. G. (2002). Arabidopsis gp91phox homologues AtrbohD and AtrbohF are required for accumulation of reactive oxygen intermediates in the plant defense response. *Proceedings of the National Academy of Sciences*, *99*(1), 517–522. https://doi.org/10.1073/pnas.012452499

V. Rajesh Kannan, K. K. B. (2015). *Sustainable Approaches to controlling plant pathogenic bacteria*.

Villamizar-Gallardo, R., Cruz, J. F. O., & Ortíz, O. O. (2016). Fungicidal effect of silver nanoparticles on toxigenic fungi in cocoa. *Pesquisa Agropecuaria Brasileira*, *51*(12), 1929–1936. https://doi.org/10.1590/S0100-204X2016001200003

Ward, E. R., Payne, G. B., Moyer, M. B., Williams, S. C., Dincher, S. S., Sharkey, K. C., … Ryals, J. a. (1991). Differential Regulation of beta-1,3-Glucanase Messenger RNAs in Response to Pathogen Infection. *Plant Physiology*, *96*(2), 390–397. https://doi.org//91 /96/0390/08/$01 .00/0

Wu, C. N., Fuh, S. C., Lin, S. P., Lin, Y. Y., Chen, H. Y., Liu, J. M., & Cheng, K. C. (2018). TEMPO-Oxidized Bacterial Cellulose Pellicle with Silver Nanoparticles for Wound Dressing. *Biomacromolecules*, *19*(2), 544–554.

https://doi.org/10.1021/acs.biomac.7b01660

Wu, J., Zheng, Y., Song, W., Luan, J., Wen, X., Wu, Z., … Guo, S. (2014). In situ synthesis of silver-nanoparticles/bacterial cellulose composites for slow-released antimicrobial wound dressing. *Carbohydrate Polymers*, *102*(1), 762–771. https://doi.org/10.1016/j.carbpol.2013.10.093

Xu, Y.-J., Wang, J.-Y., Zuo, L.-G., & Qian, X. (2016). Rapid Microwave-Assisted Synthesis and Characterization of Cellulose Fiber Containing Silver Nanoparticles in Alkaline Aqueous Solution. *Science of Advanced Materials*. https://doi.org/10.1166/sam.2016.2771

Yang, G., Xie, J., Hong, F., Cao, Z., & Yang, X. (2012). Antimicrobial activity of silver nanoparticle impregnated bacterial cellulose membrane: Effect of fermentation carbon sources of bacterial cellulose. *Carbohydrate Polymers*, *87*(1), 839–845. https://doi.org/10.1016/j.carbpol.2011.08.079

Yang, G., Yao, Y., & Wang, C. (2017). Green synthesis of silver nanoparticles impregnated bacterial cellulose-alginate composite film with improved properties. *Materials Letters*, *209*, 11–14. https://doi.org/10.1016/j.matlet.2017.07.097

Yang, J., Liu, X., Huang, L., & Sun, D. (2013). Antibacterial properties of novel bacterial cellulose nanofiber containing silver nanoparticles. *Chinese Journal of Chemical Engineering*, *21*(12), 1419–1424. https://doi.org/10.1016/S1004-9541(13)60636-9

Yoon, J., Chung, W., & Choi, D. (2009). Jasmonic Acid-Dependent Positive Regulator of Pathogen-Induced Plant Cell Death. *New Phytologist*, *184*(1), 71–84. https://doi.org/10.1111/j.1469-8137.2009.02967.x

Zeng, M., Laromaine, A., Feng, W., Levkin, P. A., & Roig, A. (2014). Origami magnetic cellulose: Controlled magnetic fraction and patterning of flexible bacterial cellulose. *Journal of Materials Chemistry C*, *2*(31), 6312–6318. https://doi.org/10.1039/c4tc00787e

Zeng, M., Laromaine, A., & Roig, A. (2014). Bacterial cellulose films: influence of bacterial strain and drying route on film properties. *Cellulose*, *21*(6), 4455–4469. https://doi.org/10.1007/s10570-014-0408-y

Zeng, M., Laromaine Sagué, A., Vallribera Massó, A., Roig Serra, A., & Barcelona., U. A. de. (2014). Bacterial cellulose: fabrication, characterization and biocompatibility studies. Retrieved from http://ddd.uab.cat/record/127658

Zhao, X., Cui, H., Wang, Y., Sun, C., Cui, B., & Zeng, Z. (2017). Development Strategies and Prospects of Nano-based Smart Pesticide Formulation. *Journal of Agricultural and Food Chemistry*, acs.jafc.7b02004. https://doi.org/10.1021/acs.jafc.7b02004

Zhao, Y., Thilmony, R., Bender, C. L., Schaller, A., He, S. Y., & Howe, G. A. (2003). Virulence systems of Pseudomonas syringae pv . tomato promote bacterial speck disease in tomato by targeting the jasmonate signaling pathway. *The Plant Journal*, *36*(4), 485–499. https://doi.org/10.1046/j.1365-313X.2003.01895.x

Chapter 2

Type III secretion-dependent and -independent phenotypes caused by *Ralstonia solanacearum* in Arabidopsis roots

Summary

The causing agent of bacterial wilt, *Ralstonia solanacearum*, is a soilborne pathogen that invades plants through their roots, traversing many tissue layers until it reaches the xylem, where it multiplies and causes plant collapse. The effects of *R. solanacearum* infection are devastating and no effective approach to fight the disease is so far available. The early steps of infection, essential for colonization, as well as the early plant defense responses, remain mostly unknown.

Here, we have set up a simple in vitro Arabidopsis-*R. solanacearum* pathosystem that has allowed us to identify three clear root phenotypes specifically associated to the early stages of infection: root growth inhibition, root hair formation and root tip cell death.

Using this method we have been able to differentiate on Arabidopsis plants the phenotypes caused by mutants in the key bacterial virulence regulators *hrpB* and *hrpG*, which remained indistinguishable using the classical soil drench inoculation pathogenicity assays. In addition, we have revealed the previously unknown involvement of auxins in the root rearrangements caused by *R. solanacearum* infection.

Our system provides an easy to use, high-throughput tool to study *R. solanacearum* aggressiveness. Furthermore, the observed phenotypes may allow the identification of bacterial virulence determinants and could even be used to screen for novel forms of early plant resistance to bacterial wilt.

The results presented in this Chapter have been published in the *Molecular Plant-Microbe Interaction* research journal (**Anexo**).

Type III secretion-dependent and -independent phenotypes caused by *Ralstonia solanacearum* in Arabidopsis roots

Haibin Lu[1☯#], Saul Lema A.[1☯], Marc Planas-Marquès[1☯], Alejandro Alonso-Díaz[1], Marc Valls[1,2,*] & Núria S. Coll[1*]

[1] Centre for Research in Agricultural Genomics (CSIC-IRTA-UAB-UB), Bellaterra, Catalonia, Spain

[2] Genetics Department, Universitat de Barcelona, Barcelona, Catalonia, Spain

☯ These authors contributed equally to this work

[#] Current address: State Key Laboratory of Crop Stress Biology for Arid Areas and College of Agronomy, Northwest A&F University, No.3 Taicheng Road, Yangling, Shaanxi, China. 712100.

* Address correspondence to: marcvalls@ub.edu, nuria.sanchez-coll@cragenomica.es

Introduction

The soilborne phytopathogen *Ralstonia solanacearum* is the causing agent of bacterial wilt, one of the most destructive bacterial crop diseases worldwide (Hayward, 1991; Mansfield *et al.*, 2012). Also referred as the *R. solanacearum* species complex because of its wide phylogenetic diversity, this bacterium can cause disease on more than 200 plant species including many important economical crops (Genin & Denny, 2012). *R. solanacearum* accesses the plant through the root and traverses many root layers until it reaches the xylem, where it profusely multiplies. From there, it spreads through the aerial part and causes wilting of the stem and leaves (Genin, 2010).

Wilting symptoms caused by *R. solanacearum* are largely dependent on the presence of a functional type III secretion system (T3SS) (Boucher *et al.*, 1985). The T3SS is a needle-like structure present in many pathogenic bacteria that allows secretion of virulence proteins –called effectors- into the host cells (Hueck, 1998; Galan & Collmer, 1999). In plant-associated bacteria, the genes responsible for the regulation and assembly of the T3SS are known as *hypersensitive response and pathogenicity* (*hrp*) genes (Lindgren *et. al.,* 1986*)*. Transcription of the *hrp* genes and their related effectors

is activated by HrpB, the downstream regulator of a well-described regulatory cascade induced by contact with the plant cell wall (Brito *et al.*, 2002). The cascade includes the membrane receptor PrhA, the signal transducer PrhI and the transcriptional regulators PrhJ and HrpG (Brito *et al.*, 2002). HrpG is downstream of PrhJ and directly controls HrpB expression (and thus expression of the T3SS genes) but it also activates a number of HrpB-independent virulence determinants such as genes for ethylene synthesis (Valls *et al.*, 2006).

Since the establishment of the *R. solanacearum* pathosystem almost two decades ago, leaf wilting has been typically used as the major readout to study the *Arabidopsis thaliana-R. solanacearum* interactions (Deslandes *et al.*, 1998). Soil drenching with a bacterial suspension followed by leaf symptom evaluation over a time course constitutes a solid measure to quantify the degree of resistance/susceptibility of the plant towards the pathogen. The disadvantages of this system are the uncontrolled influence of soil microbiota and its high variability due to infection stochasticity, as shown in potato (Cruz *et al.*, 2014). In addition, leaf wilting is the last step of *R. solanacearum* infection and does not provide information about early steps of colonization. Furthermore, soil opacity hinders direct observation of any morphological changes associated to bacterial invasion of plant tissues.

The establishment of gnotobiotic assays in which *R. solanacearum* is inoculated on plants grown axenically has opened the door to study the early steps of infection. *R. solanacearum* in vitro inoculation assays have been successfully established for tomato (Vasse *et al.*, 1995), petunia (Zolobowska & Van Gijsegem, 2006) and the model plants *Medicago truncatula* (Vailleau *et al.*, 2007) and *Arabidopsis thaliana* (Digonnet *et al.*, 2012). These studies have shed light on some common, as well as species-specific root phenomena associated to *R. solanacearum* infection. Reduced primary root elongation after infection is a common feature observed in all species analyzed. Other common root phenotypes that appeared after infection were swelling of the root tip (in tomato, petunia and *M. truncatula*), inhibition of lateral root growth (in petunia and Arabidopsis) and cell death (in *M. truncatula* and Arabidopsis). In petunia, *R. solanacearum* infection resulted as well in the formation of root lateral structures (Zolobowska & Van Gijsegem, 2006). These structures resembled prematurely terminated lateral roots, were present both in resistant and susceptible lines, and were efficient colonization sites.

In vitro pathosystems have helped defining the different stages of *R. solanacearum* infection. The bacterium was found to gain access into the tomato root through wound sites or natural openings such as emerging lateral roots (Vasse *et al.*, 1995; Saile *et al.*, 1997). In *M. truncatula* and Arabidopsis the bacteria can also enter intact roots through the root apex (Vailleau *et al.*, 2007; Digonnet *et al.*, 2012). In petunia it was shown that penetration occurs equally in resistant or susceptible plants (Zolobowska & Van Gijsegem, 2006). The second stage of infection involves invasion of the root cortical area. In this stage *R. solanacearum* quickly transverses the root cylinder centripetally via intercellular spaces, directed to the vasculature (Vasse *et al.*, 1995; Digonnet *et al.*, 2012). Massive cortical cell degeneration can be observed during this phase. The fact that cells not directly in contact with the bacteria also die led to propose that certain cell wall fragments degraded by *R. solanacearum* may act as signals to induce plant programmed cell death (Digonnet *et al.*, 2012). During the third stage of infection *R. solanaceraum* enters into the vascular cylinder and colonizes the xylem. In Arabidopsis, it was shown that vascular invasion is promoted by collapse of two xylem pericycle cells (Digonnet *et al.*, 2012). Once inside the xylem, bacteria start proliferating and moving between adjacent vessels by degrading the cell walls, but remain confined in the xylem. In the last stage of infection, disease symptoms become apparent at the whole organism level, as the stem and leaves start wilting.

All these studies have significantly broadened our understanding of the root invasion process. However, the molecular mechanisms that control these phenotypes and their timing remain vastly unexplored. In addition, no clear correlation has been established between any of the observed phenotypes and the host's resistance or susceptibility to *R. solanacearum*. Here, we have set up a simple in vitro pathosystem to determine the impact of *R. solanacearum* on Arabidopsis root morphology at the first stages of infection.

Results

In vitro infection with *R. solanacearum* causes a triple phenotype on Arabidopsis roots

In order to analyze the impact of *R. solanacearum* infection on Arabidopsis root morphology, we established a simple in vitro inoculation assay. Sterile seeds were sown

on MS media plates and grown vertically for 7 days so that plant roots developed at the surface of the medium and could be easily inoculated and visualized. Plantlets were then inoculated 1 cm above the root tip with 5 µl of a solution containing *R. solanacearum*. Infection with the wild-type GMI1000 strain caused root growth arrest (Fig. 1A). To determine whether this effect depended on the inoculation point, we inoculated at the top, middle and tip of the root. As shown in Fig. S1, *R. solanacearum* causes root growth inhibition regardless of the infection point. Hence, all experiments were performed inoculating 1 cm above the root tip. Interestingly, along with root growth inhibition we observed two additional root phenotypes caused by *R. solanacearum* infection: production of root hairs at the root tip maturation zone (Fig. 1B), and cell death at the root tip. Cell death was visualized as either Evans blue (Fig. 1C) or propidium iodide staining (Fig. S2), both of them commonly used as cell death markers as they are excluded from living cells by the plasma membrane (Gaff & Okong'O-gola, 1971; Curtis & Hays, 2007).

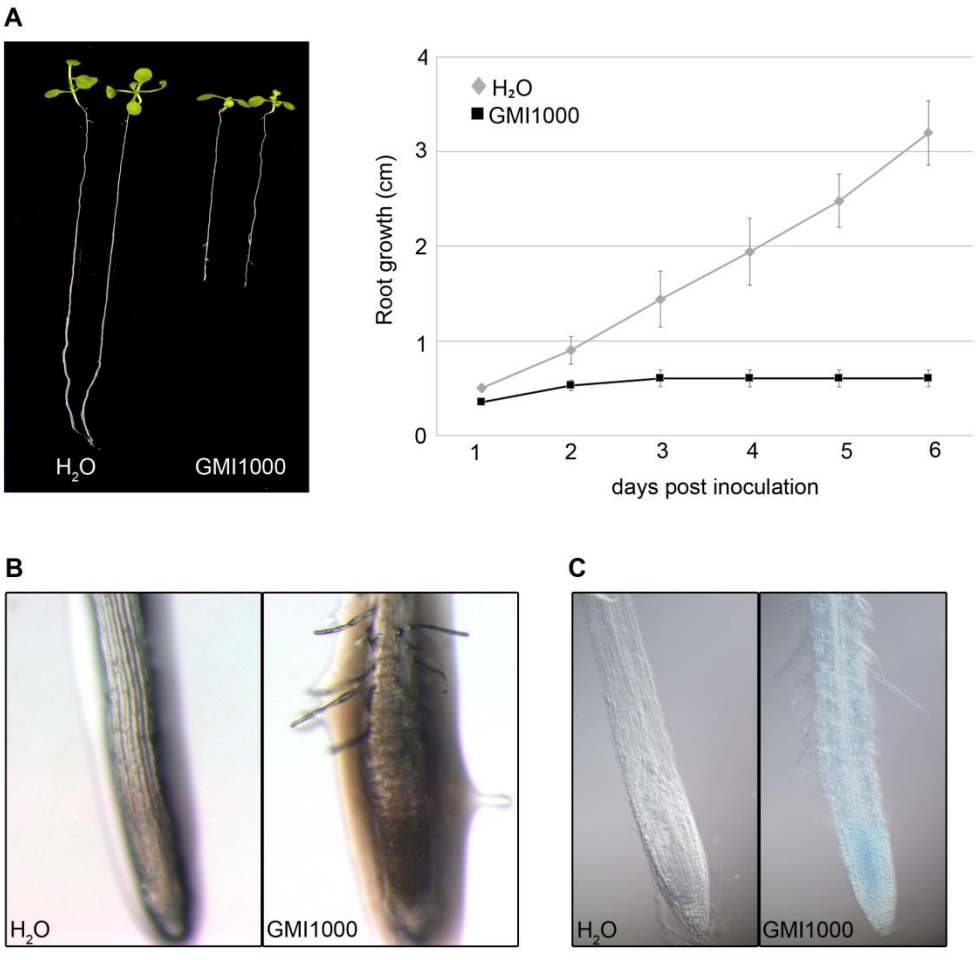

Figure 1. Root phenotypes caused by *R. solanacearum* GMI1000 (GMI1000) in vitro infection. 6-day-old Col-0 seedlings were inoculated with 5µL of a GMI1000 solution or with water as a control. (A) GMI1000 inhibition of root growth. Left panel: stereoscope images of the plantlets under white light at 6 days post inoculation (dpi). Right panel: root length at different times after infection. (B) Root hair formation on the root tip caused by GMI1000 infection. Root tip pictures obtained as before at 6 dpi. (C) Observation of cell death at root tips visualized by Evans blue staining. Representative Nomarski microscope pictures of stained roots obtained 6 dpi.10-15 plants were used in 3 independent experiments.

R. solanacearum hrp mutants are altered in their capacity to cause the triple root phenotype

With these three phenotypes in hand we set out to identify their causative bacterial genetic determinants. For this, we analyzed the triple root phenotypes on plants inoculated with *R. solanacearum* GMI1000 carrying mutations on the master regulators of virulence HrpG and HrpB. Bacteria bearing a disrupted *hrpG* lost the ability to inhibit root growth, but not those bearing disrupted *hrpB* versions (*hrpB* and *hrpBΩ*, figure 2a). Inoculation with the *ΔhrpG*, in which the whole ORF had been deleted, and its complemented strain *ΔhrpG(hrpG)* confirmed the requirement of HrpG but not HrpB to induce the phenotypes. Similarly, bacterial strains disrupted in the membrane receptor *prhA*, the signal transducer *prhI* and, to a lesser extent, the transcriptional regulator *prhJ* were all strongly affected in their capacity to inhibit root growth (Fig. 3). This is logical, since all these mutants show decreased *hrpG* transcription (Brito *et al.*, 2002). *hrp* mutants are all non-pathogenic (Boucher *et al.*, 1985), so the key role of HrpG in root inhibition compared to HrpB could be due to the fact that HrpG controls a larger number of bacterial virulence activities that have been proposed to be required for xylem colonization (Vasse *et al.*, 2000; Valls *et al.*, 2006). To check if root phenotypes correlated with bacterial colonization, 4-week-old Arabidopsis Col-0 plants were inoculated with the wild type *R. solanacearum* GMI1000 or its *hrpB* and *hrpG* deletion mutant counterparts. Bacterial loads were measured in aerial tissues of inoculated Arabidopsis plants 14 days after inoculation as colony forming units (CFUs) per gram of tissue. Fig. S3 shows that the capacity to colonize Arabidopsis plants of *hrpB* is significantly higher than of *hrpG* mutants. Thus, although *hrp* mutants had been already described to multiply *in planta* (Hanemian *et. al.*, 2013), HrpG seems to be more

essential than HrpB for the bacterium to colonize the plant xylem and reach the aerial tissues.

Finally, we also observed that mutations in the *hrpB* and the *hrpG* regulators abolished root hair formation and cell death caused by *R. solanacearum* on roots (figure 2b and 2c). In summary, we proved that root hair production and cell death induction are T3SS-dependent phenotypes. In contrast, root growth inhibition, for which HrpG is required, does not depend on a functional T3SS.

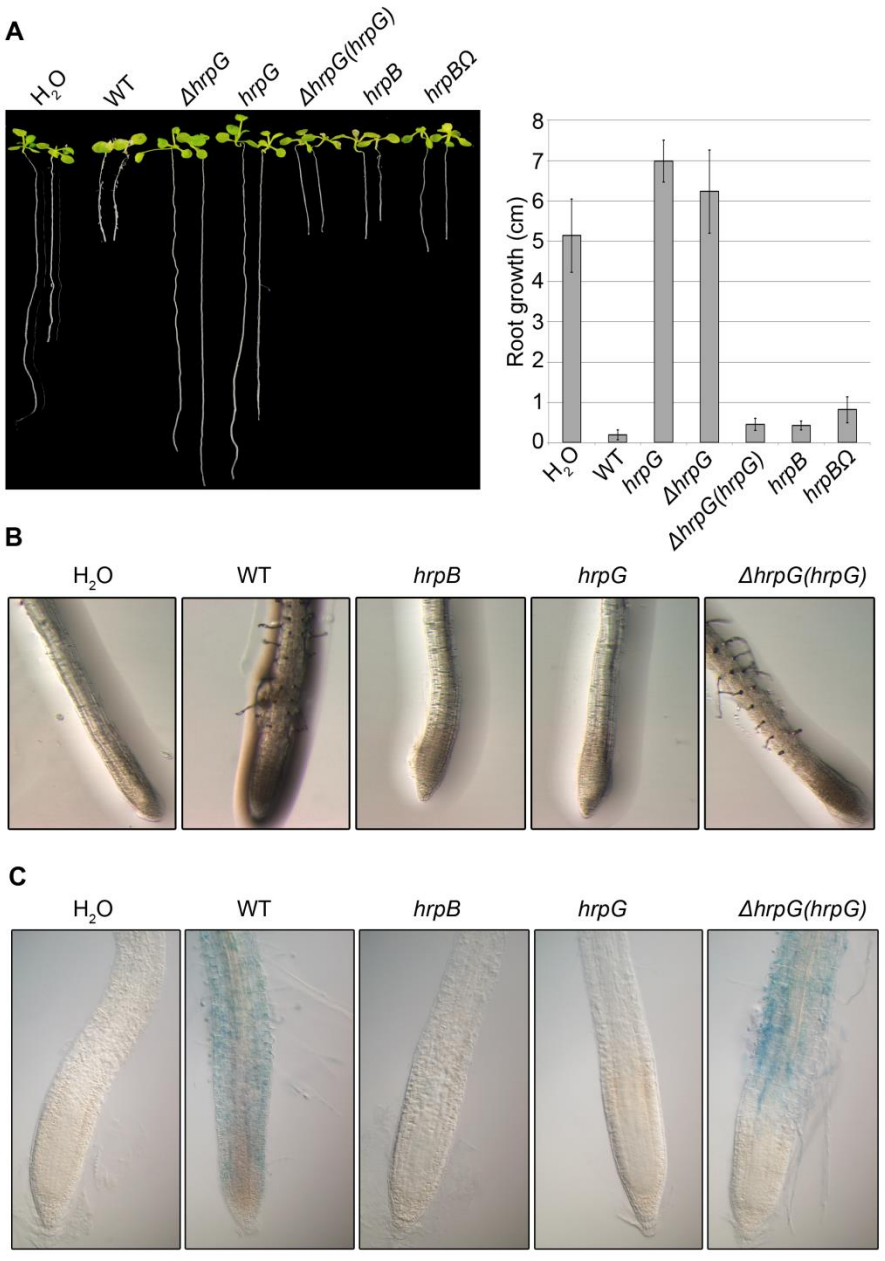

Figure 2. HrpG is required for all the phenotypes caused by GMI1000 while HrpB is only essential for cell death and root hair formation. 6-day-old Col-0 seedlings were inoculated

with water (control) or with the following strains: GMI1000 wild type (WT), *ΔhrpG* (whole gene deletion), *hrpG* (Tn5 transposon insertion), *ΔhrpG*(*hrpG*), *hrpB* (Tn5 transposon insertion) and *hrpBΩ* (Ω cassette insertion). (A) Mutations on HrpG but not HrpB abolish growth inhibition. Left panel: picture taken at 9 dpi. Right panel: root growth measurements at 9 dpi. (B) Both *hrpG* and *hrpB* mutations abolish root hair formation. Pictures were taken at 6 dpi. (C) Neither *hrpG* nor *hrpB* mutant cause root tip cell death. Pictures of infected seedlings at 6 dpi stained with Evans blue as in figure 1C. Each experiment was repeated at least 3 times using 5-10 plants.

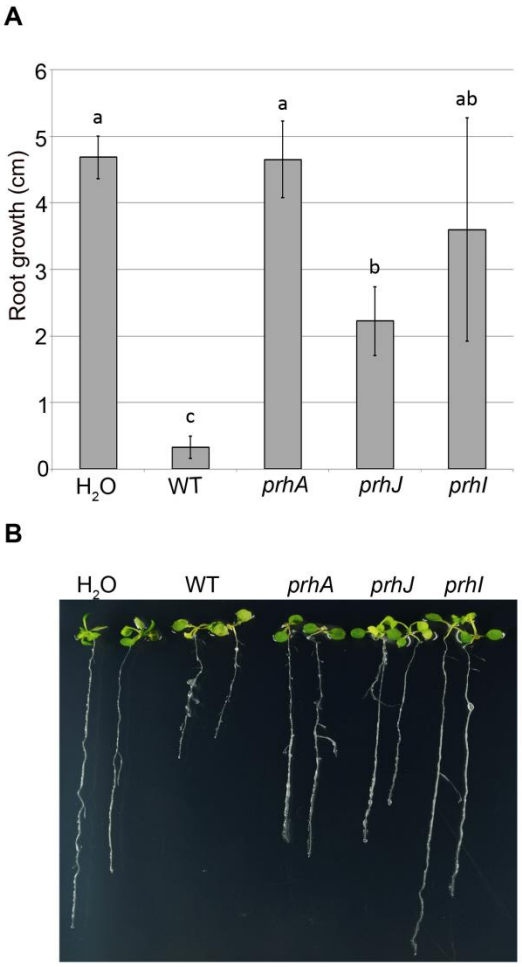

Figure 3. Detection of plant signals is essential for GMI1000 to cause root growth inhibition. Six-day-old Col-0 seedlings were inoculated with GMI1000 (WT), its derivative strains disrupted for components of the *hrp* signaling cascade or treated with water. (A) Root growth was measured at 9 dpi and (B) pictures were taken at 9 dpi. Letters above bars indicate statistical significance; bars not sharing letters represent significant mean differences by one-way ANOVA ($p < 0.05$, $\alpha = 0.05$) with post-hoc Scheffé ($\alpha = 0.05$). 5-7 plants were used in 3 independent experiments.

R. solanacearum strains unable to cause the triple root phenotype are non-virulent on Arabidopsis

Our next goal was to determine whether the ability to cause the triple phenotype in Arabidopsis roots was conserved across different *R. solanacearum* strains and if there was a correlation to aggressiveness. For this, we inoculated in vitro-grown Arabidopsis Col-0 roots with *R. solanacearum* strains belonging to different phylotypes: our reference strain GMI1000 and strain Rd15 (phylotype I); CIP301 and CFBP2957 (phylotype IIA); NCPPB3987, UY031 and UW551 (phylotype IIB); and CMR15 (phylotype III). Interestingly, infection with phylotype IIA strains CIP301 and CFBP2957 resulted in root growth inhibition (Fig. 4a), root hair production (Fig. 4b) and cell death at the root tip (Fig. 4c), similar to what we observed with phylotype I and III strains. In contrast, phylotype IIB strains NCPPB3987, UY031 and UW551 did not cause growth inhibition, nor root hair production or cell death on infected roots. Thus, different *R. solanacearum* strains vary in their ability to cause the triple root phenotype. To determine whether these phenotypes correlated with pathogenicity, we performed root infection assays on Arabidopsis plants grown on soil and recorded the appearance of wilting symptoms over time (Fig. 4d). Infection of wild-type Col-0 plants with the strains that were unable to cause the triple root phenotype (NCPPB3987, UY031 and UW551) did not result in wilting, which indicates a direct correlation between absence of root phenotypes in vitro and absence of symptoms in plants grown in soil. On the contrary, from all *R. solanacearum* strains causing the triple root phenotype, only GMI1000, Rd15 and CMR15 resulted in plant wilting. As seen before for the *hrpG* and *hrpB* mutants, symptom scoring has limitations to evaluate slight *R. solanacearum* pathogenicity differences. Thus, we inoculated Arabidopsis plants with all studied bacterial strains and measured bacterial numbers in the aerial part 14 dpi. The results, shown in figure 4e, indicated that the two phylotype IIA strains (CIP301 and CFBP2957) that showed the triple phenotype but were not causing disease colonized the aerial part of the plants to higher numbers than the strains not causing the root responses. These results show that Arabidopsis root phenotypes partially correlate with the capacity of *R. solanacearum* to colonize Arabidopsis Col-0 plants: the strains that are not able to produce the triple root phenotype are non-virulent.

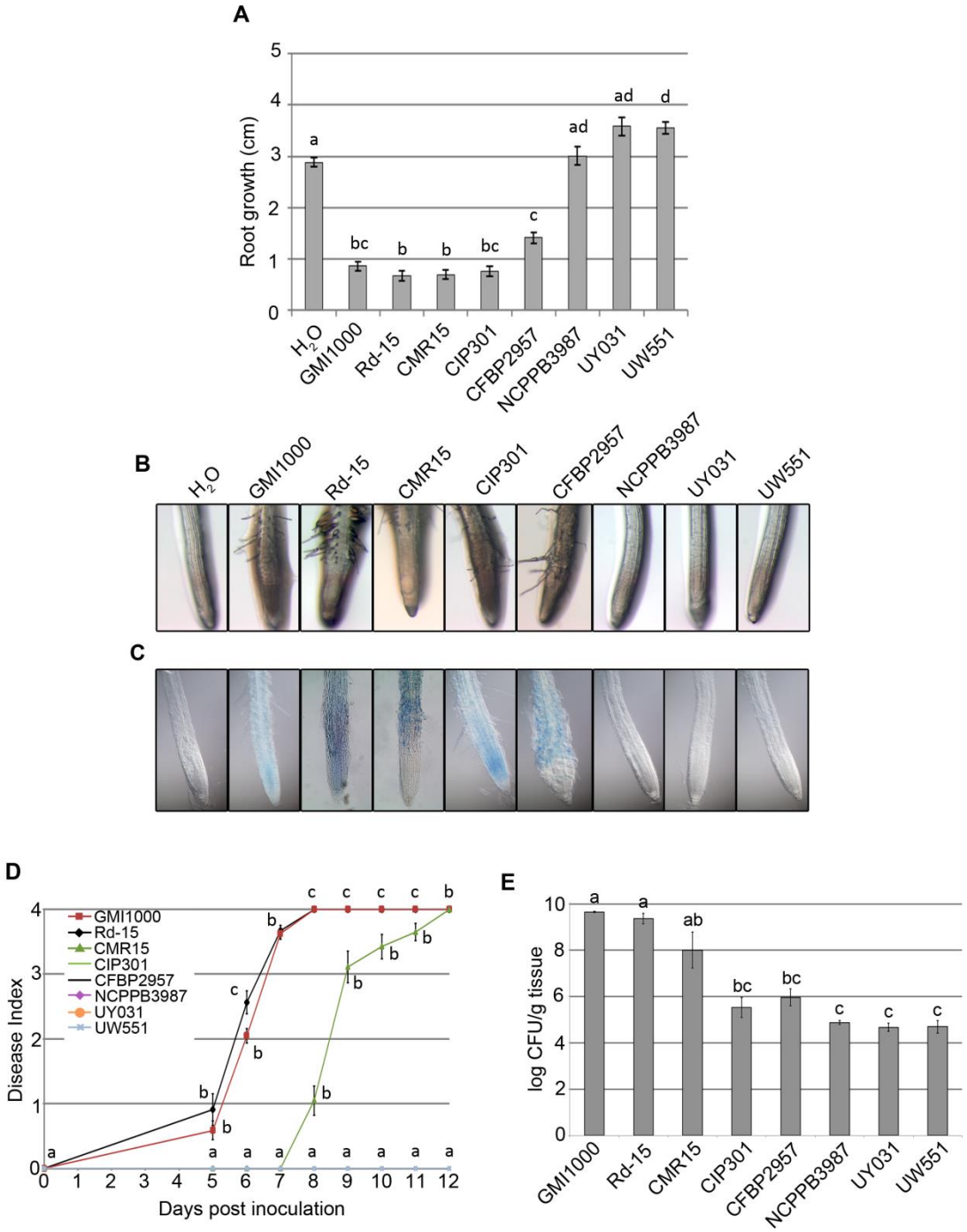

Figure 4. The ability to cause root growth inhibition, root hair formation and cell death varies across different *R. solanacearum* strains. Six-day-old Col-0 seedlings were inoculated with the indicated *R. solanacearum* wild-type strains or water. (A) Root growth after infection at 6 dpi. (B) Pathogenicity assay. (C) Bacterial multiplication in planta measured 14 days after inoculation. For graphs (A-C) letters indicate statistical significance; values not sharing letters represent significant mean differences by one-way ANOVA ($p < 0.05$, $\alpha = 0.05$) with post-hoc Scheffé ($\alpha = 0.05$). In (B), the statistical test was applied separately for each dpi. (D) Root hair

formation at 6 dpi. (E) Roots from infected seedlings at 6 dpi stained with Evans blue. Each experiment was repeated at least 3 times using 10-15 plants.

R. solanacearum-triggered root hair formation is mediated by plant auxins

In order to ascertain whether any of the phenotypes triggered by *R. solanacearum* infection were mediated by known plant defense regulators, we tested how different Arabidopsis mutants responded to the pathogen (Fig. S4). Our results showed that reactive oxygen species (ROS) produced by the membrane NADPH oxidases AtRbohD and AtRbohF were not required for root growth inhibition, root hair production or cell death in response to infection. Plants that were insensitive to jasmonic acid (*jai3-1*) or that could not synthetize it (*dde2*) or its conjugated form (*jar1-1*) showed root growth inhibition, root hair production and cell death similar to the wild-type. Similarly, the *sid2* mutant, defective in salicylic acid biosynthesis, and the ethylene insensitive mutant *ein2*, responded with the same root morphologies as wild-type to *R. solanacearum* infection. On the contrary, the auxin insensitive mutants *tir1* and *tir1/afb2* showed growth inhibition (Fig. 5a) and root tip cell death (Fig. 5b) but were not able to produce root hairs in response to infection (Fig. 5c). This result indicates that root hair production triggered by *R. solanacearum* infection requires auxin signaling. To monitor potential changes in auxin levels during infection, we analyzed expression of the auxin signaling reporter *DR5rev::GFP* in roots of infected versus control plants. As shown in Fig. 5d, *R. solanacearum* inoculation induced a strong vascular GFP signal 48 hours post-infection, suggesting that infection may result in increased auxin signaling levels in the vascular cylinder.

R. solanacearum encodes a HrpG-regulated ethylene-forming enzyme (*efe*) gene (Valls *et al.*, 2006). To assess whether bacterial ethylene mediated root growth inhibition, we infected wild-type Arabidopsis with *R. solanacearum* GMI1000 wild-type strain or with the *efe* mutant. Fig. S5(a) show that infection with the mutant resulted in root growth inhibition, indicating that ethylene produced by the bacteria is not responsible for this phenotype. Bacterial ethylene was also not required for the root hair formation phenotype, because infection with the *efe* mutant did not affect root hair formation (Fig. S5b), as expected if HrpB –which does not activate the *efe* operon– controls this phenotype (figure 2b).

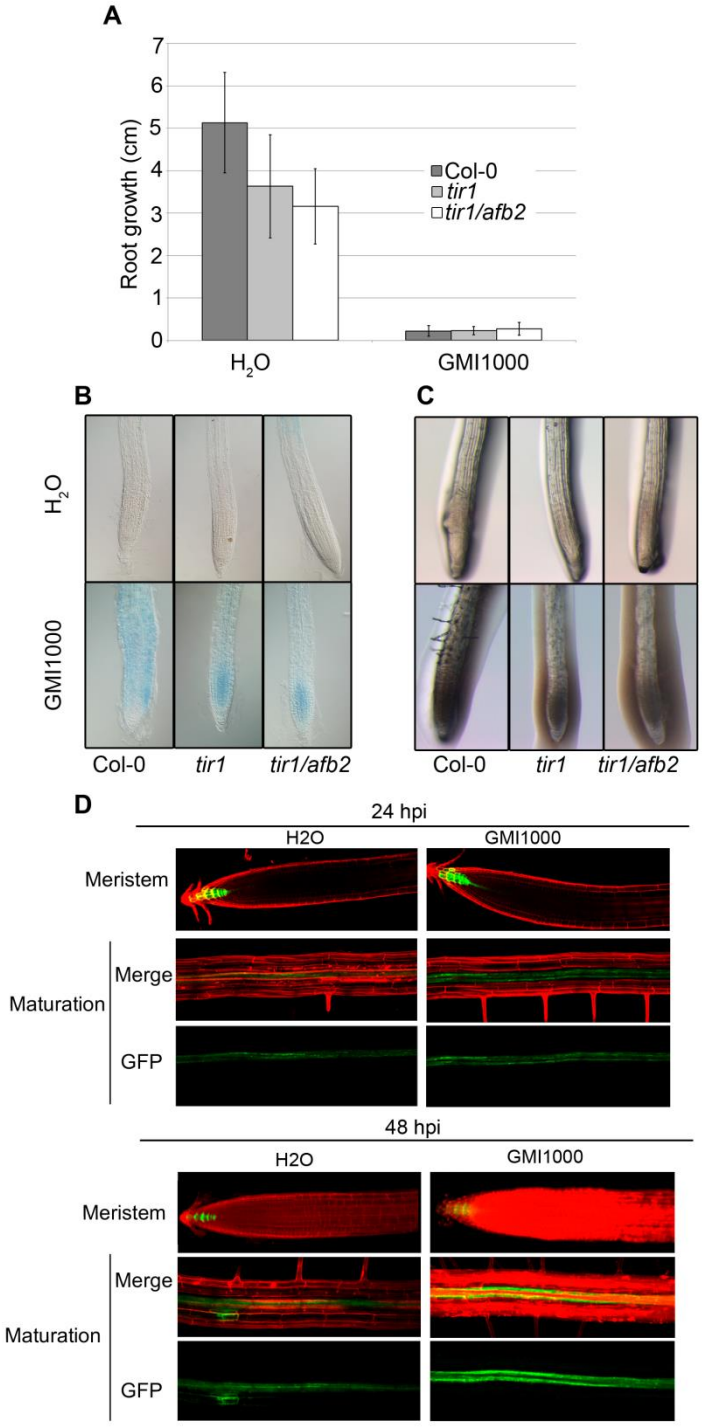

Figure 5. Auxin signaling is required for *R. solanacearum*-triggered root hair formation in Arabidopsis, but not for root growth inhibition and cell death. Six-day-old Col-0, *tir1* and *tir1/afb2* seedlings were inoculated with *R. solanacearum* GMI1000 or water and: (A) root growth was measured 6 dpi; (B) root hair formation was evaluated at 6 dpi; and (C) roots from infected seedlings at 6 dpi were stained with Evans blue. (D) Expression of the auxin signaling marker *DR5* was analyzed under the confocal microscope in roots of transgenic Col-0 *DR5rev::GFP* plants infected with *R. solanacearum* GMI1000 or water at 24 and 48 hours after

inoculation (hpi). Representative pictures of both the meristem area and maturation zone are shown. 6-10 plants were used in 3 different experimental replicates.

Absence of the triple root phenotype in Arabidopsis might reveal new sources of resistance to strain GMI1000

Next, we wanted to determine the degree of conservation of the correlation between absence of the triple phenotype and resistance to *R. solanaceraum*. For this, besides Col-0, we selected the accessions C24, Cvi-0, Ler-1, Bl-1, Rrs-7 among the 20 proposed as representatives of the maximum variability of Arabidopsis (Delker *et al.*, 2010). In addition, we included Nd-1, known to be resistant to *R. solanacearum* (Deslandes et al., 1998) and Tou-A1-74, which does not show the triple phenotype (see below). Despite the differences in root length among accessions, the majority of them displayed the triple root phenotype after inoculation with *R. solanacearum* (Fig. 6a, b, c). Only Rrs-7 and Tou-A1-74 did not show any of the three phenotypes in response to infection. To determine whether the presence/absence of the triple phenotype correlated to susceptibility to *R. solanacearum* GMI1000, we performed a pathogenicity assay using these accessions (Fig. 6d). Interestingly, Rrs-7 –but not Tou-A1-74- was resistant to *R. solanacearum*, indicating that absence of the root phenotypes could be used to identify some sources of resistance to the pathogen. Resistance to *R. solanacearum* was not found in random accessions showing the triple root phenotype, which however did not correlate with susceptibility, since the resistant accessions Nd-1 (Deslandes *et al.*, 1998) and Bl-1 reacted with root growth inhibition, root hair production and cell death after infection (Fig. 6d).

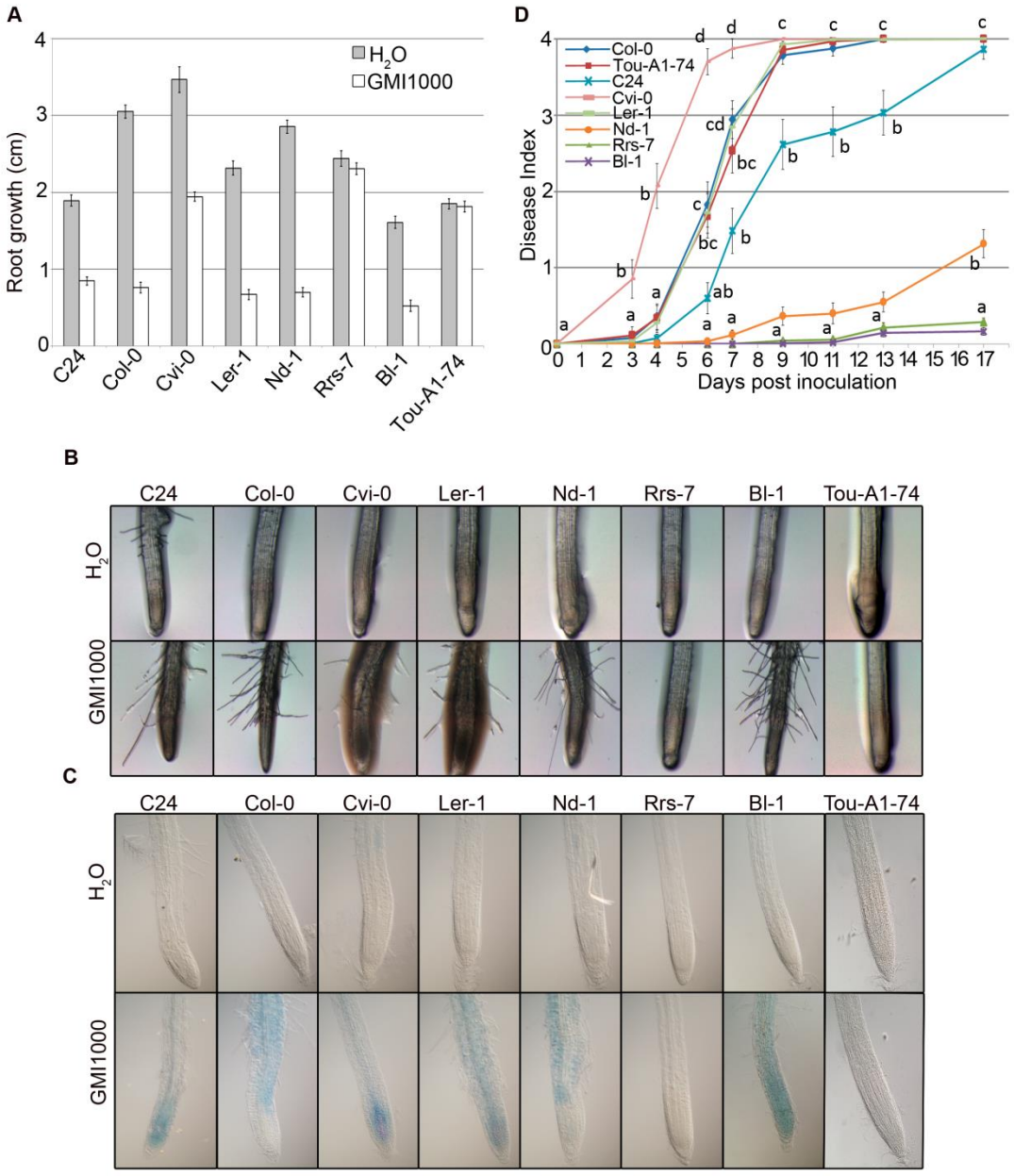

Figure 6. The absence of the triple phenotype caused by *R. solanacearum* in Arabidopsis is indicative of resistance. Six-day-old Arabidopsis seedlings from ecotypes C24, Col-0, Cvi-0, Ler-1, Nd-1, Rrs-7, Bl-1 and Tou-A1-74 were inoculated with *R. solanacearum* GMI1000 or water and at 6 dpi root growth was measured (A), root hair was visualized (B) and cell death was observed after Evans blue staining (C). (D) Five-week old plants grown in Jiffy pots were inoculated with GMI1000. Disease Index indicates the symptoms measured in a 1 to 4 scale as described in methods. Letters indicate statistical significance; values not sharing letters represent significant mean differences by one-way ANOVA ($p < 0.05$, $\alpha = 0.05$) with post-hoc Scheffé ($\alpha = 0.05$). The statistical test was applied separately for each dpi. 7-13 plants were used in each of 3 independent experiments.

Discussion

Plant host root phenotypes appear as early symptoms of colonization by *R. solanacearum*

The use of *in vitro* pathosystems to study the interactions between the vascular pathogen *R. solanacearum* and some of its plant hosts has emerged as a very powerful technique to understand the early stages of infection (Vasse *et al.*, 1995; Vasse *et al.*, 2000; Zolobowska & Van Gijsegem, 2006; Vailleau *et al.*, 2007; Turner *et al.*, 2009; Digonnet *et al.*, 2012). In this work, we have used *in vitro*-grown Arabidopsis as the model host to deepen our knowledge on the first steps of *R. solanacearum* root invasion. In vitro infection has several advantages: i) it reveals easily screenable root phenotypes associated with the infection that would remain hidden when using the soil-drench inoculation; ii) it facilitates microscopy studies to determine the penetration point and the infection itinerary through the root cell layers; iii) it is a useful tool to study the genetic determinants controlling both *R. solanacearum* virulence and host defense.
A very detailed microscopic analysis of the gnotobiotic Arabidopsis-*R. solanacearum* interaction has been recently published (Digonnet *et al.*, 2012). This study revealed the path followed by *R. solanacearum* through Arabidopsis roots, highlighting the sites of bacterial multiplication and the specific cell wall barriers degraded by the bacterium. Moving forward this knowledge, our data defines a set of root phenotypes associated to infection that can be correlated to bacterial aggressiveness and plant resistance and are genetically amenable both from the bacterial and the plant side.

In our system, infection of intact roots with a droplet of *R. solanacearum* resulted in root growth inhibition, root hair production and cell death. Root growth inhibition or delayed elongation has been previously observed as a result of *R. solanacearum* infection when using gnotobiotic systems (Vasse *et al.*, 1995; Zolobowska & Van Gijsegem, 2006; Vailleau *et al.*, 2007; Turner *et al.*, 2009; Digonnet *et al.*, 2012). One could hypothesize that root growth inhibition is the direct cause of the massive cell death observed after infection in the root cortex of Arabidopsis (this work and (Digonnet *et al.*, 2012)) or other species (Vasse *et al.*, 1995; Turner *et al.*, 2009). However, this does not seem to be the case, since a *hrpB* mutant strain causes root growth inhibition in the absence of cell death. Considering this, root growth inhibition would rather reflect xylem colonization, which takes place both for wild-type *R. solanacearum* GMI1000 and the *hrpB* mutant. In agreement with this interpretation, the

hrpG mutant, which has an extremely reduced capacity to invade the xylem (Fig. S3, (Vasse *et al.*, 1995; Vasse *et al.*, 2000)), does not cause root growth inhibition after infection. This further highlights the proposed role of HrpG as a central regulator controlling still-unknown activities essential for the bacterium to reach and multiply in the plant xylem (Vasse *et al.*, 2000; Valls *et al.*, 2006). These activities are likely encoded in genes regulated by HrpG independently of HrpB, as the latter is able to colonize the xylem. Amongst the 184 genes specifically regulated by HrpG, an obvious candidate responsible for the root growth inhibition is the gene controlling bacterial production of the phytohormone ethylene. However, we found that bacterial mutant defective in this gene still inhibited root growth (figure S5a), indicating that xylem colonization and subsequent root inhibition is controlled by other still-undefined HrpG-regulated genes.

Auxin signaling alterations caused by *R. solanacearum* infection likely trigger root structure rearrangements, resulting in root hair formation

Our plant mutant analysis showed that neither of the defense regulators salicylic acid, jasmonic acid, ethylene or NADPH-produced ROS were required for any of the root phenotypes observed after *R. solanacearum* GMI1000 infection. On the contrary, we showed that auxin signaling was clearly required for infection-triggered root hair formation. This is not surprising, since auxin is one of the main orchestrators of root hair formation (Lee & Cho, 2013; Grierson *et al.*, 2014) and can promote this process (Pitts *et al.*, 1998). Root hairs are outgrowths of epidermal cells that contribute to nutrient and water absorption (Grierson *et al.*, 2014), but they also participate in plant-microbe interactions. For instance, root hairs are the entry point of both mutualistic rhizobacteria (Rodriguez-Navarro *et al.*, 2007) and pathogenic bacteria such as *Plasmodiophora brassicaceae*, the causing agent of the clubroot disease (Kageyama & Asano, 2009). Interestingly, auxin signaling was proposed to promote cell wall remodeling to allow root hair growth (Breakspear *et al.*, 2014) and it has been shown to be a key component of both pathogenic and mutualistic root hair infections (Jahn *et al.*, 2013; Laplaze *et al.*, 2015).

During *R. solanacearum*-Arabidopsis interactions, auxin signaling may have additional important roles beyond its involvement in root hair formation. *R. solanacearum* inoculation resulted in an induction of *DR5rev::GFP* expression in the root vascular

cylinder at early stages of infection, indicative of increased auxin signaling levels. Furthermore, plant infection results in increased expression of several auxin-related genes (Zuluaga *et al.*, 2015). On a hypothetic scenario, *R. solanacearum* could directly and specifically –for example, via a T3SS effector– manipulate the host auxin signaling pathway(s) to its own benefit. There are many examples of effector-mediated manipulation of the host auxin pathway, extensively reviewed by Kazan & Lyons (2014). In most cases the pathogen uses its type III effector arsenal to specifically increase auxin levels in the host by targeting auxin biosynthesis, signaling or transport. Elevated auxin levels are beneficial for many pathogens, towards which auxin promotes susceptibility. This is the case of *Pseudomonas syringae*, *Xanthomonas oryzae* and *Magnaporte oryzae*, among others. In rice, elevated susceptibility has been linked to auxin-induced loosening of the protective cell wall, which would facilitate pathogen colonization. Other pathogens increase the host susceptibility by secreting auxin into the host, which in turn induces auxin production inside the host's cells and promotes susceptibility (Fu *et al.*, 2011). Our data points towards a potential link between increased auxin levels as a result of invasion, although further work needs to be done to determine whether this is directly correlated with an increase in susceptibility. In this context, it also remains to be clarified whether auxin-mediated root hair formation during infection facilitates *R. solanacearum* invasion or it is a mere consequence of elevated auxin levels in certain root cells. Also, it is not known whether root hairs may constitute favorite entry points for the bacteria.

Absence of the triple root phenotype to screen for *R. solanacearum* virulence factors or resistance in Arabidopsis

When analyzing different *R. solanacearum* strains, the absence of the root phenotypes is directly linked to the inability of the bacterium to cause symptoms. Thus, strains not capable to induce the triple root phenotype show low pathogenicity on Arabidopsis, as it is the case of NCPPB3987, UY031 and UW551. Presence of the phenotype is not always correlated with increased aggressiveness of a particular strain. CIP301 and CFBP2957 are not pathogenic on Arabidopsis Col-0 plants despite causing the triple root phenotype. Gene-for-gene interactions may mask these root phenotypic features and block *R. solanacearum* before it starts causing wilt. This may indicate that the Col-0 accession possesses resistance proteins that recognize effectors secreted by the two phylotype IIA strains or that phylotype IIA strains lack one or several virulence factors

required to establish disease on Arabidopsis or repress some plant defenses. Similarly, the *hrpG* mutant, which has an extremely reduced capacity to invade the xylem, does not cause root inhibition (see above).

Our data show that the lack of the triple root phenotype can be linked to resistance to *R. solanacearum*. This is the case of Arabidopsis accession Rrs-7, that appears completely resistant to *R. solanacearum* GMI1000 and does not display any of described root phenotypes. Resistance to *R. solanacearum* is very rare amongst Arabidopsis accessions. The clear enrichment of resistant accessions amongst those lacking the capacity to cause the triple phenotype indicates that the root phenotypes described here can be used to screen plant varieties in search for resistance. The fact that other resistant accessions present the phenotypes may indicate that they possess alternative forms of resistance or that other factors, including gene-for-gene interactions, override the observed phenotypes. This could be the case of the resistant accession Nd-1, which is able to detect *R. solanacearum* GMI1000 infection through recognition of the effector PopP2 by the resistance protein RRS1-R (Deslandes *et al.*, 2003). This system could thus be used to differentiate ecotypes with resistances due to a gene-for-gene recognition (Nd-1 resistance associated to the presence of the triple response) compared to other resistance mechanisms (Rrs-7 resistance associated to absence of the triple root response). Along this line, the Arabidopsis Bl-1, which also does not wilt but shows clear infection indicated by the appearance of the root phenotypes, may also recognize *R. solanacearum* through an alternative effector–resistance protein pair and stop invasion.

Taken together, our results on both the bacterial and the plant side favor the notion that absence of the root phenotypes is indicative of ineffective colonization that may reflect novel forms of resistance. Thus, the absence of the root phenotypes described here could help in the search for plant varieties with higher resistance to the devastating bacterial wilt disease.

Materials and Methods

Biological material

Arabidopsis thaliana ecotypes Bl-1, C24, Col-0, Cvi-0, Ler-1, Nd-1, Rrs-7 (Delker *et al.*, 2010, Clark *et al.*, 2007), Tou-A1-74 (Horton *et al*., 2012), and the Col-0 mutants: *sid2-2* (Tsuda *et al.*, 2009), *dde2-2* (Tsuda *et al.*, 2009), *ein2-1* (Tsuda *et al.*, 2009), *tir1-1* (Dharmasiri *et al.*, 2005), *tir1-1/afb2-3* (Parry *et al.*, 2009), *jar1-1* (Staswick & Tiryaki, 2004), *jai3-1* (Chini *et al.*, 2007), *atrbohD* and *atrbohF* (Torres *et al.*, 2002) were used. The Col-0 transgenic line *DR5rev::GFP* (Friml *et al.*, 2003) was used to monitor auxin signaling.

All *R. solanacearum* strains used are described in Supplementary Table1. Bacteria were grown at 28°C in solid or liquid rich B medium (1% Bactopeptone , 0.1% Yeast extract and 0.1% Casamino acids -all from Becton, Dickinson and Co., Franklin Lakes, NJ, USA) adding the appropriate antibiotics, as described in (Monteiro *et al.*, 2012).

In vitro inoculation assay

Seeds were sterilized with a solution containing 30% bleach and 0.02% Triton-X 100 for 10 min, washed five times with Milli-Q water and sown (20 seeds/plate) on MS-plates containing vitamins (Duchefa Biochemie B.V., Haarlem, the Nederlands) and 0.8% Agar (Becton, Dickinson and Co., Franklin Lakes, NJ, USA). Sown plates were stratifiedat 4°C in the dark for two days. Then plates were transferred to chambers and grown for 6-7 days under constant conditions of 21-22°C, 60% humidity and a 16h light/8h dark photoperiod.

For inoculation, *R. solanacearum* was collected by centrifugation (4000 rpm, 5 min) from overnight liquid cultures, resuspended with water and adjusted to a final OD_{600} of 0.01. Six to seven-day-old Arabidopsis seedlings grown on plates as detailed above were inoculated with 5 µL of the bacterial solution, which was applied 1cm above the root tip, as described previously (Digonnet *et al.*, 2012). Plates with the infected seedlings were sealed with micropore tape (3M Deutschland GmbH, Neuss, Germany) and transferred to a controlled growth chamber at 25°C, 60% humidity and a 12h light/12h dark photoperiod. Root length of infected seedlings was recorded over time. For root hair evaluation, pictures were taken 6 days post inoculation (dpi) with an Olympus DP71 stereomicroscope (Olympus, Center Valley, PA, USA) at 11.5x. To

analyze cell death, roots from seedlings grown on plates were collected 6 dpi and immediately stained by carefully submerging them into a solution containing 0.05% w/v of Evans blue (Sigma-Aldrich, Buchs, Switzerland) for 30 min at room temperature. Roots were then washed twice with distilled water and photographed under a 20× lens with a Nomarski Axiophot DP70 microscope (Zeiss, Oberkochen, Germany). For propidium iodide staining, roots of infected seedlings were soaked into 1μg/ml staining solution (Sigma-Aldrich, Buchs, Switzerland), and immediately photographed with a 20x magnification on an Olympus FV1000 (Olympus, Center Valley, PA, USA) or a Leica SP5 (Wetzlar, Germany) confocal microscope.

Pathogenicity assays

R. solanacearum pathogenicity tests were carried out using the soil-drench method (Monteiro *et al.*, 2012). Briefly, Arabidopsis was grown for 4-to-5 weeks on Jiffy pots (Jiffy Group, Lorain, OH, USA) in a controlled chamber at 22°C, 60% humidity and a 8h light/16h dark photoperiod. Jiffys were cut at 1/3 from the bottom and immediately submerged for 30 min into a solution of overnight-grown *R. solanacearum* adjusted to OD_{600}=0.1 with distilled water (35 ml of bacterial solution per plant). Then inoculated plants were transferred to trays containing a thin layer of soil drenched with the same *R. solanacearum* solution and kept in a chamber at 28°C, 60% humidity and 12h light/12h dark. Plant wilting symptoms were recorded every day and expressed according to a disease index scale (0: no wilting, 1: 25% wilted leaves, 2: 50%, 3: 75%, 4: death). At least 30 plants were used in each assay, performed at least in three replicate experiments.

R. solanacearum vessel colonization was tested in Arabidopsis plants inoculated with a lower inoculum (OD_{600}= 0.01). To quantify bacterial colonization, the plant aerial parts were cut 14 days after inoculation and homogenized. Dilutions of the homogenate plant material were plated on rich B medium supplemented with the appropriate antibiotics and the bacterial content measured as colony formation units (cfu) per gram of fresh plant tissue. At least 20 plants were inoculated per *R. solanacearum* strain and the experiment was repeated three times.

Supplementary information

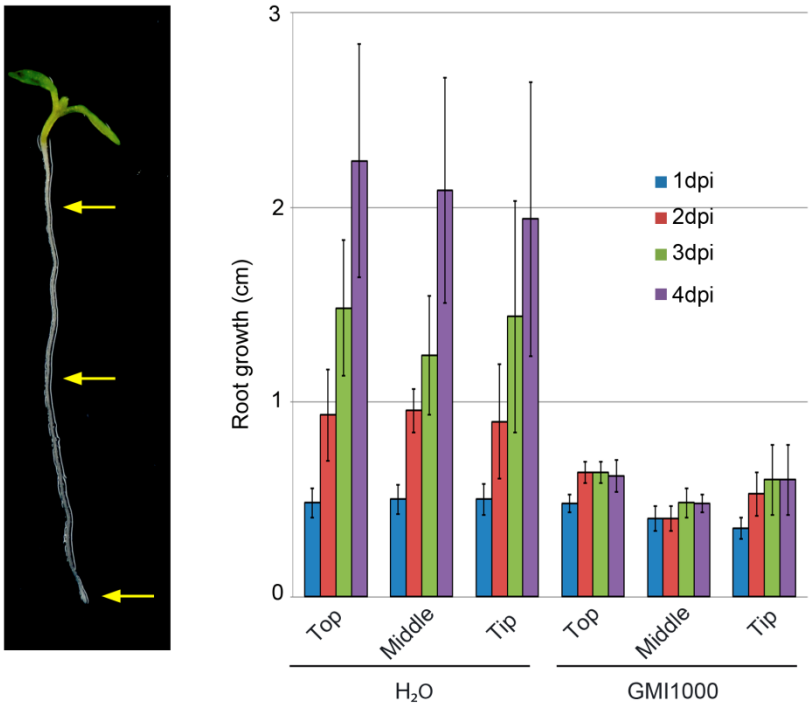

Figure S1. The root site of infection does not have effect on growth inhibition caused by *R. solanacearum* GMI1000. Six-day-old Col-0 seedlings were inoculated with GMI1000 or water. Left panel: Picture of a 6-day-old seedling before infection, with yellow arrows pointing at the selected positions for R. solanacearum infection. Right panel: root growth inhibition occurs independently of the site of infection. 5-8 plants were used in at least 3 different experiments.

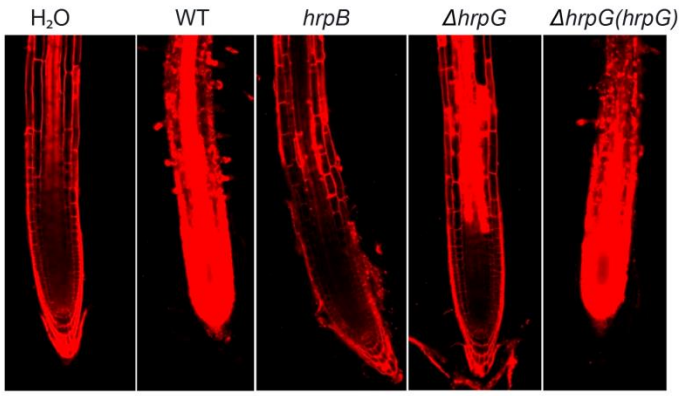

Figure S2. *R. solanacearum*-triggered cell death at the root tip visualized using propidium iodide staining. Photographs were taken using confocal microscopy at 6 dpi.

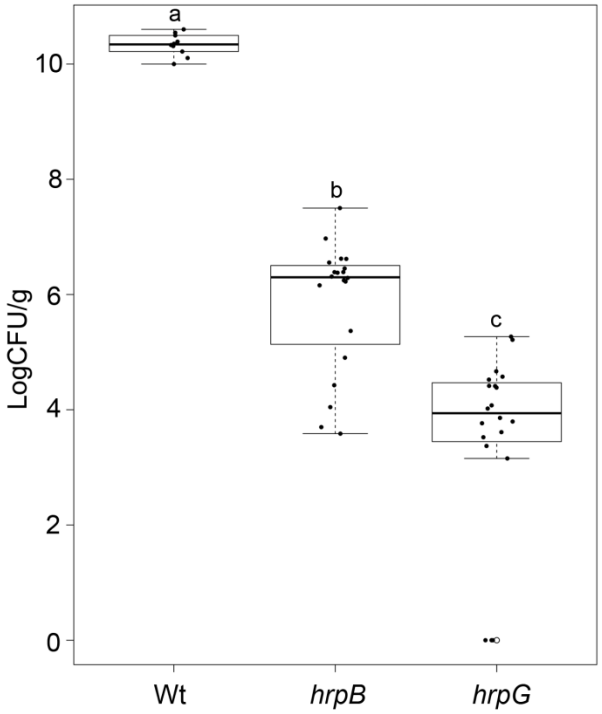

Figure S3. *R. solanacearum* GMI1000 Wt, *hrpB* and *hrpG* mutants show different plant colonization capacity compared to Wt. Four-week old plants grown in Jiffy pots were inoculated with the following strains: GMI1000 Wt, hrpB (Tn5 transposon insertion) and hrpG (Tn5 transposon insertion) at OD600 of 0.01 (10^7 cfu/mL). At 14 dpi bacterial load was calculated; three different experiments are plotted, with a total of 10 plants for the Wt control, 20 plants for hrpB and 20 plants for hrpG. Letters indicate statistical significance; values not sharing letters represent significant mean differences by post-hoc Tukey´s ($p < 0.05$).

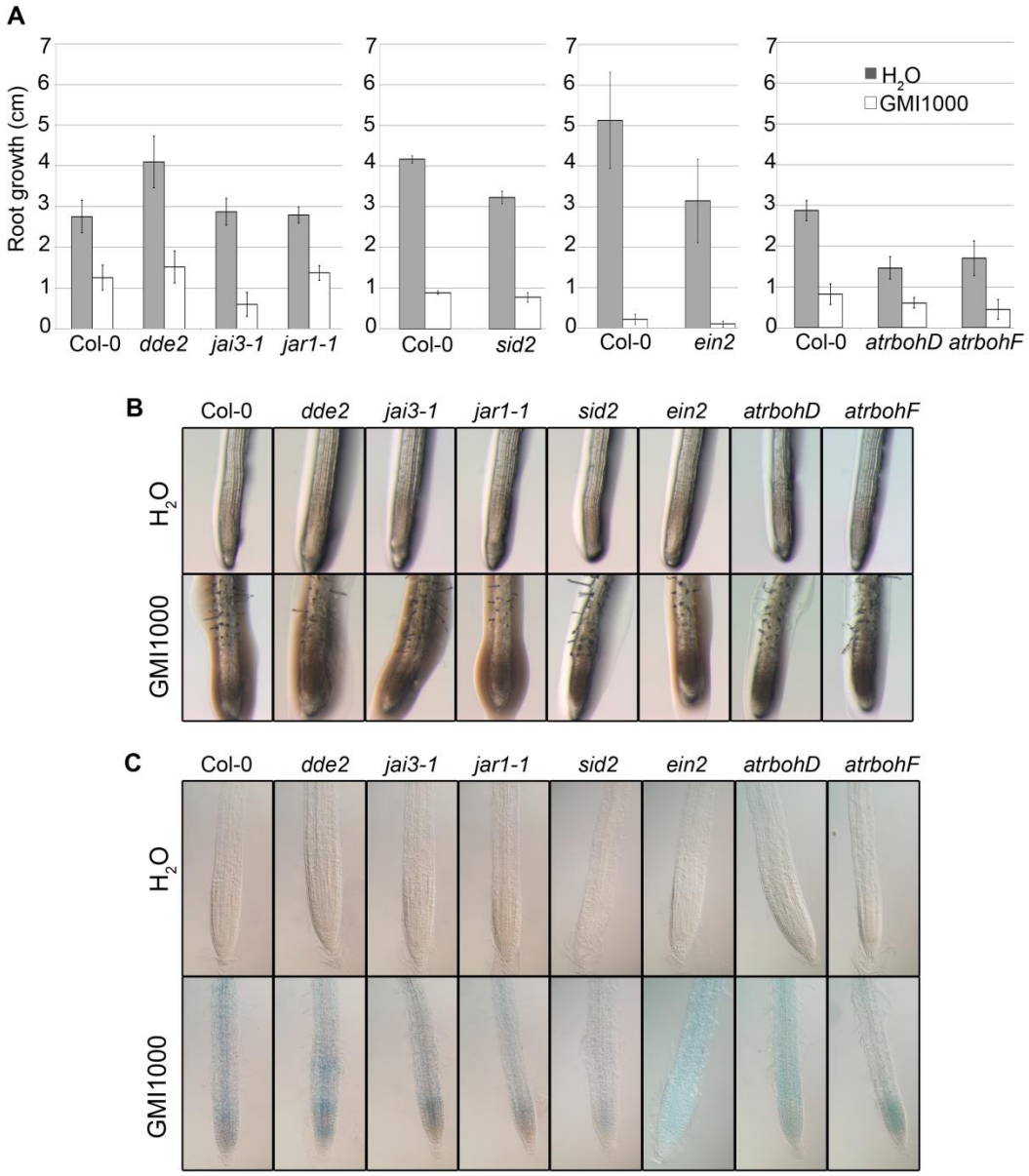

Figure S4. The plant defense regulators jasmonic acid, ethylene, salicylic acid and reactive oxygen species are not essential for the triple phenotype caused by R. solanacearum GMI1000 infection. Six-day-old mutant dde2, jai3-1, jar1-1, sid2, ein2, atrbohD, atrbohF and wild type Col-0 seedlings were inoculated with GMI1000 or water. (A) Root growth was measured at 6 dpi. (B) Root hair formation was photographed at 6 dpi. (C) Cell death was observed by Evans blue staining at 6 dpi using Nomarski microscopy. Around 6-10 plants were used in at least 3 different experiments.

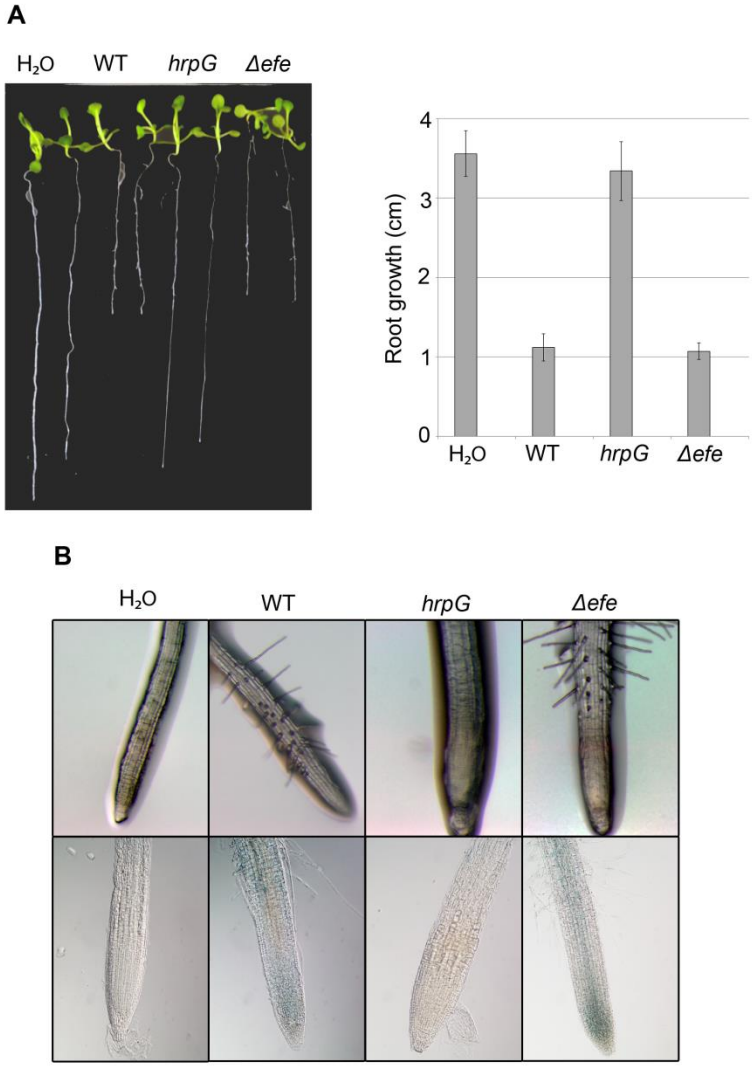

Figure S5. Ethylene produced by GMI1000 is not required for root growth inhibition, root hair formation nor cell death. (A) Disruption of the ethylene forming enzyme gene efe does not abolish root growth inhibition and (B) it does not affect root hair formation nor cell death caused by GMI1000. 6-day-old Col-0 seedlings were inoculated with GMI1000 or water. Infected seedlings were photographed at 9 dpi and root growth was measured at 9 dpi. Root hair formation and cell death was stained as in fig. 1 and photographed at 6 dpi. 10-14 plants were used in 3 independent experiments.

Strain	Description	Reference
GMI1000	Phylotype I strain isolated from *S. lycopersicum*	(Wicker *et al.*, 2012)
Rd15	Phylotype I strain isolated from radish	(Yang *et al.* 1998)
CIP301	Phylotype IIA strain isolated from *S. tuberosum*	(Wicker *et al.*, 2012)
CFBP2957	Phylotype IIA strain isolated from *S. lycopersicum*	(Wicker *et al.*, 2012)
NCPPB3987	Phylotype IIB strain isolated from *S. tuberosum*	(Wicker *et al.*, 2012)
UY031	Phylotype IIB strain isolated from *S. tuberosum*	(Wicker *et al.*, 2012)
UW551	Phylotype IIB strain isolated from *Pelargonium*	(Wicker *et al.*, 2012)
CMR15	Phylotype III strain isolated from *S. lycopersicum*	(Wicker *et al.*, 2012)
ΔhrpG	GMI1775: GMI1000 deleted of the *hrpG* ORF	(Valls *et al.* 2006)
hrpG	GMI1425: GMI1000 with *hrpG* disrupted by *Tn*5 transposon insertion	(Arlat *et al.* 1992)
ΔhrpG (hrpG)	*Δhrpg* strain complemented with *hrpG* on the genome	(Monteiro *et al.* 2012)
hrpB	GMI1492: GMI1000 with *hrpB* disrupted by *Tn*5 transposon insertion	(Arlat *et al.*, 1992)
hrpBΩ	GMI1525: GMI1000 with *hrpB* disrupted by Ω interposon insertion	(Genin *et al.* 1992)
efeΩ	GMI1000 with *efe* disrupted by Ω interposon insertion	(Valls *et al.*, 2006)
prhAΩ	GMI1575: GMI1000 with *prhA* disrupted by Ω interposon insertion	(Marenda *et al.* 1998)
prhIΩ	GMI1580: GMI1000 with *prhI* disrupted by Ω interposon insertion	(Brito *et al.* 2002)
prhJΩ	GMI1579: GMI1000 with *prhJ* disrupted by Ω interposon insertion	(Brito *et al.* 1999)
prhRΩ	GMI1581: GMI1000 with *prhR* disrupted by Ω interposon insertion	(Arlat *et al.*, 1992)

Supplementary Table 1 *R. solanacearum* strains were used in this study.

Acknowledgements

We are grateful to M. Estelle (University of California San Diego) for the *tir1* and *tir1/afb2* seeds; to K. Tsuda (Max Planck Institute from plant breeding research) for the *sid2*, *ein2* and *dde2* seeds; to R. Solano (Spanish National Center for Biotechnolgy, CNB) for the *jai3-1* and *jar1-1* seeds; and to M. Quint (Leibniz institute of Plant Biochemistry), for the Arabidopsis accessions Bl-1, C24, Cvi-0, Ler-1, Nd-1 and RRS-7. We would like to thank M.A. Moreno-Risueño for helpful comments and critically reading the manuscript. We also thank S. Poussier, I. Robène, E. Wicker, S. Genin, CP. Cheng, P Hanson and P. Prior for providing *R. solanacearum* strains and for their advice in the choice of relevant ones. This work was funded by MINECO projects AGL2013-46898-R and AGL2016-78002-R to N.S.C. and M.V. and RyC 2014-1658 to N.S.C. and EU-Marie Curie Actions (PCDMC-321738 and PIIF-331392) and BP_B 00030 from the Catalan Government to N.S.C. We also want to acknowledge the support of the COST Action SUSTAIN (FA1208), the "Severo Ochoa Programme for Centres of Excellence in R&D" 2016-2019 (SEV-2015-0533) from the MINECO and by the CERCA Programme / Generalitat de Catalunya.

Bibliography

Boucher CA, Barberis PA, Trigalet AP, Demery DA. 1985. Transposon mutagenesis of *Pseudomonas solanacearum*: isolation of Tn5-induced avirulent mutants. *J.Gen.Microbiol.* 131: 2449-2457.

Breakspear A, Liu C, Roy S, Stacey N, Rogers C, Trick M, Morieri G, Mysore KS, Wen J, Oldroyd GE, et al. 2014. The root hair "infectome" of Medicago truncatula uncovers changes in cell cycle genes and reveals a requirement for Auxin signaling in rhizobial infection. *Plant Cell* 26(12): 4680-4701.

Brito B, Aldon D, Barberis P, Boucher C, Genin S. 2002. A signal transfer system through three compartments transduces the plant cell contact-dependent signal controlling R. solanacearum hrp genes. *Mol Plant Microbe Interact* 15(2): 109-119.

Clark RM, Schweikert G, et al. 2007. Common Sequence Polymorphisms Shaping Genetic Diversity in Arabidopsis thaliana. *Science* 317(5836): 338-342.

Cruz AP, Ferreira V, Pianzzola MJ, Siri MI, Coll NS, Valls M. 2014. A novel, sensitive method to evaluate potato germplasm for bacterial wilt resistance using a luminescent Ralstonia solanacearum reporter strain. *Mol Plant Microbe Interact* 27(3): 277-285.

Curtis MJ, Hays JB. 2007. Tolerance of dividing cells to replication stress in UVB-irradiated Arabidopsis roots: requirements for DNA translesion polymerases eta and zeta. *DNA Repair (Amst)* 6(9): 1341-1358.

Chini A, Fonseca S, Fernandez G, Adie B, Chico JM, Lorenzo O, Garcia-Casado G, Lopez-Vidriero I, Lozano FM, Ponce MR, et al. 2007. The JAZ family of repressors is the missing link in jasmonate signalling. *Nature* 448(7154): 666-671.

Delker C, Poschl Y, Raschke A, Ullrich K, Ettingshausen S, Hauptmann V, Grosse I, Quint M. 2010. Natural variation of transcriptional auxin response networks in Arabidopsis thaliana. *Plant Cell* 22(7): 2184-2200.

Deslandes L, Olivier J, Peeters N, Feng DX, Khounlotham M, Boucher C, Somssich I, Genin S, Marco Y. 2003. Physical interaction between RRS1-R, a protein conferring resistance to bacterial wilt, and PopP2, a type III effector targeted to the plant nucleus. *Proc Natl Acad Sci U S A* 100(13): 8024-8029.

Deslandes L, Pileur F, Liaubet L, Camut S, Can C, Williams K, Holub E, Beynon J, Arlat M, Marco Y. 1998. Genetic characterization of RRS1, a recessive locus in Arabidopsis thaliana that confers resistance to the bacterial soilborne pathogen Ralstonia solanacearum. *Mol Plant Microbe Interact* 11(7): 659-667.

Dharmasiri N, Dharmasiri S, Estelle M. 2005. The F-box protein TIR1 is an auxin receptor. *Nature* 435(7041): 441-445.

Digonnet C, Martinez Y, Denance N, Chasseray M, Dabos P, Ranocha P, Marco Y, Jauneau A, Goffner D. 2012. Deciphering the route of Ralstonia solanacearum colonization in Arabidopsis thaliana roots during a compatible interaction: focus at the plant cell wall. *Planta* 236(5): 1419-1431.

Friml J, Vieten A, Sauer M, Weijers D, Schwarz H, Hamann T, Offringa R, Jurgens G. 2003. Efflux-dependent auxin gradients establish the apical-basal axis of Arabidopsis. *Nature* 426(6963): 147-153.

Fu J, Liu H, Li Y, Yu H, Li X, Xiao J, Wang S. 2011. Manipulating broad-spectrum disease resistance by suppressing pathogen-induced auxin accumulation in rice. *Plant Physiol* 155(1): 589-602.

Gaff DF, Okong'O-gola O. 1971. The use of non-permeating pigments for testing the survival of cells. *J Exp Bot* 22: 757-758.

Galan JE, Collmer A. 1999. Type III secretion machines: Bacterial devices for protein delivery into host cells. *Science* 284(5418): 1322-1328.

Genin S. 2010. Molecular traits controlling host range and adaptation to plants in Ralstonia solanacearum. *New Phytol* 187(4): 920-928.

Genin S, Denny TP. 2012. Pathogenomics of the Ralstonia solanacearum species complex. *Annu Rev Phytopathol* 50: 67-89.

Grierson C, Nielsen E, Ketelaarc T, Schiefelbein J. 2014. Root hairs. *Arabidopsis Book* 12: e0172.

Hayward AC. 1991. Biology and epidemiology of bacterial wilt caused by pseudomonas solanacearum. *Annu Rev Phytopathol* 29: 65-87.

Hanemian M., Zhou B., Deslandes L., Marco Y., Trémousaygue D. 2013. Hrp mutant bacteria as biocontrol agents: Toward a sustainable approach in the fight against plant pathogenic bacteria. *Plant Signaling & Behavior*, 8(10), e25678.

Horton MW, Hancock AM, Huang YS, Toomajian C, Atwell S, Auton A, Muliyati NW, Platt A, Sperone FG, Vilhjálmsson BJ, Nordborg M, Borevitz JO, Bergelson J. 2012. Genome-wide patterns of genetic variation in worldwide *Arabidopsis thaliana* accessions from the RegMap panel. *Nat Genet*. 2012 44(2):212-216.

Hueck CJ. 1998. Type III protein secretion systems in bacterial pathogens of animals and plants. *Microbiol Mol Biol Rev* 62(2): 379-433.

Jahn L, Mucha S, Bergmann S, Horn C, Staswick P, Steffens B, Siemens J, Ludwig-Müller J. 2013. The Clubroot Pathogen (Plasmodiophora brassicae) Influences Auxin Signaling to Regulate Auxin Homeostasis in Arabidopsis. *Plants* 2(4): 726-749.

Kageyama K, Asano T. 2009. Life Cycle of Plasmodiophora brassicae. *Journal of Plant Growth Regulation* 28(3): 203-211.

Kazan K, Lyons R. 2014. Intervention of Phytohormone Pathways by Pathogen Effectors. *Plant Cell* 26(6): 2285-2309.

Laplaze L, Lucas M, Champion A. 2015. Rhizobial root hair infection requires auxin signaling. *Trends Plant Sci* 20(6): 332-334.

Lee RD, Cho HT. 2013. Auxin, the organizer of the hormonal/environmental signals for root hair growth. *Front Plant Sci* 4: 448.

Lindgren PB, Peet RC, Panopoulos NJ. 1986. Gene cluster of Pseudomonas syringae pv. phaseolicola controls pathogenicity of bean plants and hypersensitivity of nonhost plants. *Journal of Bacteriology*, *168*(2), 512–522.

Mansfield J, Genin S, Magori S, Citovsky V, Sriariyanum M, Ronald P, Dow M, Verdier V, Beer SV, Machado MA, et al. 2012. Top 10 plant pathogenic bacteria in molecular plant pathology. *Mol Plant Pathol* 13(6): 614-629.

Monteiro F, Sole M, van Dijk I, Valls M. 2012. A chromosomal insertion toolbox for promoter probing, mutant complementation, and pathogenicity studies in Ralstonia solanacearum. *Mol Plant Microbe Interact* 25(4): 557-568.

Parry G, Calderon-Villalobos LI, Prigge M, Peret B, Dharmasiri S, Itoh H, Lechner E, Gray WM, Bennett M, Estelle M. 2009. Complex regulation of the TIR1/AFB family of auxin receptors. *Proc Natl Acad Sci U S A* 106(52): 22540-22545.

Pitts RJ, Cernac A, Estelle M. 1998. Auxin and ethylene promote root hair elongation in Arabidopsis. *Plant J* 16(5): 553-560.

Rodriguez-Navarro DN, Dardanelli MS, Ruiz-Sainz JE. 2007. Attachment of bacteria to the roots of higher plants. *FEMS Microbiol Lett* 272(2): 127-136.

Saile E, McGarvey JA, Schell MA, Denny TP. 1997. Role of Extracellular Polysaccharide and Endoglucanase in Root Invasion and Colonization of Tomato Plants by Ralstonia solanacearum. *Phytopathology* 87(12): 1264-1271.

Staswick PE, Tiryaki I. 2004. The oxylipin signal jasmonic acid is activated by an enzyme that conjugates it to isoleucine in Arabidopsis. *Plant Cell* 16(8): 2117-2127.

Torres MA, Dangl JL, Jones JD. 2002. Arabidopsis gp91phox homologues AtrbohD and AtrbohF are required for accumulation of reactive oxygen intermediates in the plant defense response. *Proc Natl Acad Sci U S A* 99(1): 517-522.

Tsuda K, Sato M, Stoddard T, Glazebrook J, Katagiri F. 2009. Network properties of robust immunity in plants. *PLoS Genet* 5(12): e1000772.

Turner M, Jauneau A, Genin S, Tavella MJ, Vailleau F, Gentzbittel L, Jardinaud MF. 2009. Dissection of bacterial Wilt on Medicago truncatula revealed two type III secretion system effectors acting on root infection process and disease development. *Plant Physiol* 150(4): 1713-1722.

Vailleau F, Sartorel E, Jardinaud MF, Chardon F, Genin S, Huguet T, Gentzbittel L, Petitprez M. 2007. Characterization of the interaction between the bacterial wilt pathogen Ralstonia solanacearum and the model legume plant Medicago truncatula. *Mol Plant Microbe Interact* 20(2): 159-167.

Valls M, Genin S, Boucher C. 2006. Integrated regulation of the type III secretion system and other virulence determinants in Ralstonia solanacearum. *PLoS Pathog* 2(8): e82.

Vasse J, Frey P, Trigalet A. 1995. Microscopic studies of intercellular infection and protoxylem invasion of tomato roots by Pseudomonas solanacearum. *Molecular Plant-Microbe Interactions* 8(2): 241-251.

Vasse J, Genin S, Frey P, Boucher C, Brito B. 2000. The hrpB and hrpG regulatory genes of Ralstonia solanacearum are required for different stages of the tomato root infection process. *Mol Plant Microbe Interact* 13(3): 259-267.

Zolobowska L, Van Gijsegem F. 2006. Induction of lateral root structure formation on petunia roots: A novel effect of GMI1000 Ralstonia solanacearum infection impaired in Hrp mutants. *Mol Plant Microbe Interact* 19(6): 597-606.

Zuluaga AP, Sole M, Lu H, Gongora-Castillo E, Vaillancourt B, Coll N, Buell CR, Valls M. 2015. Transcriptome responses to Ralstonia solanacearum infection in the roots of the wild potato Solanum commersonii. *BMC Genomics* 16: 246.

CONCLUSIONES

Aplicaciones de la BC-AgNPs (capítulo 1)

1- El híbrido BC-AgNPs tiene propiedades antibacterianas y antifúngicas en cultivo *in vitro* y en plantas de tabaco y tomate.
2- La unión covalente de nanopartículas de plata a BC evita su liberación al medio, facilitando su uso en aplicaciones agrícolas.

Análisis del patosistema *A. thaliana*-*R solanacearum* (Capítulo 2):

3- El sistema infección *in vitro* que se ha utilizado ha permitido establecer una clara correlación entre la ausencia del triple fenotipo en raíz y la resistencia a *R. solanacearum*.
4- La infección *in vitro* es de gran utilidad para facilitar: el escrutinio de fenotipos asociados a la infección, los estudios de microscopía y la búsqueda de determinantes genéticos asociados a la defensa de la planta.

BIBLIOGRAFIA

Bibliografía

Almeida, I. F., Pereira, T., Silva, N. H. C. S., Gomes, F. P., Silvestre, A. J. D., Freire, C. S. R., … Costa, P. C. (2014). Bacterial cellulose membranes as drug delivery systems: An in vivo skin compatibility study. *European Journal of Pharmaceutics and Biopharmaceutics*, *86*(3), 332–336. https://doi.org/10.1016/j.ejpb.2013.08.008

Alonso-Díaz, A., Floriach-Clark, J., Fuentes, J., Capellades, M., Coll, N. S., & Laromaine, A. (2019). Enhancing Localized Pesticide Action through Plant Foliage by Silver-Cellulose Hybrid Patches. *ACS Biomaterials Science and Engineering*, *5*(2), 413–419. https://doi.org/10.1021/acsbiomaterials.8b01171

Álvarez, B., Vasse, J., López, M. M., & Trigalet, A. (2007). Comparative Behavior of Ralstonia solanacearum Biovar 2 in Diverse Plant Species, *98*(1), 59–68.

Amnuaikit, T., Chusuit, T., Raknam, P., & Boonme, P. (2011). Effects of a cellulose mask synthesized by a bacterium on facial skin characteristics and user satisfaction. *Medical Devices: Evidence and Research*, (June 2011), 77. https://doi.org/10.2147/mder.s20935

Araud-razou, I., Vasse, J., Montrozier, H., & Etchebar, C. (1998). Detection and visualization of the major acidic exopolysaccharide of Ralstonia solanacearum and its role in tomato root infection and vascular colonization, 795–796.

Bielecki, S., Krystynowicz, A., Turkiewicz, M., & Kalinowska, H. (2002). Bacterial Cellulose. *Biomaterials from Nature for Advanced Devices and Therapies*, 384–399. https://doi.org/10.1002/9781119126218.ch21

Biyik, H., & Coban, E. P. (2017). Evaluation of different carbon, nitrogen sources and industrial wastes for bacterial cellulose production. *European Journal of Biotechnology and Bioscience*, *5*(1), 74–80.

Butchosa, N., Brown, C., Larsson, P. T., Berglund, L. A., Bulone, V., & Zhou, Q. (2013). Nanocomposites of bacterial cellulose nanofibers and chitin nanocrystals: Fabrication, characterization and bactericidal activity. *Green Chemistry*, *15*(12), 3404–3413. https://doi.org/10.1039/c3gc41700j

Caruso, P., Biosca, E. G., Bertolini, E., Marco-noales, E., & Gorris, M. T. (2017). Genetic diversity reflects geographical origin of Ralstonia solanacearum strains isolated from plant and water sources in Spain, *20*(4), 155–164. https://doi.org/10.2436/20.1501.01.298.

Caruthers, S. D., Wickline, S. A., & Lanza, G. M. (2007). Nanotechnology applications in medicine. *Tumori*, *94*(2), 206–215. https://doi.org/10.1016/j.copbio.2007.01.006

Castellano, J. J., Shafii, S. M., Ko, F., Donate, G., Wright, T. E., Mannari, R. J., … Robson, M. C. (2007). Comparative evaluation of silver-containing antimicrobial dressings and drugs. *International Wound Journal*, *4*(2). https://doi.org/10.1111/j.1742-481X.2007.00316.x

Chawla, P. R., Bajaj, I. B., Survase, S. A., & Singhal, R. S. (2008). Microbial cellulose: Fermentative production and applications. *Food Technology and Biotechnology*, *47*(2), 107–124.

Choi, O., Deng, K. K., Kim, N. J., Ross, L., Surampalli, R. Y., & Hu, Z. (2008). The inhibitory effects of silver nanoparticles, silver ions, and silver chloride colloids on microbial growth. *Water Research*, *42*(12), 3066–3074. https://doi.org/10.1016/j.watres.2008.02.021

Chopra, I. (2007). The increasing use of silver-based products as antimicrobial agents: A useful development or a cause for concern? *Journal of Antimicrobial Chemotherapy*, *59*(4), 587–590. https://doi.org/10.1093/jac/dkm006

Czaja, W., Krystynowicz, A., Bielecki, S., & Brown, R. M. (2005). Microbial cellulose — the natural power to heal wounds $, *27*, 145–151. https://doi.org/10.1016/j.biomaterials.2005.07.035

Dahman, Y. (2009). Nanostructured Biomaterials and Biocomposites from Bacterial Cellulose Nanofibers. *Journal of Nanoscience and Nanotechnology*, *9*(9), 5105–5122. https://doi.org/10.1166/jnn.2009.1466

De Moura, M. R., Mattoso, L. H. C., & Zucolotto, V. (2012). Development of cellulose-based bactericidal nanocomposites containing silver nanoparticles and their use as active food packaging. *Journal of Food Engineering*, *109*(3), 520–524. https://doi.org/10.1016/j.jfoodeng.2011.10.030

Denny, T. P., & Baek, S.-R. (1990). Genetic evidence that extracellular polysaccharide is a virulence factor of pseudomonas solanacearum.pdf.

Dhanalakshmi, M., Thenmozhi, S., Devi, K. M., & Kameshwaran, S. (2013). Silver Nanoparticles and its Antibacterial Activity, *4*(5), 819–826.

Digonnet, C., Martinez, Y., Demancé, N., Chasseray, M., Dabos, P., Ranocha, P., … Goffner, D. (2012). Deciphering the route of Ralstonia solanacearum colonization in Arabidopsis thaliana roots during a compatible interaction : focus at the plant cell wall, 1419–1431. https://doi.org/10.1007/s00425-012-1694-y

Dourado, F., Gama, M., & Rodrigues, A. C. (2017). A Review on the toxicology and dietetic role of bacterial cellulose. *Toxicology Reports*, *4*(September), 543–553. https://doi.org/10.1016/j.toxrep.2017.09.005

Festucci-Buselli, R. A., Otoni, W. C., & Joshi, C. P. (2007). Structure, organization, and functions of cellulose synthase complexes in higher plants. *Brazilian Journal of Plant Physiology*, *19*(1), 1–13. https://doi.org/10.1590/s1677-04202007000100001

Gao, W. H., Chen, K. F., Yang, R. D., Yang, F., & Han, W. J. (2011). Properties of bacterial cellulose and its influence on the physical properties of paper. *BioResources*, *6*(1), 144–153.

Gudikandula, K., & Charya Maringanti, S. (2016). Synthesis of silver nanoparticles by chemical and biological methods and their antimicrobial properties. *Journal of Experimental Nanoscience*, *11*(9), 714–721. https://doi.org/10.1080/17458080.2016.1139196

Hajipour, M. J., Fromm, K. M., Akbar Ashkarran, A., Jimenez de Aberasturi, D., Larramendi, I. R. de, Rojo, T., … Mahmoudi, M. (2012). Antibacterial properties of nanoparticles. *Trends in Biotechnology*, *30*(10), 499–511. https://doi.org/10.1016/j.tibtech.2012.06.004

Hayward, A. C. (1964). P651, *27*, 265–277.

He, L. Y. (1983). Characteristics of strains of Pseudomonas solanacearum form China.PDF.

Heggers, J. P., Richard, J. W., Spencer, B. A., McCoy, L. F., Carino, E., Washington, J. W., … Goodheart, R. (2012). Acticoat versus Silverlon: The Truth. *Journal of Burn Care & Rehabilitation*. https://doi.org/10.1097/00004630-200203002-00146

HJ., K. (2000). Historical review of the use of silver in the treatment of burns.I. Early uses. *Burns*, *26*, 117–130.

Hong, J. C., Momol, M. T., Jones, J. B., Ji, P., Flor-, N., & Olson, S. M. (2008). Detection of Ralstonia solanacearum in Irrigation Ponds and Aquatic Weeds Associated with the Ponds in North Florida, *92*(12).

Huang, J., & Schell, M. (1995). Molecular characterization of the eps gene cluster of Pseudomonas solanacearum and its transcriptional regulation at a single promoter, *16*, 977–989.

Iravani, S., Korbekandi, H., & Zolfaghari, B. (2013). Synthesis of silver nanoparticles : chemical , physical and biological methods Synthesis of silver NPs. *Research in Pharmaceutical Sciences*, *9*(6), 385–406. https://doi.org/10.1111/j.1551-2916.2006.01044.x

Jo, Y.-K., Kim, B. H., & Jung, G. (2009). Antifungal Activity of Silver Ions and Nanoparticles on Phytopathogenic Fungi. *Plant Disease*, *93*(10), 1037–1043. https://doi.org/10.1094/PDIS-93-10-1037

Johnston, H. J., Hutchison, G., Christensen, F. M., Peters, S., Hankin, S., & Stone, V. (2010). A review of the in vivo and in vitro toxicity of silver and gold particulates: particle attributes and biological mechanisms responsible for the observed toxicity. *Critical Reviews in Toxicology*, *40*(4), 328–346. https://doi.org/10.3109/10408440903453074

Jonas, R., & Farah, L. F. (1998). Production and application of microbial cellulose. *Polymer Degradation and Stability*, *59*(1–3), 101–106. https://doi.org/10.1016/S0141-3910(97)00197-3

Kang, Y., Liu, H., Genin, S., Schell, M. A., & Denny, T. P. (2002). Ralstonia solanacearum requires type 4 pili to adhere to multiple surfaces and for natural transformation and virulence, 427–437.

Kędziora, A., Speruda, M., Krzyżewska, E., Rybka, J., Łukowiak, A., & Bugla-Płoskońska, G. (2018). Similarities and differences between silver ions and silver in nanoforms as antibacterial agents. *International Journal of Molecular Sciences*, *19*(2). https://doi.org/10.3390/ijms19020444

Kimura, S., & Itoh, T. (2007). Biogenesis and Function of Cellulose in the Tunicates. *Cellulose: Molecular and Structural Biology*, 217–236. https://doi.org/10.1007/978-1-4020-5380-1_13

Kishanji, M., Mamatha, G., Obi Reddy, K., Varada Rajulu, A., & Madhukar, K. (2017). In situ generation of silver nanoparticles in cellulose matrix using Azadirachta indica leaf extract as a reducing agent. *International Journal of Polymer Analysis and Characterization*, *22*(8), 734–740. https://doi.org/10.1080/1023666X.2017.1369612

Klemm, D., Kramer, F., Moritz, S., Lindström, T., Ankerfors, M., Gray, D., & Dorris, A. (2011). Nanocelluloses: A new family of nature-based materials. *Angewandte Chemie - International Edition*, *50*(24), 5438–5466. https://doi.org/10.1002/anie.201001273

Legendre, J.-Y. (2009). Assembly comprising a substrate comprising biocellulose, and a powdered cosmetic composition to be brought into contact with the substrate, *1*(19). https://doi.org/10.1016/j.(73)

Li, Y. T., Lin, S. Bin, Chen, L. C., & Chen, H. H. (2017). Antimicrobial activity and controlled

release of nanosilvers in bacterial cellulose composites films incorporated with montmorillonites. *Cellulose*, *24*(11), 4871–4883. https://doi.org/10.1007/s10570-017-1487-3

Liu, H., Kang, Y., Genin, S., Schell, M. A., & Denny, T. P. (2001). Twitching motility of Ralstonia solanacearum requires a type IV pilus system, (2001), 3215–3229.

M. Iguchi;, S. Yamanaka;, & A. Budhiono; (2000). Bacterial cellulose - a masterpiece of nature's arts. *Journal of Materials Science*, *35*(2), 261–270. https://doi.org/10.1023/A

Maneerung, T., Tokura, S., & Rujiravanit, R. (2008). Impregnation of silver nanoparticles into bacterial cellulose for antimicrobial wound dressing. *Carbohydrate Polymers*, *72*(1), 43–51. https://doi.org/10.1016/j.carbpol.2007.07.025

Mcgarvey, J. A., Bell, C. J., Denny, T. P., & Schell, M. A. (1998). Analysis of Extracellular Polysaccharide I In Culture and In Planta Using Immunological Methods : New Insights and Implications.

Mcgarvey, J. A., Denny, T. P., & Schell, M. A. (1999). Spatial-Temporal and Quantitative Analysis of Growth and EPS I Production by Ralstonia solanacearum in Resistant and Susceptible Tomato Cultivars, *89*(12), 1233–1239.

Melaiye, A., & Youngs, W. J. (2005). Silver and its application as an antimicrobial agent. *Expert Opinion on Therapeutic Patents*, *15*(2), 125–130. https://doi.org/10.1517/13543776.15.2.125

Mohite, B. V., & Patil, S. V. (2016). In situ development of nanosilver-impregnated bacterial cellulose for sustainable released antimicrobial wound dressing. *Journal of Applied Biomaterials & Functional Materials*. https://doi.org/10.5301/jabfm.5000257

Monge, M. (2009). Nanopartículas de plata: métodos de síntesis en disolución y propiedades bactericidas. *An. Quím*, 33–41. https://doi.org/ISSN 1575-3417

Morgan, J. L. W., Strumillo, J., & Zimmer, J. (2012). Crystallographic snapshot of cellulose synthesis and membrane translocation. *Nature*, *000*, 181–186. https://doi.org/10.1038/nature11744

Moyer, C. A., Brentano, L., Gravens, D. L., Margraf, H. W., & Monafo, W. W. (1965). Treatment of large human burns with 0.5% silver nitrate solution, (December).

Nishi, Y., Uryu, M., Yamanaka, S., Watanabe, K., Kitamura, N., Iguchi, M., & Mitsuhashi, S. (1990). The structure and mechanical properties of sheets prepared from bacterial cellulose - Part 2 Improvement of the mechanical properties of sheets and their applicability to diaphragms of electroacoustic transducers. *Journal of Materials Science*, *25*(6), 2997–3001. https://doi.org/10.1007/BF00584917

Oikawa, T., Ohtori, T., & Ameyama, M. (1995). Production of cellulose from d-mannitol by acetobacter xylinum ku-1. *Bioscience, Biotechnology and Biochemistry*, *59*(2), 331–332. https://doi.org/10.1080/bbb.59.331

Oka, H., Tomioka, T., Tomita, K., Nishino, a, & Ueda, S. (1994). Inactivation of enveloped viruses by a silver-thiosulfate complex. *Metal-Based Drugs*, *1*(5–6), 511. https://doi.org/10.1155/MBD.1994.511

Okiyama, A., Motoki, M., & Yamanaka, S. (1993). Bacterial cellulose IV. Application to

processed foods. *Topics in Catalysis*, *6*(6), 503–511. https://doi.org/10.1016/S0268-005X(09)80074-X

Orgambides, G., Montroziers, H., Servins, P., Roussels, J., & Trigalet-demeryll, D. (1991). High Heterogeneity of the Exopolysaccharides of Pseudomonas solanacearum Strain GMI 1000 and the Complete Structure of the Major Polysaccharide *.

Pinto, R. J. B., Daina, S., Sadocco, P., Neto, C. P., & Trindade, T. (2013). Antibacterial Activity of Nanocomposites of Copper and Cellulose. *BioMed Research International*, *2013*(December), 1–6. https://doi.org/10.1155/2013/280512

Portela, R., Leal, C. R., Almeida, P. L., & Sobral, R. G. (2019). Bacterial cellulose: a versatile biopolymer for wound dressing applications. *Microbial Biotechnology*, *201*, 1–25. https://doi.org/10.1111/1751-7915.13392

Purwadaria, T., Gunawan, L., & Gunawan, A. W. (2010). The Production of Nata Colored by Monascus purpureus J1 Pigments as Functional Food. *Microbiology Indonesia*, *4*(1), 6–10. https://doi.org/10.5454/mi.4.1.2

R. Malcolm Brown Jr. (1996). The biosynthesis of cellulose. *Journal of Macromolecular Science, Part A: Pure and Applied Chemistry Publication*, (10), 1345–1373.

Ratte, H. T. (1998). Bioaccumulation and toxicity of silver compounds: a review. *Environmental Toxicology and Chemistry*, *18*(1), 89–108.

Rieger, K. A., Cho, H. J., Yeung, H. F., Fan, W., & Schiffman, J. D. (2016). Antimicrobial Activity of Silver Ions Released from Zeolites Immobilized on Cellulose Nanofiber Mats. *ACS Applied Materials and Interfaces*, *8*(5), 3032–3040. https://doi.org/10.1021/acsami.5b10130

Roig-Sanchez, S., Jungstedt, E., Anton-Sales, I., Malaspina, D. C., Faraudo, J., Berglund, L. A., … Roig, A. (2019). Nanocellulose films with multiple functional nanoparticles in confined spatial distribution. *Nanoscale Horizons*, *4*, 634–641. https://doi.org/10.1039/c8nh00310f

Römling, U. (2002). Molecular biology of cellulose production in bacteria. *Research in Microbiology*, *153*(4), 205–212. https://doi.org/10.1016/S0923-2508(02)01316-5

Ross, P., Mayer, R., & Benziman, M. (1991). Cellulose Biosynthesis and Function in Bacteria. *Microbiological Reviews*, *55*(1), 35–58. https://doi.org/10.1016/j.bbalip.2012.08.009

Rouabhia, M., Asselin, J., Tazi, N., Messaddeq, Y., Levinson, D., & Zhang, Z. (2014). Production of biocompatible and antimicrobial bacterial cellulose polymers functionalized by RGDC grafting groups and gentamicin. *ACS Applied Materials and Interfaces*, *6*(3), 1439–1446. https://doi.org/10.1021/am4027983

Russell, R., Bond, P., Roco, M., Murday, J., Teague, C., Hays, S., & Merzbacher, C. (2004). The National Nanotechnology Initiaive: Strategic Plan, iii. Retrieved from www.nano.gov/sites/default/files/pub.../nni_strategic_plan_2004.pdf

Saeed, K., & Ibrahim. (2013). Carbon nanotubes-properties and applications: a review. *Carbon Letters*, *14*(3), 131–144. https://doi.org/10.5714/CL.2013.14.3.131

Sambhy, V., MacBride, M. M., Peterson, B. R., & Sen, A. (2006). Silver bromide nanoparticle/polymer composites: Dual action tunable antimicrobial materials. *Journal of the American Chemical Society*, *128*(30), 9798–9808. https://doi.org/10.1021/ja061442z

Sarkar, P., Bosneaga, E., & Auer, M. (2009). Plant cell walls throughout evolution: Towards a molecular understanding of their design principles. *Journal of Experimental Botany*, *60*(13), 3615–3635. https://doi.org/10.1093/jxb/erp245

Savage, N., Thomas, T. a, & Duncan, J. S. (2007). Nanotechnology applications and implications research supported by the US Environmental Protection Agency STAR grants program. *J. Environ. Monit.*, *9*(10), 1046–1054. https://doi.org/10.1039/b704002d

Schell, M. A. (2000). G ENES OF R ALSTONIA S OLANACEARUM BY AN.

Schouten, H. J. (1989). A possible role in pathogenesis for the swelling of extracellular slime of Erwinia amylovora at increasing water potential, *c*, 169–170.

Stoica-Guzun, A., Stroescu, M., Tache, F., Zaharescu, T., & Grosu, E. (2007). Effect of electron beam irradiation on bacterial cellulose membranes used as transdermal drug delivery systems. *Nuclear Instruments and Methods in Physics Research, Section B: Beam Interactions with Materials and Atoms*, *265*(1), 434–438. https://doi.org/10.1016/j.nimb.2007.09.036

Stone, B. (2005). Cellulose: Structure and Distribution. *Encyclopedia of Life Sciences*, 1–8. https://doi.org/10.1038/npg.els.0000695

Sun, D., Yang, J., Li, J., Yu, J., Xu, X., & Yang, X. (2009). Novel Pd-Cu/bacterial cellulose nanofibers: Preparation and excellent performance in catalytic denitrification. *Applied Surface Science*, *256*(7), 2241–2244. https://doi.org/10.1016/j.apsusc.2009.10.034

Surma-ślusarska, B., & Presler, S. (2008). Characteristics of Bacterial Cellulose Obtained from Acetobacter xylinum Culture for Application in Papermaking Characteristics of Bacterial Cellulose Obtained from Acetobacter Xylinum Culture for Application in Papermaking, (11530002).

Thompson, D. N., & Hamilton, M. A. (2001). Production of bacterial cellulose from alternate feedstocks. *Applied Biochemistry and Biotechnology - Part A Enzyme Engineering and Biotechnology*, *91–93*(12), 503–513. https://doi.org/10.1385/ABAB:91-93:1-9:503

Ullah, H., Santos, H. A., & Khan, T. (2016). Applications of bacterial cellulose in food, cosmetics and drug delivery. *Cellulose*, *23*(4), 2291–2314. https://doi.org/10.1007/s10570-016-0986-y

Van Alfen, N. K. (1989). Reassessment of plant wilt toxins, (63).

Vance, M. E., Kuiken, T., Vejerano, E. P., McGinnis, S. P., Hochella, M. F., & Hull, D. R. (2015). Nanotechnology in the real world: Redeveloping the nanomaterial consumer products inventory. *Beilstein Journal of Nanotechnology*, *6*(1), 1769–1780. https://doi.org/10.3762/bjnano.6.181

Vasse, J., Frey, P., & Trigalet, A. (1995). Microscopic studies of intercellular infection and protoxylem invasion of tomato roots by Pseudomonas solanacearum, (January 1995).

Watanabe, K., Tabuchi, M., Ishikawa, A., TAkemura, H., Tsuchida, Ta., Morinaga, Y., & Yoshinaga, F. (1998). Acetobacter Mutant With High Cell Productivity.Pdf.

Wu, C. N., Fuh, S. C., Lin, S. P., Lin, Y. Y., Chen, H. Y., Liu, J. M., & Cheng, K. C. (2018). TEMPO-Oxidized Bacterial Cellulose Pellicle with Silver Nanoparticles for Wound Dressing. *Biomacromolecules*, *19*(2), 544–554. https://doi.org/10.1021/acs.biomac.7b01660

Yang, G., Yao, Y., & Wang, C. (2017). Green synthesis of silver nanoparticles impregnated bacterial cellulose-alginate composite film with improved properties. *Materials Letters*, *209*, 11–14. https://doi.org/10.1016/j.matlet.2017.07.097

Yao, J., & Allen, C. (2006). Chemotaxis Is Required for Virulence and Competitive Fitness of the Bacterial Wilt Pathogen Ralstonia solanacearum, *188*(10), 3697–3708. https://doi.org/10.1128/JB.188.10.3697

Zeng, M., Laromaine, A., & Roig, A. (2014). Bacterial cellulose films: influence of bacterial strain and drying route on film properties. *Cellulose*, *21*(6), 4455–4469. https://doi.org/10.1007/s10570-014-0408-y

Adepu, S., & Khandelwal, M. (2018). Broad-spectrum antimicrobial activity of bacterial cellulose silver nanocomposites with sustained release. *Journal of Materials Science*, *53*(3), 1596–1609. https://doi.org/10.1007/s10853-017-1638-9

Agency, U. S. E. P. (1992). Silver in Business. Retrieved from http://www.empower-yourself-with-color-psychology.com/silver-in-business.html

Agrios, G. N. (2005). *Plant Pathology. Quinta edición. Academic Press. Nueva York.*

Araújo, I. M. S., Silva, R. R., Pacheco, G., Lustri, W. R., Tercjak, A., Gutierrez, J., … Barud, H. S. (2017). Hydrothermal synthesis of bacterial cellulose–copper oxide nanocomposites and evaluation of their antimicrobial activity. *Carbohydrate Polymers*, *179*(2018), 341–349. https://doi.org/10.1016/j.carbpol.2017.09.081

Barud, H. S., Regiani, T., Marques, R. F. C., Lustri, W. R., Messaddeq, Y., & Ribeiro, S. J. L. (2011). Antimicrobial bacterial cellulose-silver nanoparticles composite membranes. *Journal of Nanomaterials*, *2011*. https://doi.org/10.1155/2011/721631

Boateng, J., & Catanzano, O. (2015). Advanced Therapeutic Dressings for Effective Wound Healing - A Review. *Journal of Pharmaceutical Sciences*, *104*(11), 3653–3680. https://doi.org/10.1002/jps.24610

De Moura, M. R., Mattoso, L. H. C., & Zucolotto, V. (2012). Development of cellulose-based bactericidal nanocomposites containing silver nanoparticles and their use as active food packaging. *Journal of Food Engineering*, *109*(3), 520–524. https://doi.org/10.1016/j.jfoodeng.2011.10.030

FAO. (2014). *Food and Agriculture Organization, the international code of conduct on pesticide management*.

Gonzalez-Moragas, L., Yu, S. M., Murillo-Cremaes, N., Laromaine, A., & Roig, A. (2015). Scale-up synthesis of iron oxide nanoparticles by microwave-assisted thermal decomposition. *Chemical Engineering Journal*, *281*, 87–95. https://doi.org/10.1016/j.cej.2015.06.066

Hajipour, M. J., Fromm, K. M., Akbar Ashkarran, A., Jimenez de Aberasturi, D., Larramendi, I. R. de, Rojo, T., … Mahmoudi, M. (2012). Antibacterial properties of nanoparticles. *Trends in Biotechnology*, *30*(10), 499–511. https://doi.org/10.1016/j.tibtech.2012.06.004

Heredia, A., Jiménez, A., Guillén, R., & Guillénn, R. (1995). Composition of plant cell walls. *Zeitschrift Für Lebensmittel-Untersuchung Und -Forschung*, *200*(1), 24–31. https://doi.org/10.1007/BF01192903

Hestrin, S., & Schramm, M. (1954). Synthesis of cellulose by Acetobacter xylinum. 2. Preparation of freeze-dried cells capable of polymerizing glucose to cellulose*. *Biochemical Journal*, *58*(2), 345–352. https://doi.org/10.1042/bj0580345

Jonas, R., & Farah, L. F. (1998). Production and application of microbial cellulose. *Polymer Degradation and Stability*, *59*(1–3), 101–106. https://doi.org/10.1016/S0141-3910(97)00197-3

Kim, S. W., Jung, J. H., Lamsal, K., Kim, Y. S., Min, J. S., & Lee, Y. S. (2012). Antifungal effects of silver nanoparticles (AgNPs) against various plant pathogenic fungi. *Mycobiology*, *40*(1), 53–58. https://doi.org/10.5941/MYCO.2012.40.1.053

Kishanji, M., Mamatha, G., Obi Reddy, K., Varada Rajulu, A., & Madhukar, K. (2017). In situ generation of silver nanoparticles in cellulose matrix using Azadirachta indica leaf extract as a reducing agent. *International Journal of Polymer Analysis and Characterization*, *22*(8), 734–740. https://doi.org/10.1080/1023666X.2017.1369612

Klemm, D., Kramer, F., Moritz, S., Lindström, T., Ankerfors, M., Gray, D., & Dorris, A. (2011). Nanocelluloses: A new family of nature-based materials. *Angewandte Chemie - International Edition*, *50*(24), 5438–5466. https://doi.org/10.1002/anie.201001273

Lemire, J. a, Harrison, J. J., & Turner, R. J. (2013). Antimicrobial activity of metals: mechanisms, molecular targets and applications. *Nature Reviews. Microbiology*, *11*(6), 371–384. https://doi.org/10.1038/nrmicro3028

Li, Y. T., Lin, S. Bin, Chen, L. C., & Chen, H. H. (2017). Antimicrobial activity and controlled release of nanosilvers in bacterial cellulose composites films incorporated with montmorillonites. *Cellulose*, *24*(11), 4871–4883. https://doi.org/10.1007/s10570-017-1487-3

Li, Z., Wang, L., Chen, S., Feng, C., Chen, S., Yin, N., … Xu, Y. (2015). Facilely green synthesis of silver nanoparticles into bacterial cellulose. *Cellulose*, *22*(1), 373–383. https://doi.org/10.1007/s10570-014-0487-9

Maneerung, T., Tokura, S., & Rujiravanit, R. (2008). Impregnation of silver nanoparticles into bacterial cellulose for antimicrobial wound dressing. *Carbohydrate Polymers*, *72*(1), 43–51. https://doi.org/10.1016/j.carbpol.2007.07.025

Maria, L. C. S., Santos, A. L. C., Oliveira, P. C., Valle, A. S. S., Barud, H. S., Messaddeq, Y., & Ribeiro, S. J. L. (2010). Preparation and antibacterial activity of silver nanoparticles impregnated in bacterial cellulose. *Polímeros*, *20*(1), 72–77. https://doi.org/10.1590/S0104-14282010005000001

Mohite, B. V., & Patil, S. V. (2016). In situ development of nanosilver-impregnated bacterial

cellulose for sustainable released antimicrobial wound dressing. *Journal of Applied Biomaterials & Functional Materials*. https://doi.org/10.5301/jabfm.5000257

Nasrollahi, Y.-K., Kim, B. H., & Jung, G. (2009). Antifungal Activity of Silver Nanoparticles on some fungi. *Plant Disease*, *93*(10), 1037–1043. https://doi.org/10.1094/PDIS-93-10-1037

Oirdi, M. El, & Bouarab, K. (2007). Plant signalling components EDS1 and SGT1 enhance disease caused by the necrotrophic pathogen Botrytis cinerea, *175*(1), 131–139. https://doi.org/10.1111/j.1469-8137.2007.02086.x

Oka, H., Tomioka, T., Tomita, K., Nishino, a, & Ueda, S. (1994). Inactivation of enveloped viruses by a silver-thiosulfate complex. *Metal-Based Drugs*, *1*(5–6), 511. https://doi.org/10.1155/MBD.1994.511

Pontier, D., & Tronchet, M. (1998). Activation of hsr 203, a plant gene expressed during incompatible plant-pathogen interactions, is correlated with programmed cell death. *Mol Plant Microbe Interact*, *11*(6), 544–554. https://doi.org/10.1094/MPMI.1998.11.6.544

Pratley, J. E., & Haig, T. (2018). *Metal-Based nanomaterials and oxidative stress in plants: current aspects and overview.* (Vol. 26). https://doi.org/10.1007/978-3-319-76708-6

Rieger, K. A., Cho, H. J., Yeung, H. F., Fan, W., & Schiffman, J. D. (2016). Antimicrobial Activity of Silver Ions Released from Zeolites Immobilized on Cellulose Nanofiber Mats. *ACS Applied Materials and Interfaces*, *8*(5), 3032–3040. https://doi.org/10.1021/acsami.5b10130

Sundström, J. F., Albihn, A., Boqvist, S., Ljungvall, K., Marstorp, H., Martiin, C., … Magnusson, U. (2014). Future threats to agricultural food production posed by environmental degradation, climate change, and animal and plant diseases - a risk analysis in three economic and climate settings. *Food Security*, *6*(2), 201–215. https://doi.org/10.1007/s12571-014-0331-y

Torres, M. A. (2010). ROS in biotic interactions. *Physiologia Plantarum*, *138*(4), 414–429. https://doi.org/10.1111/j.1399-3054.2009.01326.x

Torres, M. A., Dangl, J. L., & Jones, J. D. G. (2002). Arabidopsis gp91phox homologues AtrbohD and AtrbohF are required for accumulation of reactive oxygen intermediates in the plant defense response. *Proceedings of the National Academy of Sciences*, *99*(1), 517–522. https://doi.org/10.1073/pnas.012452499

V. Rajesh Kannan, K. K. B. (2015). *Sustainable Approaches to controlling plant pathogenic bacteria*.

Villamizar-Gallardo, R., Cruz, J. F. O., & Ortíz, O. O. (2016). Fungicidal effect of silver nanoparticles on toxigenic fungi in cocoa. *Pesquisa Agropecuaria Brasileira*, *51*(12), 1929–1936. https://doi.org/10.1590/S0100-204X2016001200003

Ward, E. R., Payne, G. B., Moyer, M. B., Williams, S. C., Dincher, S. S., Sharkey, K. C., …

Ryals, J. a. (1991). Differential Regulation of beta-1,3-Glucanase Messenger RNAs in Response to Pathogen Infection. *Plant Physiology*, *96*(2), 390–397. https://doi.org//91 /96/0390/08/$01 .00/0

Wu, C. N., Fuh, S. C., Lin, S. P., Lin, Y. Y., Chen, H. Y., Liu, J. M., & Cheng, K. C. (2018). TEMPO-Oxidized Bacterial Cellulose Pellicle with Silver Nanoparticles for Wound Dressing. *Biomacromolecules*, *19*(2), 544–554. https://doi.org/10.1021/acs.biomac.7b01660

Wu, J., Zheng, Y., Song, W., Luan, J., Wen, X., Wu, Z., … Guo, S. (2014). In situ synthesis of silver-nanoparticles/bacterial cellulose composites for slow-released antimicrobial wound dressing. *Carbohydrate Polymers*, *102*(1), 762–771. https://doi.org/10.1016/j.carbpol.2013.10.093

Xu, Y.-J., Wang, J.-Y., Zuo, L.-G., & Qian, X. (2016). Rapid Microwave-Assisted Synthesis and Characterization of Cellulose Fiber Containing Silver Nanoparticles in Alkaline Aqueous Solution. *Science of Advanced Materials*. https://doi.org/10.1166/sam.2016.2771

Yang, G., Xie, J., Hong, F., Cao, Z., & Yang, X. (2012). Antimicrobial activity of silver nanoparticle impregnated bacterial cellulose membrane: Effect of fermentation carbon sources of bacterial cellulose. *Carbohydrate Polymers*, *87*(1), 839–845. https://doi.org/10.1016/j.carbpol.2011.08.079

Yang, G., Yao, Y., & Wang, C. (2017). Green synthesis of silver nanoparticles impregnated bacterial cellulose-alginate composite film with improved properties. *Materials Letters*, *209*, 11–14. https://doi.org/10.1016/j.matlet.2017.07.097

Yang, J., Liu, X., Huang, L., & Sun, D. (2013). Antibacterial properties of novel bacterial cellulose nanofiber containing silver nanoparticles. *Chinese Journal of Chemical Engineering*, *21*(12), 1419–1424. https://doi.org/10.1016/S1004-9541(13)60636-9

Yoon, J., Chung, W., & Choi, D. (2009). Jasmonic Acid-Dependent Positive Regulator of Pathogen-Induced Plant Cell Death. *New Phytologist*, *184*(1), 71–84. https://doi.org/10.1111/j.1469-8137.2009.02967.x

Zeng, M., Laromaine, A., Feng, W., Levkin, P. A., & Roig, A. (2014). Origami magnetic cellulose: Controlled magnetic fraction and patterning of flexible bacterial cellulose. *Journal of Materials Chemistry C*, *2*(31), 6312–6318. https://doi.org/10.1039/c4tc00787e

Zeng, M., Laromaine, A., & Roig, A. (2014). Bacterial cellulose films: influence of bacterial strain and drying route on film properties. *Cellulose*, *21*(6), 4455–4469. https://doi.org/10.1007/s10570-014-0408-y

Zeng, M., Laromaine Sagué, A., Vallribera Massó, A., Roig Serra, A., & Barcelona., U. A. de. (2014). Bacterial cellulose: fabrication, characterization and biocompatibility studies. Retrieved from http://ddd.uab.cat/record/127658

Zhao, X., Cui, H., Wang, Y., Sun, C., Cui, B., & Zeng, Z. (2017). Development Strategies and

Prospects of Nano-based Smart Pesticide Formulation. *Journal of Agricultural and Food Chemistry*, acs.jafc.7b02004. https://doi.org/10.1021/acs.jafc.7b02004

Zhao, Y., Thilmony, R., Bender, C. L., Schaller, A., He, S. Y., & Howe, G. A. (2003). Virulence systems of Pseudomonas syringae pv . tomato promote bacterial speck disease in tomato by targeting the jasmonate signaling pathway. *The Plant Journal*, *36*(4), 485–499. https://doi.org/10.1046/j.1365-313X.2003.01895.x

Boucher CA, Barberis PA, Trigalet AP, Demery DA. 1985. Transposon mutagenesis of *Pseudomonas solanacearum*: isolation of Tn5-induced avirulent mutants. *J.Gen.Microbiol.* 131: 2449-2457.

Breakspear A, Liu C, Roy S, Stacey N, Rogers C, Trick M, Morieri G, Mysore KS, Wen J, Oldroyd GE, et al. 2014. The root hair "infectome" of Medicago truncatula uncovers changes in cell cycle genes and reveals a requirement for Auxin signaling in rhizobial infection. *Plant Cell* 26(12): 4680-4701.

Brito B, Aldon D, Barberis P, Boucher C, Genin S. 2002. A signal transfer system through three compartments transduces the plant cell contact-dependent signal controlling R. solanacearum hrp genes. *Mol Plant Microbe Interact* 15(2): 109-119.

Clark RM, Schweikert G, et al. 2007. Common Sequence Polymorphisms Shaping Genetic Diversity in Arabidopsis thaliana. *Science* 317(5836): 338-342.

Cruz AP, Ferreira V, Pianzzola MJ, Siri MI, Coll NS, Valls M. 2014. A novel, sensitive method to evaluate potato germplasm for bacterial wilt resistance using a luminescent Ralstonia solanacearum reporter strain. *Mol Plant Microbe Interact* 27(3): 277-285.

Curtis MJ, Hays JB. 2007. Tolerance of dividing cells to replication stress in UVB-irradiated Arabidopsis roots: requirements for DNA translesion polymerases eta and zeta. *DNA Repair (Amst)* 6(9): 1341-1358.

Chini A, Fonseca S, Fernandez G, Adie B, Chico JM, Lorenzo O, Garcia-Casado G, Lopez-Vidriero I, Lozano FM, Ponce MR, et al. 2007. The JAZ family of repressors is the missing link in jasmonate signalling. *Nature* 448(7154): 666-671.

Delker C, Poschl Y, Raschke A, Ullrich K, Ettingshausen S, Hauptmann V, Grosse I, Quint M. 2010. Natural variation of transcriptional auxin response networks in Arabidopsis thaliana. *Plant Cell* 22(7): 2184-2200.

Deslandes L, Olivier J, Peeters N, Feng DX, Khounlotham M, Boucher C, Somssich I, Genin S, Marco Y. 2003. Physical interaction between RRS1-R, a protein conferring resistance to bacterial wilt, and PopP2, a type III effector targeted to the plant nucleus. *Proc Natl Acad Sci U S A* 100(13): 8024-8029.

Deslandes L, Pileur F, Liaubet L, Camut S, Can C, Williams K, Holub E, Beynon J, Arlat M, Marco Y. 1998. Genetic characterization of RRS1, a recessive locus in Arabidopsis

thaliana that confers resistance to the bacterial soilborne pathogen Ralstonia solanacearum. *Mol Plant Microbe Interact* 11(7): 659-667.

Dharmasiri N, Dharmasiri S, Estelle M. 2005. The F-box protein TIR1 is an auxin receptor. *Nature* 435(7041): 441-445.

Digonnet C, Martinez Y, Denance N, Chasseray M, Dabos P, Ranocha P, Marco Y, Jauneau A, Goffner D. 2012. Deciphering the route of Ralstonia solanacearum colonization in Arabidopsis thaliana roots during a compatible interaction: focus at the plant cell wall. *Planta* 236(5): 1419-1431.

Friml J, Vieten A, Sauer M, Weijers D, Schwarz H, Hamann T, Offringa R, Jurgens G. 2003. Efflux-dependent auxin gradients establish the apical-basal axis of Arabidopsis. *Nature* 426(6963): 147-153.

Fu J, Liu H, Li Y, Yu H, Li X, Xiao J, Wang S. 2011. Manipulating broad-spectrum disease resistance by suppressing pathogen-induced auxin accumulation in rice. *Plant Physiol* 155(1): 589-602.

Gaff DF, Okong'O-gola O. 1971. The use of non-permeating pigments for testing the survival of cells. *J Exp Bot* 22: 757-758.

Galan JE, Collmer A. 1999. Type III secretion machines: Bacterial devices for protein delivery into host cells. *Science* 284(5418): 1322-1328.

Genin S. 2010. Molecular traits controlling host range and adaptation to plants in Ralstonia solanacearum. *New Phytol* 187(4): 920-928.

Genin S, Denny TP. 2012. Pathogenomics of the Ralstonia solanacearum species complex. *Annu Rev Phytopathol* 50: 67-89.

Grierson C, Nielsen E, Ketelaarc T, Schiefelbein J. 2014. Root hairs. *Arabidopsis Book* 12: e0172.

Hayward AC. 1991. Biology and epidemiology of bacterial wilt caused by pseudomonas solanacearum. *Annu Rev Phytopathol* 29: 65-87.

Hanemian M., Zhou B., Deslandes L., Marco Y., Trémousaygue D. 2013. Hrp mutant bacteria as biocontrol agents: Toward a sustainable approach in the fight against plant pathogenic bacteria. *Plant Signaling & Behavior*, 8(10), e25678.

Horton MW, Hancock AM, Huang YS, Toomajian C, Atwell S, Auton A, Muliyati NW, Platt A, Sperone FG, Vilhjálmsson BJ, Nordborg M, Borevitz JO, Bergelson J. 2012. Genome-wide patterns of genetic variation in worldwide *Arabidopsis thaliana* accessions from the RegMap panel. *Nat Genet*. 2012 44(2):212-216.

Hueck CJ. 1998. Type III protein secretion systems in bacterial pathogens of animals and plants. *Microbiol Mol Biol Rev* 62(2): 379-433.

Jahn L, Mucha S, Bergmann S, Horn C, Staswick P, Steffens B, Siemens J, Ludwig-Müller J. 2013. The Clubroot Pathogen (Plasmodiophora brassicae) Influences Auxin Signaling to Regulate Auxin Homeostasis in Arabidopsis. *Plants* 2(4): 726-749.

Kageyama K, Asano T. 2009. Life Cycle of Plasmodiophora brassicae. *Journal of Plant Growth Regulation* 28(3): 203-211.

Kazan K, Lyons R. 2014. Intervention of Phytohormone Pathways by Pathogen Effectors. *Plant Cell* 26(6): 2285-2309.

Laplaze L, Lucas M, Champion A. 2015. Rhizobial root hair infection requires auxin signaling. *Trends Plant Sci* 20(6): 332-334.

Lee RD, Cho HT. 2013. Auxin, the organizer of the hormonal/environmental signals for root hair growth. *Front Plant Sci* 4: 448.

Lindgren PB, Peet RC, Panopoulos NJ. 1986. Gene cluster of Pseudomonas syringae pv. phaseolicola controls pathogenicity of bean plants and hypersensitivity of nonhost plants. *Journal of Bacteriology*, *168*(2), 512–522.

Mansfield J, Genin S, Magori S, Citovsky V, Sriariyanum M, Ronald P, Dow M, Verdier V, Beer SV, Machado MA, et al. 2012. Top 10 plant pathogenic bacteria in molecular plant pathology. *Mol Plant Pathol* 13(6): 614-629.

Monteiro F, Sole M, van Dijk I, Valls M. 2012. A chromosomal insertion toolbox for promoter probing, mutant complementation, and pathogenicity studies in Ralstonia solanacearum. *Mol Plant Microbe Interact* 25(4): 557-568.

Parry G, Calderon-Villalobos LI, Prigge M, Peret B, Dharmasiri S, Itoh H, Lechner E, Gray WM, Bennett M, Estelle M. 2009. Complex regulation of the TIR1/AFB family of auxin receptors. *Proc Natl Acad Sci U S A* 106(52): 22540-22545.

Pitts RJ, Cernac A, Estelle M. 1998. Auxin and ethylene promote root hair elongation in Arabidopsis. *Plant J* 16(5): 553-560.

Rodriguez-Navarro DN, Dardanelli MS, Ruiz-Sainz JE. 2007. Attachment of bacteria to the roots of higher plants. *FEMS Microbiol Lett* 272(2): 127-136.

Saile E, McGarvey JA, Schell MA, Denny TP. 1997. Role of Extracellular Polysaccharide and Endoglucanase in Root Invasion and Colonization of Tomato Plants by Ralstonia solanacearum. *Phytopathology* 87(12): 1264-1271.

Staswick PE, Tiryaki I. 2004. The oxylipin signal jasmonic acid is activated by an enzyme that conjugates it to isoleucine in Arabidopsis. *Plant Cell* 16(8): 2117-2127.

Torres MA, Dangl JL, Jones JD. 2002. Arabidopsis gp91phox homologues AtrbohD and AtrbohF are required for accumulation of reactive oxygen intermediates in the plant defense response. *Proc Natl Acad Sci U S A* 99(1): 517-522.

Tsuda K, Sato M, Stoddard T, Glazebrook J, Katagiri F. 2009. Network properties of robust immunity in plants. *PLoS Genet* 5(12): e1000772.

Turner M, Jauneau A, Genin S, Tavella MJ, Vailleau F, Gentzbittel L, Jardinaud MF. 2009. Dissection of bacterial Wilt on Medicago truncatula revealed two type III secretion system effectors acting on root infection process and disease development. *Plant Physiol* 150(4): 1713-1722.

Vailleau F, Sartorel E, Jardinaud MF, Chardon F, Genin S, Huguet T, Gentzbittel L, Petitprez M. 2007. Characterization of the interaction between the bacterial wilt pathogen Ralstonia solanacearum and the model legume plant Medicago truncatula. *Mol Plant Microbe Interact* 20(2): 159-167.

Valls M, Genin S, Boucher C. 2006. Integrated regulation of the type III secretion system and other virulence determinants in Ralstonia solanacearum. *PLoS Pathog* 2(8): e82.

Vasse J, Frey P, Trigalet A. 1995. Microscopic studies of intercellular infection and protoxylem invasion of tomato roots by Pseudomonas solanacearum. *Molecular Plant-Microbe Interactions* 8(2): 241-251.

Vasse J, Genin S, Frey P, Boucher C, Brito B. 2000. The hrpB and hrpG regulatory genes of Ralstonia solanacearum are required for different stages of the tomato root infection process. *Mol Plant Microbe Interact* 13(3): 259-267.

Zolobowska L, Van Gijsegem F. 2006. Induction of lateral root structure formation on petunia roots: A novel effect of GMI1000 Ralstonia solanacearum infection impaired in Hrp mutants. *Mol Plant Microbe Interact* 19(6): 597-606.

Zuluaga AP, Sole M, Lu H, Gongora-Castillo E, Vaillancourt B, Coll N, Buell CR, Valls M. 2015. Transcriptome responses to Ralstonia solanacearum infection in the roots of the wild potato Solanum commersonii. *BMC Genomics* 16: 246.